INFORMATION TO USERS

This manuscript has been reproduced from the microfilm master. UMI films the text directly from the original or copy submitted. Thus, some thesis and dissertation copies are in typewriter face, while others may be from any type of computer printer.

The quality of this reproduction is dependent upon the quality of the copy submitted. Broken or indistinct print, colored or poor quality illustrations and photographs, print bleedthrough, substandard margins, and improper alignment can adversely affect reproduction.

In the unlikely event that the author did not send UMI a complete manuscript and there are missing pages, these will be noted. Also, if unauthorized copyright material had to be removed, a note will indicate the deletion.

Oversize materials (e.g., maps, drawings, charts) are reproduced by sectioning the original, beginning at the upper left-hand corner and continuing from left to right in equal sections with small overlaps.

Photographs included in the original manuscript have been reproduced xerographically in this copy. Higher quality 6" x 9" black and white photographic prints are available for any photographs or illustrations appearing in this copy for an additional charge. Contact UMI directly to order.

Bell & Howell Information and Learning
300 North Zeeb Road, Ann Arbor, MI 48106-1346 USA

UMI®
800-521-0600

NEW INSTRUMENTATION FOR THE DETECTION OF SULFUR DIOXIDE IN THE REMOTE ATMOSPHERE

A

THESIS

Presented to the Faculty

of the University of Alaska Fairbanks

in Partial Fulfillment of the Requirements

for the Degree of

DOCTOR OF PHILOSOPHY

By

Dennis K. Nicks Jr., B.S.

Fairbanks, Alaska

December 1999

NEW INSTRUMENTATION FOR THE DETECTION OF SULFUR DIOXIDE IN THE REMOTE ATMOSPHERE

by

Dennis K. Nicks Jr.

RECOMMENDED:

Glen E. Shaw

Richard J. Hoflen

Richard L. Benner
Advisory Committee Chair

Thom P. Clare
Department Head, Chemistry and Biochemistry

APPROVED:

Thomas Clarke for Dave Woodall
Dean, College of Science, Engineering and Mathematics

Dean of the Graduate School

11-15-99
Date

Abstract

Sulfur gases are an important chemical component of the atmosphere. Gaseous sulfur compounds effect the acidity of rainwater and are important precursors to aerosol particles which affect public health, climate and visibility of scenic vistas such as the Grand Canyon. Sulfate aerosols are also known to participate in ozone catalysis in the stratosphere. A vast majority of the gaseous sulfur cycling through the atmosphere will exist as sulfur dioxide (SO_2) at some time during its atmospheric lifetime. Since SO_2 is a primary component of the atmospheric sulfur cycle, quality measurements of this gas are important to understanding the cycling of sulfur through the atmosphere. The mixing ratio of SO_2 in the atmosphere can be as low as a few 10's of parts-per-trillion by volume (pptv) in unpolluted areas and as high as 100's of parts-per-billion by volume (ppbv) near industrial centers. Obtaining SO_2 measurements with mixing ratios that can differ by 10^5 in magnitude is a difficult task, especially for mixing ratios less than a few hundred pptv.

The Diffusion Denuder/Sulfur Chemiluminescence Detector (DD/SCD) was developed further and tested in a rigorously blind comparison under controlled laboratory conditions. The DD/SCD exhibited excellent sensitivity and little-to-no interference from other trace gases. The DD/SCD performance was comparable to that of other state-of-the-art instruments developed for measuring SO_2 in the remote atmosphere.

The Continuous SO_2 Detector was developed to overcome the limitation of long sampling times (4 to 90 minutes) inherent in the DD/SCD and other state-of-the-art techniques. The Continuous SO_2 Detector (CSD) was developed based on the design of the DD/SCD, but has been optimized for sensitive, high-time resolved measurements of SO_2 in air. Sensitive, high-time resolved measurements would be beneficial for studying atmospheric SO_2 over large geographical areas from a moving sampling platform such as an aircraft. The current prototype of the CSD is capable of measuring SO_2 at mixing ratios of less than 100 pptv on the order of seconds. The DD/SCD, CSD and an automated, computer controlled dynamic dilution system described in this thesis represent a suite of instruments for the measurement of SO_2 in the remote atmosphere.

Table of Contents

List of Figures

List of Tables

Acknowledgments

This work would not have been possible without the support of many people and organizations. Special thanks goes out to Richard Benner who took me on as a graduate student and apprentice. Rich has lots of good ideas and I was fortunate to have the opportunity to work with him in implementing some of them. He encourages creativity and innovation, and stresses that a simple elegant solution is always better than a complex and expensive one. I was also fortunate to have a great committee. Glenn Shaw, Richard Stolzberg, Bill Simpson and Rob Disselkamp did an excellent job of offering suggestions and keeping me on track.

Several sources of funding were made available through research grants, travel grants, teaching assistantships and competitive student awards. I would like to acknowledge support from the National Science Foundation, the National Oceanic and Atmospheric Administration, the University of Alaska Fairbanks department of Chemistry and Biochemistry, the Geophysical Institute, the Center for Climate Change and Arctic System Research and the Crooks Memorial Fund Scholarship.

I would also like to thank my many friends and colleagues, specifically Will Cantrell, Clara Jodwalis, and Dave Veazey. Lastly, I would like to thank Kim Schoenbachler. Throughout the highs and lows of graduate school, Kim was there to offer her support and encouragement when I needed it most. I can't imagine finishing my thesis without her.

Chapter 1

Introduction:

The cycling of sulfur gases through the atmosphere have important ramifications in many environmental issues. The environmental issues range from acidification of rain water to the degradation of visibility, climatological effects and concerns regarding public health. Emissions of sulfur gases to the atmosphere can be divided into three categories: biogenic, volcanic and anthropogenic. Biogenic sources of sulfur emit compounds such as hydrogen sulfide (H_2S), carbon disulfide (CS_2), carbonyl sulfide (COS) and dimethylsulfide (DMS). The sources of the biogenic sulfur gases are diverse, including the oceans, soils, plants and swamps. The biogenically produced sulfur gases are oxidized in the atmosphere. The primary oxidant for trace gases in the atmosphere is the OH radical, which is a byproduct of the photolysis of tropospheric ozone. Other oxidation pathways for reduced sulfur gases have also been observed, such as ozone, peroxyl radical and nitrate radical. The oxidation pathways for these reduced sulfur gases are complex, but the major intermediate species in the oxidation process is sulfur dioxide (SO_2). Sulfur dioxide is also emitted directly from the biota through biomass burning, however this direct source of SO_2 pales in magnitude when compared to volcanic and anthropogenic emissions.

Anthropogenic emissions of sulfur gases are primarily in the form of SO_2. These emissions are the result of the combustion of fossil fuels such as coal, fuel oil and gasoline. Since these materials are traded commodities, and historical sales and production are well

documented, the resulting estimates of anthropogenic sulfur emissions from fossil fuel combustion are very reliable. These emissions have increased considerably since the Industrial Revolution which began in the late 1800s. Global estimates of anthropogenic sulfur gas emissions are said to be between 80-140 x 10^{12} g S $year^{-1}$ [Cullis and Hirschler, 1980]. Despite stringent pollution control regulations in developed countries, global anthropogenic sulfur emissions are still increasing. Sulfur emissions from the developed world are small compared to developing nations, even though the fossil fuel consumption of developed countries is much higher. For instance, estimates of sulfur emissions of greater than 20 x 10^{12} g S $year^{-1}$ from China in 1986 overshadow the estimates from the entire continent of North America (an estimate of less than 15 x 10^{12} g S $year^{-1}$) [Seinfeld and Pandis, 1997]. This is due primarily to the use of cheaper fossil fuel-based energy sources, such as high sulfur coal, in developing countries. Environmental regulation and controls for SO_2 emissions are lax, or non-existent in developing countries due to the costs of implementation. As further economic development is inevitable, the trend in anthropogenic SO_2 emissions will increase for the foreseeable future.

Environmental problems due to sulfur dioxide are well known. Mixing ratios of SO_2 in the hundreds of parts per billion by volume (ppbv) combined with other conditions such as a high number of acidic aerosol particles contributed to an estimated 4000 premature deaths during a few days in London England in 1952 [Samet and Utell, 1991; Ito et al., 1993]. Sulfur dioxide is also a major contributor to atmospheric acidity. Increased sulfur dioxide in the atmosphere results in increased acidity of cloud droplets and rain water. The increased acidity of rainwater is believed to have an adverse effect on

plants and has been suspected as a cause of reduced productivity in forests [Bunce, 1991]. These problems occur down wind from heavily industrialized areas, where high mixing ratios of sulfur dioxide are common.

Atmospheric sulfur dioxide is reactive and can be removed from the atmosphere through both wet and dry deposition. It also undergoes further oxidation in the atmosphere, which is caused primarily by reaction with the OH radical. The oxidative reactions are as follows [Seinfeld and Pandis, 1997]:

$$SO_2 + OH\cdot + M \rightarrow HOSO_2\cdot + M \quad (1.1)$$

$$HOSO_2\cdot + O_2 \rightarrow HO_2\cdot + SO_3 \quad (1.2)$$

$$SO_3 + H_2O + M \rightarrow H_2SO_4 \quad (1.3)$$

Reaction (1.1) is the initial reaction with the OH radical. The second reaction with O_2 (1.2) forms the peroxy radical and SO_3. Finally, in the presence of water vapor, SO_3 reacts rapidly to form sulfuric acid (1.3). Since sulfuric acid has a vapor pressure that is effectively zero, it ends up in the aerosol phase either through homogeneous nucleation or through condensation on an existing aerosol particle. The aerosol particles are eventually removed by settling, dry deposition or through precipitation events. This oxidation step resulting in a gas-to-particle conversion is another important removal process for atmospheric sulfur dioxide.

Aerosol Effects:

Before the aerosols are removed from the atmosphere, they can contribute to the degradation of visibility in scenic vistas such as the Grand Canyon and produce visible haze in otherwise pristine arctic regions [Eatough et al., 1995; NRC, 1993; Raatz and Shaw, 1984; Shaw, 1985]. Recently, a great deal of research as been devoted to the sources, sinks, and chemical and physical properties of sulfur aerosols as potential agents of climate change. Aerosols can scatter solar radiation directly ("direct effect") or they can scatter light indirectly ("indirect effect") by changing the optical properties of clouds [Shaw, 1983; Charleson et al., 1987; 1991; 1992] . These "aerosol effects" which may effect the Earth's radiation balance and thus may have an impact on climate change, are poorly characterized. A recent study by the Intergovernmental Panel on Climate Change (IPCC) estimates contributions to global climate change from both greenhouse gases and the direct and indirect effects from aerosols [IPCC, 1996; NRC, 1996]. The warming due to increased greenhouse gases is stated with a degree of certainty. The estimates of cooling as a result of the direct effect contains large uncertainties, which is due to the lack of scientific information. The effects on climate as a result of the indirect effect are so poorly understood that they could not be estimated. Since the effect could not be estimated, only a range of possible effects was stated. Taking into account the range of uncertainty in the combined aerosol effects, it is possible that the warming due to the increase in greenhouse gases could be offset by an aerosol cooling effect [Schwartz and Andreae, 1996]. Clearly this is a call for more research into the science of atmospheric aerosols, including the formation processes from gaseous precursors such as SO_2.

The effects of atmospheric aerosols on public health are of great concern. The human body's response to high levels of air pollution have been shown to contribute to premature death and respiratory system ailments [Samet and Utell, 1991; Samet and Speizer, 1993; Dockery et al., 1993; Ito et al., 1993; Reichhardt, 1995]. Current studies have focused on acute exposure to high levels of air pollution, including sulfur dioxide and acidic aerosols. There is some disagreement in the scientific and medical communities as to what proportion of health problems are actually caused by sulfurous aerosols and SO_2 [Ito et al., 1993]. There are many problems in assessing the effects of sulfurous aerosol and SO_2. The epidemiological difficulties aside, the environmental data for aerosol composition and size does not have sufficient history, continuity, temporal resolution, sensitivity and wide-spread coverage for use in statistical models [Ito et al., 1993]. For instance, there is much speculation that fine particles referred to as $PM_{2.5}$ (also known as particulate matter with aerodynamic diameter < 2.5 μm or $PM_{2.5}$) have been suspected to be more dangerous to public health than the larger PM_{10} (particulate matter with aerodynamic diameter < 10μm) [Riechhardt et al., 1995]. If $PM_{2.5}$ is an important contributor to adverse health effects, then this exacerbates the problem, as a network of $PM_{2.5}$ samplers is just now being setup. While understanding the role of sulfurous aerosols and SO_2 on public health is important, there is still much to study both on the epidemiological and the atmospheric chemistry side. A network of sensitive SO_2 and aerosol sulfate instruments may improve the understanding of the formation of these aerosol particles. Better scientific information and environmental data should benefit the study of the effects of air pollution on public health.

A summary of the emissions, reactions and removal processes discussed in this text is illustrated in Figure 1.1. The diagram illustrates the major contributors to the atmospheric sulfur load. Estimates of the loading due to the different contributors have also been given [Kelley and Smith, 1990; Brimblecombe et al., 1989; Jodwalis, 1998]. One of the most interesting aspects of the sulfur cycle is the large uncertainty in the biogenic emissions of sulfur to the atmosphere. The ambient mixing ratios of these reduced sulfur gases are commonly less than 50 parts per trillion by volume (pptv) [Seinfeld and Pandis, 1998], which is difficult to measure with current analytical techniques. The analytical problem is compounded with the large geographical area over which these sources are located. The magnitude of anthropogenic emissions compared with the total of biogenic and volcanic emissions is also interesting. The anthropogenic emissions of sulfur gases are roughly 80% of the natural sulfur emissions [Cullis and Hirschler, 1980; Moller, 1984; Kelly and Smith, 1990]. The atmospheric sulfur cycle is highly perturbed by anthropogenic activities. The effects on the natural sulfur cycle due to this perturbation are unknown.

As mentioned previously, the reduced sulfur gases undergo an oxidation process in the atmosphere. The diagram in Figure 1.1 was also meant to illustrate this oxidation process in a simplified manner. The oxidation pathway of reduced sulfur gases is complex, and although there are a number of intermediate species, a major intermediate species in the oxidation of reduced sulfur gases is SO_2. The point of this simplified diagram of the sulfur cycle is to demonstrate that a large majority of the sulfur cycling through the atmosphere exists as SO_2 at some time during it's atmospheric lifetime. Since

SO_2 is a primary intermediate for reduced sulfur gases as well as the primary sulfur gas emitted from anthropogenic sources, having good measurements of SO_2 is crucial for understanding the global sulfur cycle and possible related environmental and climatological effects.

Measurements of sulfur dioxide:

There are numerous ways to measure SO_2 mixing ratios in the atmosphere. The methods are as diverse as the applications, giving an investigator a number of choices based on desired sensitivity, portability, selectivity and sampling time. Some of these techniques are primarily sample collection or preconcentration techniques which use common bench-top analysis, such as ion chromatography. Other instruments are specially designed to selectively measure SO_2. For the purpose of this discussion, the instruments have been divided into different categories based on either the method of detection or the method of sampling and preconcentrating the atmospheric SO_2. The instrument categories include: (1) Fluorescence, (2) Sulfur Chemiluminescence, (3) Gas Chromatographic Systems, (4) Aqueous-based Systems and (5) Filter and Diffusion Denuder methods. This section concludes with a description of the Diffusion Denduer/Sulfur Chemiluminescence Detector (DD/SCD), which is the subject of this Thesis. The information regarding these different instrumental techniques is to serve only as a brief introduction. For more information regarding a specific technique, the reader is referred to the references found in the following discussion.

Fluorescence:

A commercially available instrument for monitoring atmospheric SO_2 is based on pulsed fluorescence in an optical cavity. In the pulsed fluorescence instrument, SO_2 in the sample air is excited by a zenon flash lamp which is pulsed at 10 Hz. Internal optics isolate the excitation radiation in the 190-230 nm wavelength range, which corresponds to a strong absorption band of SO_2. Excited SO_2^* fluoresces in a broad band ranging from 240-420 nm, with an emission peak at approximately 320 nm [Okabe, et al., 1973 from Luke, 1997]. The emission is isolated using band pass filters and monitored with a photomultiplier tube. Numerous modifications have been made to the pulsed fluorescence technique to alleviate interference problems, primarily from hydrocarbons and water vapor. A Nafion drier and "hydrocarbon kicker" were incorporated into the design and used successfully by Luke during a recent instrument intercomparison [Luke, 1997]. The pulsed fluorescence technique has been used for ambient monitoring of SO_2 in both polluted and unpolluted areas. Detection limits of 20-40 pptv SO_2 have been reported for a sampling and signal averaging time of 25 minutes [Stecher et al, 1997]. Less sensitive models of the pulsed fluorescence instrument are also used for monitoring industrial emissions to the atmosphere.

Another fluorescence technique is the flame photometric detector (FPD). The FPD has been widely used for the detection of sulfur in the atmosphere. The FPD is not selective for SO_2, so some separation or chemical isolation is necessary for selective detection of SO_2. In highly polluted air masses, such as power plant plumes, where mixing ratios of SO_2 can be hundreds of ppbv, the FPD has been used to measure SO_2 without

any sort of separation [Boatman et al, 1988]. The idea behind this technique is that SO_2 would be the only sulfur species emitted from the point-source. This technique works in this application because ambient levels of all other sulfur gases combined would be less than 1 ppbv. Measurements would be taken from outside the plume, and used as reference points to be subtracted from the response within the plume. The FPD works by combusting the sample air in a hydrogen-rich flame. One of the combustion products is electronically excited disulfur, or S_2^*. The FPD montiors S_2^* levels by measuring light intensity of the 294 nm emission wavelength [Boatman et al., 1988]. Since the technique relies on the formation of S_2^*, it has a non-linear response. Due to the instrument's nearly quadratic response, the instrument sensitivity can be improved and the response can be made nearly linear by the addition of another sulfur gas to the hydrogen fuel. Additions of 50 ppbv SF_6 to the flame fuel have resulted in near linear response and a detection limit of 0.5 ppbv for SO_2 with an averaging time of 300s [Boatman et al., 1988]. The linear response from doping the flame with high background levels of sulfur is very limited in that the linear range is limited to only 1 to 1.5 orders of magnitude [Farwell and Barinaga, 1986].

Chemiluminescence:

The Sulfur Chemiluminescence Detector (SCD) was developed by Benner and Stedman [1989]. The SCD has an equimolar response to all sulfur gases, it is not selective for SO_2. It works in a manner similar to that of the FPD in that it combusts the air sample in a hydrogen rich flame. The flame product used for detection of sulfur is different and is

based on a chemically induced fluorescence, or chemiluminescence. The chemical mechanism for the SCD is well understood [Benner, 1991; Benner and Stedman, 1994] and is summarized below:

$$\text{gaseous sulfur} \xrightarrow{\Delta(T = 1800^{o}C)} S + \text{products} \quad (1.4)$$

$$S + O \rightarrow SO \quad (1.5)$$

$$SO + O \rightarrow SO_2 \quad (1.6)$$

$$SO + O_3 \rightarrow SO_2^{*} + O_2 \quad (1.7)$$

$$SO_2^{*} \xrightarrow{h\upsilon = 340nm} SO_2 \quad (1.8)$$

In the combustion zone, the sulfur gases are broken down into sulfur atoms (1.4). As the flame products cool, the sulfur atoms combine with oxygen atoms as in reactions (1.5) and (1.6). A vacuum pump (Edwards Vacuum, model 2M18, Crawley, Sussex, England) draws the flame products through a critical oriface into a vacuum. This results in a rapid expansion and adiabatic cooling , which quenches chemical reactions in the flame gases before SO can be converted into the thermodynamically favored SO_2. The goal of this quenching step is to optimize the production of SO within the flame. The SO containing flame products are then mixed with O_3, which reacts with SO to form SO_2^{*} in step (7), which relaxes from the excited state with the release of a photon at about 340 nm (8). The chemiluminescence is then detected by a photomultiplier tube.

The SCD could easily be substituted for any application developed using the FPD

for sulfur detection. Like the FPD, the SCD has been used as a total sulfur monitor for atmospheric pollution measurements [Benner and Stedman, 1994; Jodwalis and Benner, 1996]. Although the FPD and SCD have common uses, it is important to differentiate between the chemical mechanisms of the SCD and the FPD. The chemiluminescence of the SCD is based on a mechanism involving a single sulfur atom, whereas the FPD requires S_2, which contains two sulfur atoms. What this means is that the SCD has a linear response to sulfur and the FPD has a nearly quadratic response to sulfur. Another characteristic of the the FPD mechanism is that with low levels of sulfur gas in the sample, S_2 is a rare flame product [Sugden et al., 1962; Muller et al., 1979; Farwell and Barinaga, 1986]. These two factors suggest that the SCD is more sensitive than the FPD. Results from research conducted by Gaines et al. [1990], show that the SCD is between 10 and 20 times more sensitive than the FPD. Not only is the SCD more sensitive to sulfur gases, but it has a linear range of over 4 orders of magnitude. It also has no known interferences, whereas the FPD exhibits interferences from had problems with CO_2, water vapor and some hydrocarbons.

GC-based techniques

A number of gas chromatography (GC) techniques exist for measuring SO_2 in the atmosphere. The advantage of using a GC in conjunction with a suitable detector is that selectivity for SO_2 is no longer a requirement of the detector. With proper chromatographic separation, SO_2 can be differentiated from other detectable species. Early studies with a GC/FPD have been quite successful in the measurement of both SO_2

and DMS as well as other biogenically produced sulfur gases [Farwell and Barinaga, 1986]. To obtain sufficient analyte for analysis, sample air is preconcentrated using a cryogenic trap. The cryogenic trap uses liquid argon to condense sulfur gases, including SO_2, as the sample air is passed through a loop of tubing submerged in the cryogen. The trapped sulfur gases are then purged by heating and focused onto the GC column for separation and ultimately quantified by the FPD. Mixing ratios of less than 100 pptv SO_2 and DMS have been observed in remote areas such as the central Pacific Ocean using this technique [Thornton and Bandy, 1993].

The SCD has also been used successfully when coupled to a GC. The atmospheric sulfur gases can be preconcentrated on molecular sieve and then re-volatilized and focused onto the GC column. Cryogenic preconcentration can also be used for sulfur gas analysis. This technique has been used successfully in measuring biogenic sulfur gases, primarily DMS, in the Gulf of Alaska, the Bering Strait and Chukchi Sea [Jodwalis, 1998]. This technique could easily be optimized for the analysis of SO_2 in air. The GC/SCD technique is also quite sensitive. Measurements of DMS in the remote marine boundary layer ranged from a few pptv to a few hundred pptv. The SCD has been commercialized by Sievers Instruments (Boulder, CO) and is a widely used GC detector for many analytical applications [Shearer et al., 1990; Gaines et al., 1990]. The SCD has also been used as a detector for HPLC [Ryerson et al., 1992].

Another detector that has been used successfully for ambient SO_2 measurements when coupled with a GC is the mass spectrometer (MS). The GC/MS technique also uses a liquid argon based cryogenic trap to preconcentrate the analyte gases. This technique

further benefits by using an isotopically labeled internal standard, in this case $^{34}SO_2$. The isotope dilution technique allows for further quality assurance of the measurements. For instance, any sampling artifact in the measurement will be accounted for by using the internal standard as a reference. By using this information as well as the ratio of ^{34}S to ^{32}S for naturally occurring sulfur, the result can be corrected and the ambient SO_2 mixing ratio quantified. The technique has been used successfully on both ground and aircraft based sampling platforms. The technique has a detection limit of better than 20 pptv SO_2 with a sampling and preconcentration time of between 3 and 8 minutes, depending on the ambient SO_2 mixing ratio [Stecher et al., 1997; Driedger III, et al., 1987].

Aqueous-based systems:

Sulfur dioxide reacts rapidly in the presence of water and on wetted surfaces. A number of techniques use this chemical property as a way of collecting SO_2 in a substrate for future analysis. One technique that has been used successfully is based on an aqueous phase chemiluminescent reaction. The aqueous chemiluminescence technique used by Jaeschke et al. [1997] involves collecting SO_2 on a filter which is impregnated with a $HgCl_4^{2-}$ (aq) (TCM). The filter is housed in a Teflon® filter holder, which has been modified by adding a small sample reservoir on the back end of the filter, to collect the TCM which drips from the saturated filter. A peristaltic pump continuously refreshes the filter by pumping TCM from the sample reservoir, spraying it directly on the filter. As the sample air is drawn through the filter, SO_2 is removed through reaction with the TCM solution. Once a sufficient sample is collected, the TCM solution is removed from the

reservoir and diverted into a reaction chamber. The TCM solution is mixed with Ce^{4+} (aq), which initiates a chemiluminescent reaction with the sulfur containing compound. The resulting photons are detected by a photomultiplier tube. This technique has a sampling time of between 10-35 minutes and requires a sample volume of 100-350 L of air. The detection limit of this technique under these conditions has been determined to be better than 20 pptv SO_2 [Stecher et al, 1997].

Another technique uses an aqueous absorber solution which is circulated through a gas to liquid exchange coil. The aqueous absorber solution contains 10 μM formaldehyde with 0.840 mM Na_2EDTA. The resulting aqueous solution containing sulfur dioxide, bisulfite and sulfite is then pumped through a continuous reaction system. It is sequentially reacted with ethanolamine in a pH = 9 buffer and o-phthalaldehyde. This series of reactions convert the absorbed SO_2 into a highly fluorescent isoindole derivative. A strong acetate buffer of pH = 5.7 is then added to aid in the HPLC analysis and also to preserve the fluorescent product. The sample is then separated by HPLC and detected by a continuous fluorescence spectrophotometer which utilizes an excitation wavelength of 330 nm and an detection wavelength of 380 nm. This system has been used extensively in the field, specifically in remote oceanic areas where the mixing ratio of SO_2 can be less than 50 pptv [Yvon and Saltzman, 1996]. With a sampling time of 4 minutes the instrument has a detection limit of better than 20 pptv SO_2 [Stecher et al, 1997; Gallagher et al., 1997].

A third aqueous based system is one that incorporates a mist chamber with an ion chromatograph (IC). The mist/IC instrument works in the following way. The sample air

is accelerated to a high velocity through one nozzle and is immediately passed by a second nozzle positioned orthogonal to the first. This creates a localized pressure drop at the second nozzle due to the Bernoulli Effect. The low pressure regime causes a sample of ultra-pure water to be drawn from a reservoir at the base of the second nozzle. The water is aspirated from the second nozzle into the jet of air from the first. This creates a dense, fine mist that efficiently scavenges SO_2 from the sample air. The aspirated water is collected in a reservoir at the bottom of the mist chamber. The water is re-circulated from the mist chamber through the second nozzle, until a suitable amount of SO_2 is collected for analysis. The water is then removed from the reservoir and weighed to determine the mass, which is then used to determine the aqueous sample volume. Two aliquots of the water are then analyzed for SO_4^{2-} by IC [Talbot et al., 1997]. This technique works best with high sample flow rates and can obtain detection limits better than 20 pptv SO_2 with a sampling time of between 5 and 30 minutes [Stecher et al., 1997].

Filter and diffusion denuder collection methods:

Another method of preconcentrating SO_2 for analysis is on a collection surface which is coated with an aqueous substrate that is allowed to dry. The dried substrate reacts with SO_2, removing it from the sample air. This substrate can then be extracted and analyzed with using ion chromatography as the analytical technique. These methods are similar to the aqueous techniques, however a differentiation has been made because the sample is collected on a dry substrate. There are two widely accepted methods of collecting SO_2 on a reactive substrate, filter methods and diffusion denuder methods.

One of the most widely accepted filter techniques for collecting ambient SO_2 utilizes a paper filter which is impregnated with a carbonate substrate. The filter is first pre-cleaned with a dilute HCl, deionized water solution and then rinsed several times. The filter is then soaked in a 1% K_2CO_3 / 10% glycerin solution. The filters are then allowed to dry in an SO_2-free clean room. The filter holder consists of an aerosol pre-filter which is followed by the CO_3^{2-} impregnated filter. As sample air is drawn through the filters, the aerosol sulfur is removed in the pre-filter and the SO_2 is allowed to pass through to the second filter. The SO_2 reacts on the surface of the second filter, and is removed from the air stream. When an adequate sample has been collected, the filter is removed from the housing and stored until analysis. The sample is extracted by the addition of a 0.01% H_2O_2 solution which converts the sulfur in the sample to SO_4^{2-}(aq). The extract is then passed through a cation exchange resin, which exchanges H^+ for any of the K^+ ions left from the sample collection substrate. The resulting H_2SO_4 is then analyzed by ion chromatography. For clean ambient air, with SO_2 mixing ratios less than 50 pptv, a sample volume of 6,000 liters is required for an uncertainly level of ± 7 pptv [Ferek et al., 1997; Ferek et al., 1991].

Since the use and theory of diffusion denuders is important to this work, the description given will be more detailed than the other SO_2 techniques. The most basic diffusion denuder design consists of a hollow tube, which is coated with a substrate which is a "perfect" sink for the analyte gas. Perfect means is that when the analyte gas comes in contact with the coated inner wall of the denuder tube, it will react instantaneously and be irreversibly removed from the sample air. Any gases that do not react with the denuder

surface is passed through the denuder unaffected. The diagram in Figure 1.2 demonstrates the use of a diffusion denuder. As the name implies, the collection properties and efficiency of the diffusion denuder is based on the diffusivity of the analyte gas in a the bulk fluid. In this case, the bulk fluid is air. To be able to predict the diffusivity of a particular gas in air, laminar flow conditions are required. One criteria for assessing laminar flow is when the Reynolds number is less than about 2000. The Reynolds number is calculated by:

$$\mathrm{Re} = \frac{4F}{\pi \nu d} \tag{1.9}$$

In this equation, F is the volumetric flow rate (cm^3s^{-1}), ν is the kinematic viscosity of air at 20° C (0.152 cm^2s^{-1}) and d is the internal diameter of the cylindrical tube (cm). Under laminar flow conditions, the removal efficiency of a diffusion denuder can be predicted by the Gormley and Kennedy equation [Gormley and Kennedy, 1949]. The equation is as follows:

$$1 - \frac{C}{C^\circ} = 0.819e^{(-14.6272\Delta)} + 0.0976e^{(-89.22\Delta)} + 0.01896e^{(-212\Delta)} \tag{1.10}$$

Where:

$$\Delta = \frac{DL}{\gamma(\mathrm{Re})d} \qquad (1.11)$$

In these equations, C is the amount of analyte gas remaining in the denuder effluent, C^o is the original amount of analyte entering the denuder, D is the molecular diffusivity of the analyte gas in air (cm^2s^{-1}), L is the length of the dunuder (cm), γ is the permitivity of free space (cm^2s^{-1}), Re is the Reynold's number and d is the internal diameter of the denuder (cm). The second and third terms of the Gormley-Kennedy equation become less crucial when the delta is greater than 0.2. The length L of the denuder should be chosen so that the removal efficiency approaches 100%. The temperature dependence of the diffusion denuder is reflected in the diffusion coefficient. A comprehensive review of the theory and uses of diffusion denuders can be obtained from Murphy and Fahey [1987], Febo et al. [1989], and Zulifiqur et al. [1989].

Once the dimensions of the denuder have been determined theoretically, a suitable collection substrate must be chosen for the denuder coating. For the collection of SO_2, a CO_3^{2-} substrate has been most commonly used [Ferm, 1985; Koutrakis et al., 1988; Dasch et al., 1989; Lee et al., 1993]. The CO_3^{2-} substrate consists of 5% by mass K_2CO_3, 5% by mass glycerine, diluted with a 50:50 methanol:water solution. The uncoated denuder tube is capped on one end with a PTFE Teflon® plug. Approximately 4 ml of the CO_3^{2-} solution is added to the tube, which is then capped off completely with another PTFE Teflon® plug. The tube is inverted and rolled several times to ensure uniform coating of

the inner walls of the denuder tube. The solution is then drained and the denuder tube is dried by flushing compressed helium through the tube at a flow rate of approximately 20 cm^3min^{-1} for about 2 hours. The coated tube is then capped off with Swagelock fittings and stored until needed [Wu, 1996; Benner et al., 1997].

Sample air is drawn through the diffusion denuder until a suitable sample has been absorbed by the denuder coating. Once a suitable sample has been obtained, the coating can be extracted and analyzed. The extraction and analysis process is similar to the impregnated filter technique. The denuder is washed with an ultra-pure water and peroxide solution, which is then analyzed for SO_4^{2-} by ion chromatography.

Both the filter and diffusion denuder preconcentration techniques require large sample volumes to obtain detectable levels of SO_4^{2-}. The large sample volumes frequently require long sampling times. As a result, these techniques are used primarily to obtain average mixing ratios of atmospheric SO_2 over periods of time ranging from hours to days.

Diffusion Denuder/Sulfur Chemiluminescence Detector (DD/SCD)

The SCD is an ideal detector for atmospheric sulfur gases. It is sensitive, selective for sulfur, has a linear response over at least four orders of magnitude, has no major interference problems and has a fast response time [Benner, 1991]. Since the SCD cannot differentiate between different sulfur gases, a separation or isolation step is required for specificity to SO_2. As mentioned previously, interfacing the SCD to a GC would achieve specificity for different sulfur gases. The addition of a GC for separation and cryogen for

preconcentration complicates the analysis, especially in a field sampling application where simplicity is preferred. The preconcentration and GC steps require additional time sampling and separation. The additional time requirement increases the time between measurements, so much of the SCD's fast response advantage is not realized. Specificity for SO_2 can also be achieved by interfacing a CO_3^{2-} coated diffusion denuder to the SCD. A schematic diagram of this Diffusion Denuder/Suflur Chemiluminescence Detector (DD/SCD) is shown in Figure 1.3. The principles behind the DD/SCD are straight forward. Sample air is diverted through a CO_3^{2-} denuder where SO_2 is selectively and quantitatively removed. The response to this sample air, scrubbed of SO_2, is recorded by the SCD. Next, a 3-way solenoid valve redirects the sample flow through an uncoated tube, directly to the SCD, bypassing the CO_2^{2-} denuder. The response to the sample air containing SO_2 is measured by the SCD. The difference between the SCD response from the air containing SO_2 (high response) and that of the air scrubbed of SO_2 (low response) is proportional to the mixing ratio of SO_2 contained in the sample air. This describes the workings of the DD/SCD at the most basic level. Chapters 2 and 4 will expand on the theory and practice of the DD/SCD.

The DD/SCD was first used by Schoran et al. [1994] to measure ambient SO_2 mixing ratios in the Grand Canyon. The DD/SCD worked well throughout the experiment, but had not undergone rigorous testing and evaluation before field deployment. The same technique was developed independently at the University of Alaska Fairbanks as part of a National Science Foundation (NSF) Research Experience for Undergraduates (REU) program in 1993. The results from the prototype developed at

UAF were promising and the technique was further developed [Wu, 1995]. The DD/SCD is novel in that it obtains specificity for SO_2 with a total sulfur detector, without preconcentration and chromatographic separation. This simplifies analysis and is also ideal for remote field deployment. The DD/SCD also takes advantage of the real-time characteristics of the SCD.

Instrument Intercomparision

With so many different instruments being used to measure SO_2, it is difficult to compare and contrast the field measurements from each of these instruments. Each technique has different operational characteristics such as sampling time, interferences and limit of detection. Without understanding the differences between these instruments, it is difficult to compare and contrast the resulting field measurements. In 1989, the Chemical Instrumentation Test and Evaluation mission 3 (CITE3) was conducted as part of the NASA Global Tropospheric Experiment. One of the primary objectives for CITE3 was to test and evaluate via airborne field intercomparisons the capacity to make reliable measurement of many atmospheric sulfur species, including SO_2. The state-of-the-art instruments at the time, were flown during the extensive field mission, which logged almost 100 flight hours. Having the intercomparison on a moving platform made it difficult to compare techniques with different sampling or preconcentration times. The results from the intercomparison of the SO_2 instruments were less than definitive. The instruments showed no correlation for mixing ratios less than 250 pptv. This was particularly troubling since mixing ratios of SO_2 are commonly less than 100 pptv. The

CITE3 data clearly indicated that detection limits for SO_2 must be better than 50-100 pptv for many tropospheric applications [Hoell et al, 1993; Gregory et al., 1993].

In response to the CITE3 results, the NSF funded the Gas Phase Sulfur Intercomparison Experiment (GASIE). This experiment was intended to evaluate the state-of-the-art SO_2 instrumentation under a controlled laboratory environment. By controlling the mixing ratio of SO_2 for a period of time, instruments could be evaluated with the same sample air regardless of the sampling time required. The addition of potential interfering gases into the sample air matrix could also be controlled. The interfering gases consisted of CO_2, CO, CH_4, DMS, NO_x, O_3 and water vapor. By controlling the input of potential interfering gases, interference problems with individual instruments could be identified. The intercomparison was conducted in a rigorously blind fashion. Throughout the experiment, the group delivering the test gas mixtures was not aware of the results from the different instruments being tested. Similarly, the operators of the instruments being evaluated did not know the mixing ratios of the sample air being delivered or the results of the other operators. An independent oversight committee coordinated the experiment and ensured that the process remained blind. A complete description of the experimental design and execution of GASIE is described elsewhere [Luther et al.,1997; Stecher et al., 1997; MacTaggart et al., 1997].

Many of the instruments evaluated in GASIE are described earlier in this text. The instruments which were evaluated in GASIE included a pulsed fluorescence technique [Luke, 1997], high-performance liquid chromatography (HPLC)/fluorescence [Gallagher et al., 1997], mist chamber/ion chromatography (IC) [Talbot et al., 1997], diffusion

scrubber/IC [Kok, et al., 1990], aqueous chemiluminescence [Jaeschke et al., 1997], isotope dilution-gas chromatograph (GC)/mass spectrometer (MS) [Bandy et al., 1993], a carbonate filter/IC [Ferek et al., 1993] and the diffusion denuder/sulfur chemiluminescence detector (DD/SCD) [Benner et al., 1997].

The GASIE results demonstrate the substantial improvements in SO_2 detection since CITE3. A comprehensive analysis of GASIE can be obtained from Stecher et al. [1997]. The graph in Figure 1.4 summarizes the results found in GASIE. In this graph, the measurements from each of the instruments found to have no significant interferences from the different sample air matrices used in GASIE, were combined to form an average measurement (DD/SCD measurements were omitted from this average). The results demonstrate excellent linearity from zero to 500 pptv SO_2. The only significant difference in slope occurred with the sample air which contained water vapor at 50% relative humidity (RH). This small effect from water vapor was accounted for by the quality assurance instruments and was attributed to losses within the sample air delivery system. The DD/SCD and Filter/IC techniques were the only instruments that demonstrated analytical problems when water vapor was introduced into the sample air matrix. The general conclusions from GASIE were that, aside from the DD/SCD, the instruments compared well and showed little to no detectable effects from interfering gases. All of the instruments tested were capable of measuring SO_2 at mixing ratios of less than 50 pptv [Stecher et al., 1997].

The DD/SCD experienced numerous problems during the GASIE experiment. At the time that GASIE was conducted, the DD/SCD technique was still in early stages of

development. The technique had not undergone rigorous testing before the experiment, thus GASIE was the first chance for the technique to be evaluated in a blind experiment. The instrument fared poorly in the test compared with the more developed, field tested systems. The graph in Figure 1.5 shows the results and demonstrates the problems uncovered in GASIE. The problems include a major interference from water vapor and minor interferences from the sample air containing CO_2, CO, CH_4 and DMS as well as minor interference from the sample air containing NO_x and O_3 [Wu, 1995; Stecher et al., 1997].

Problems with the DD/SCD during GASIE

Water Vapor:

The DD/SCD demonstrated a significant problem when water vapor was added to the sample air matrix at 50% relative humidity. This was surprising because the SCD does not suffer an interference from water vapor [Benner and Stedman, 1989]. This lead to a thorough investigation of the DD/SCD sample train and denuder manifold. By repeating the humidity experiments after the GASIE results had been released, it became evident that parts of the fittings and sampling train tubing as well as the CO_3^{2-} denuder itself were emitting an unknown sulfur gas under high humidity. Further experimentation revealed that the CO_3^{2-} denuder released SO_2 only when it had been heavily loaded with sulfur. It is interesting to note that the Filter/IC technique, which also uses a CO_3^{2-} substrate had only a minor problem with water vapor. The filter used in the Filter/IC method is replaced after each run, so large amounts of sulfur are not collected on the filter. The CO_3^{2-} denuder was

not changed throughout the experiment as it is used as a removal device, not a preconcentration device (like the CO_3^{2-} filter). The sulfur load on the denuder was much higher than that of the CO_3^{2-} filter. These results indicate that the effect from water is dependent on sulfur load on the CO_3^{2-} substrate.

Interferences:

The addition of CO_2 (350 ppmv), CH_4 (2 ppmv), CO (120 ppbv) and DMS (100 pptv) resulted in a negative offset of ~40 pptv in the DD/SCD results. The DD/SCD had been tested for DMS removal prior to GASIE, but no interference had been found. In re-tests after the GASIE results had been released, DMS was found to be removed, not by the CO_3^{2-} denuder, but by the uncoated tube that is meant to remove no sulfur gases. One explanation for this change is that condensed water introduced into the denuder manifold during one water vapor tests during GASIE may have changed the chemical characteristics of the uncoated tube [Wu, 1995; Benner et al., 1997].

During GASIE, the addition of O_3 (100 ppbv) and NO_x (10 ppbv) to the sample air matrix resulted in a positive intercept of 50 to 100 pptv in the DD/SCD measurement. The SCD has no interference problems with NO_x [Benner and Stedman, 1989] and tests conducted after the GASIE showed that the response due to O_3 at 100 ppbv was much less than 5%.

Post-GASIE Modifications:

It was evident after reviewing the results from GASIE and conducting further

research into the problems with the denuder manifold that water vapor must be removed from the sample air. A Nafion (Permapure, Toms River, NJ) dryer was added to the DD/SCD at the inlet to the sampling train. The DD/SCD and Nafion dryer were rigorously tested and showed no interference from water vapor [Wu, 1995; Benner et al., 1997]. The entire sampling train and denuder manifold were also redesigned. Special attention was made to ensure that new materials used in the sampling train and denuder manifold were more compatible with SO_2. The modifications to the DD/SCD solved the problems that were revealed in GASIE. These modifications are described in Benner et al., [1997] and further described in Chapter 2 of this Thesis.

Contents of Thesis:

This Thesis describes the further development and testing of the DD/SCD and is divided into the following sections. Chapter 2 describes the Gas Phase Sulfur Intercomparison Experiment, Phase 2 (GASIE-2), a re-test of the DD/SCD. The re-test was designed to evaluate the improved DD/SCD to see that the modifications had addressed the interference problems discovered in GASIE. Chapter 2 includes a description of these changes to the DD/SCD, the results of GASIE-2 as well as a re-analysis of some of the original GASIE data. Chapter 2 has been submitted for publication in the *Journal of Geophysical Research*, so much of the introduction and historical background from Chapter 1 may be repeated. Chapter 3 describes a new dynamic dilution system for fabricating calibration gases. This dilution system was used extensively in GASIE-2 for supplying the gas mixtures for the calibration of the DD/SCD. The dilution

system was designed, developed and rigorously calibrated so that it was capable of diluting reactive calibration gases such as SO_2 from stock calibration standard in the ppmv range to mixing ratios as low as 10 pptv. Chapter 4 describes a new SO_2 instrument dubbed the Continuous SO_2 Detector (CSD). The new technique is based on the DD/SCD, but benefits from a completely new design of the diffusion denuder manifold. The CSD is capable of measuring SO_2 in the 10's of pptv in time scales of less than a minute. This is a significant improvement over the DD/SCD technique, which required a 10 min measurement time. Chapter 5 contains a summary of this Thesis work, as well as ideas and plans for future work using this research.

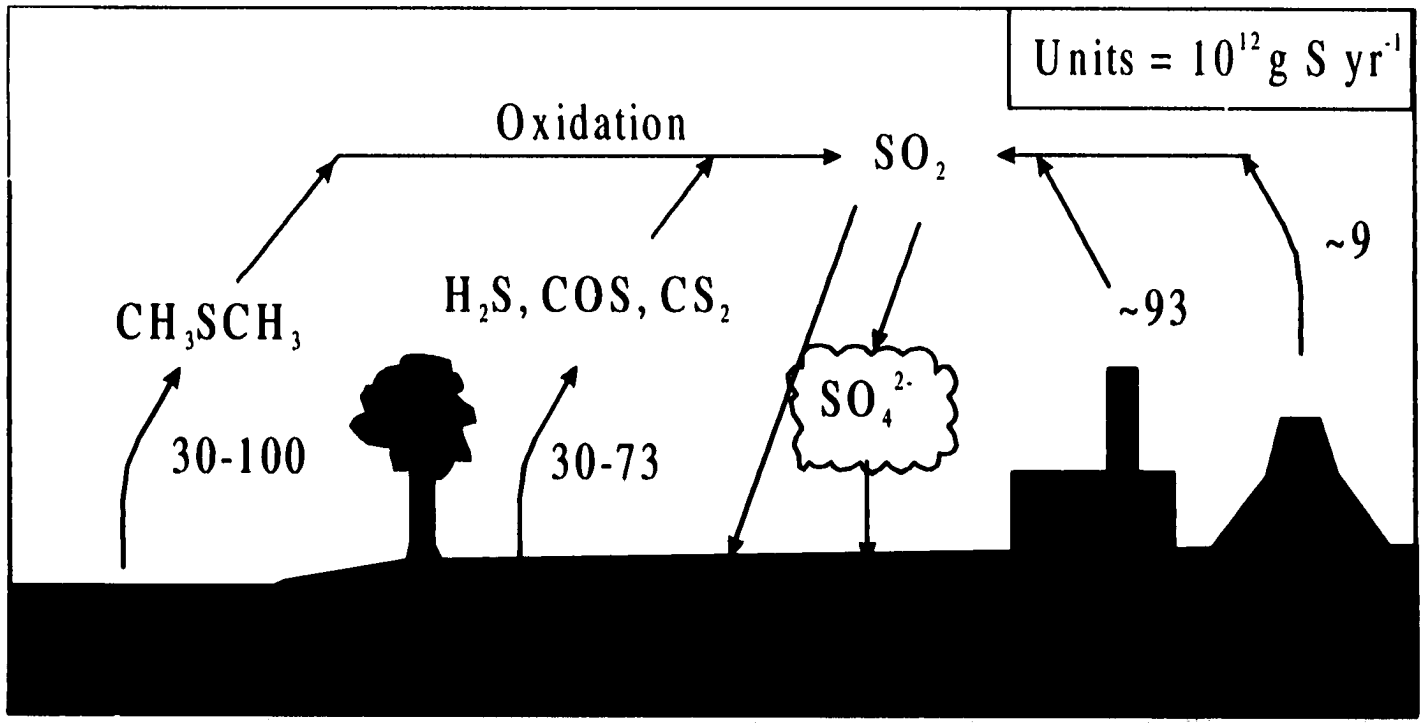

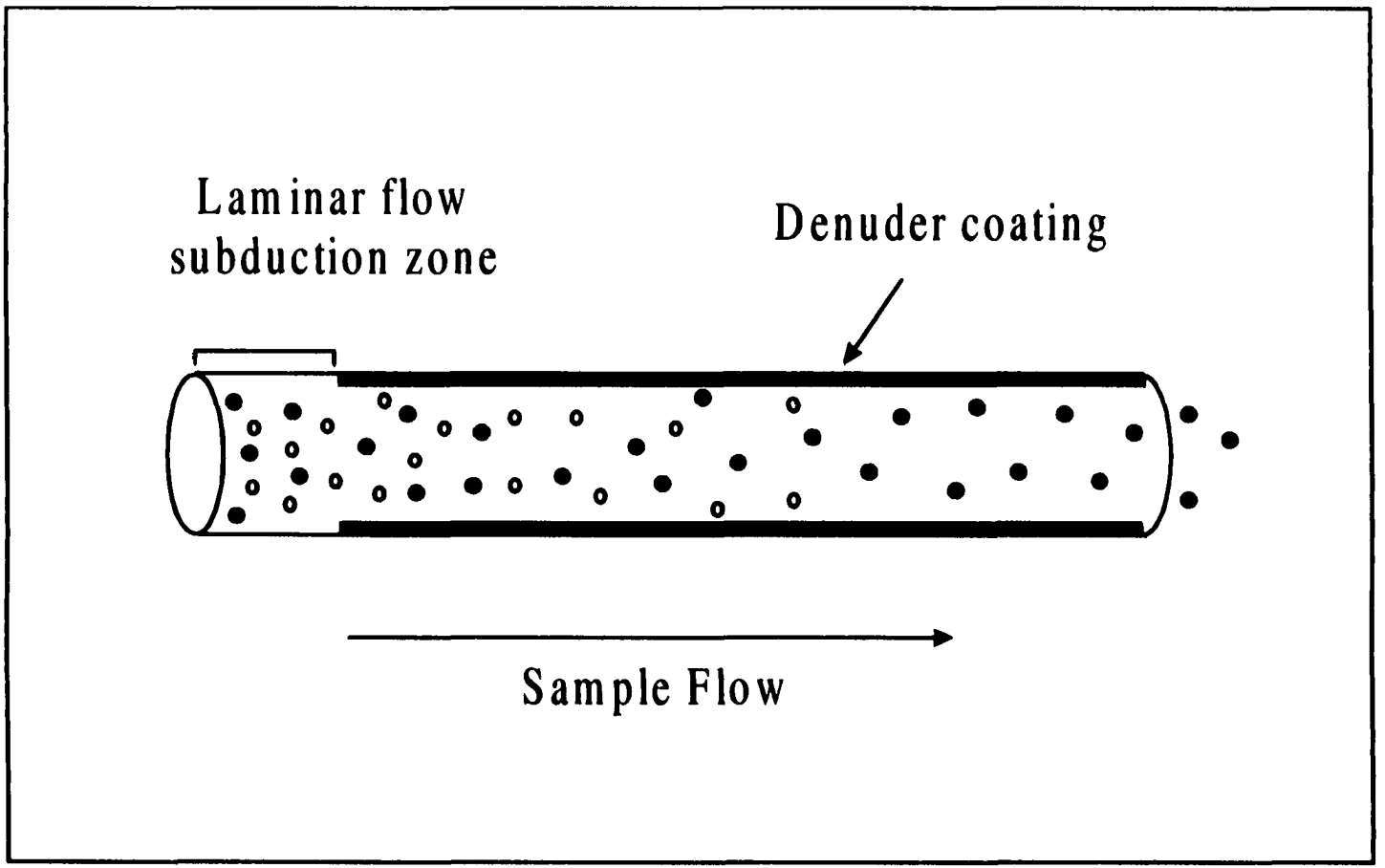

Figure 1.2 Schematic drawing of a diffusion denuder
The sample air enters the diffusion denuder from the left, where laminar low is established. The analyte gas, represented by the yellow circles, diffuses to the inner surface of the denuder tube. when the analyte gas comes in contact with the coated surface, it reacts instantaneously and irreversibly with the substrate and is removed from the sample air. The other molecules within the air sample pass through the diffusion denuder unaffected.

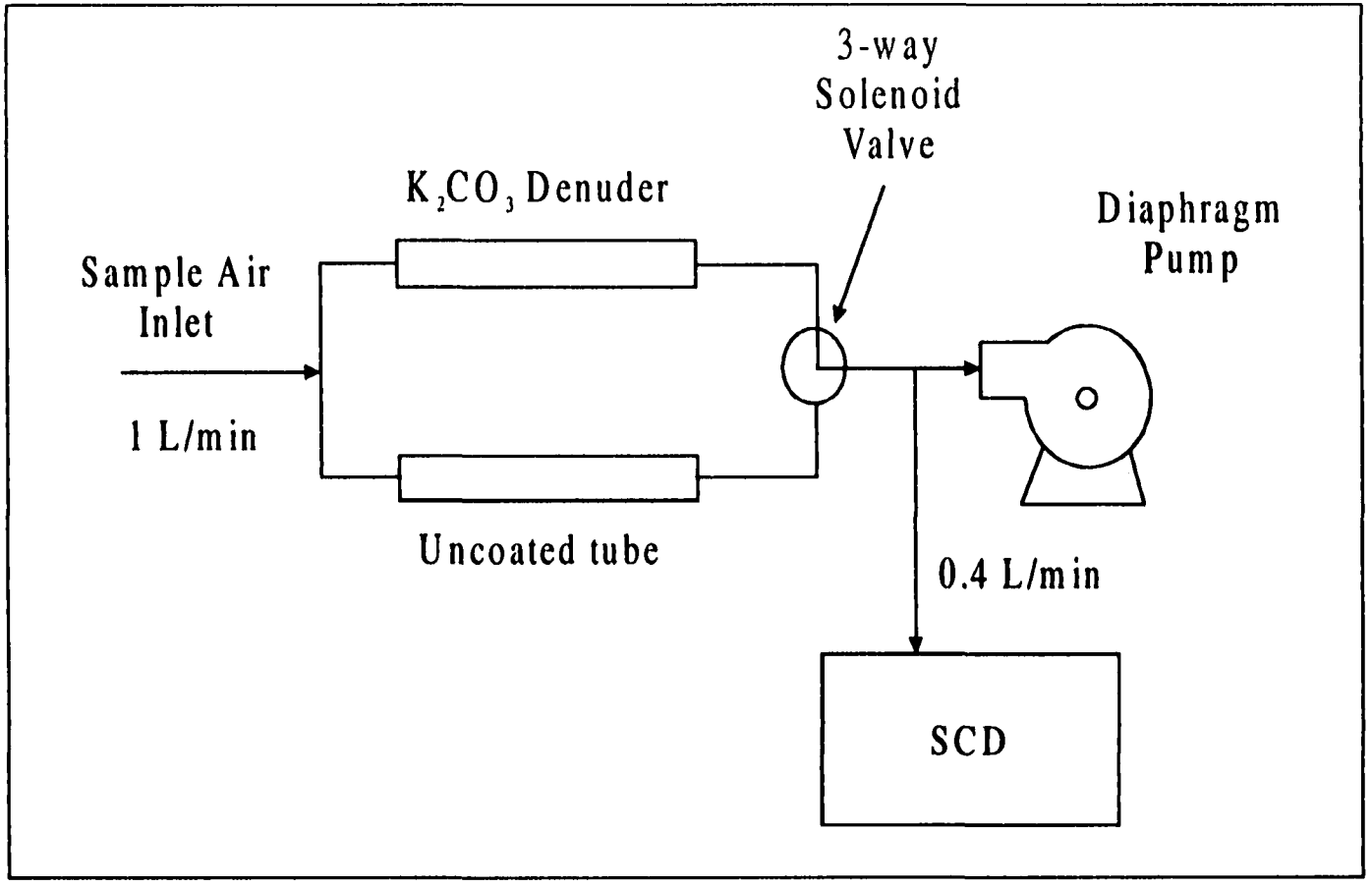

Figure 1.3 Schematic diagram of an early prototype of the DD/SCD
The sample air is drawn into the denuder manifold. A 3-way solenoid valve alternately directs the sample flow through either a carbonate coated diffusion denuder or an uncoated tube of the same dimensions and material as the diffusion denuder. The carbonate denuder seleetively and quantitatively removes sulfur dioxide, whereas the uncoated tube does not. This results in a modulation in the SCD response, between the air scrubbed of sulfur dioxide exiting the carbonate denuder (low response) and the air exiting the uncoated tube (high response). The amplitude of the modulation is proportional to the sulfur dioxide mixing ratio of the sample air.

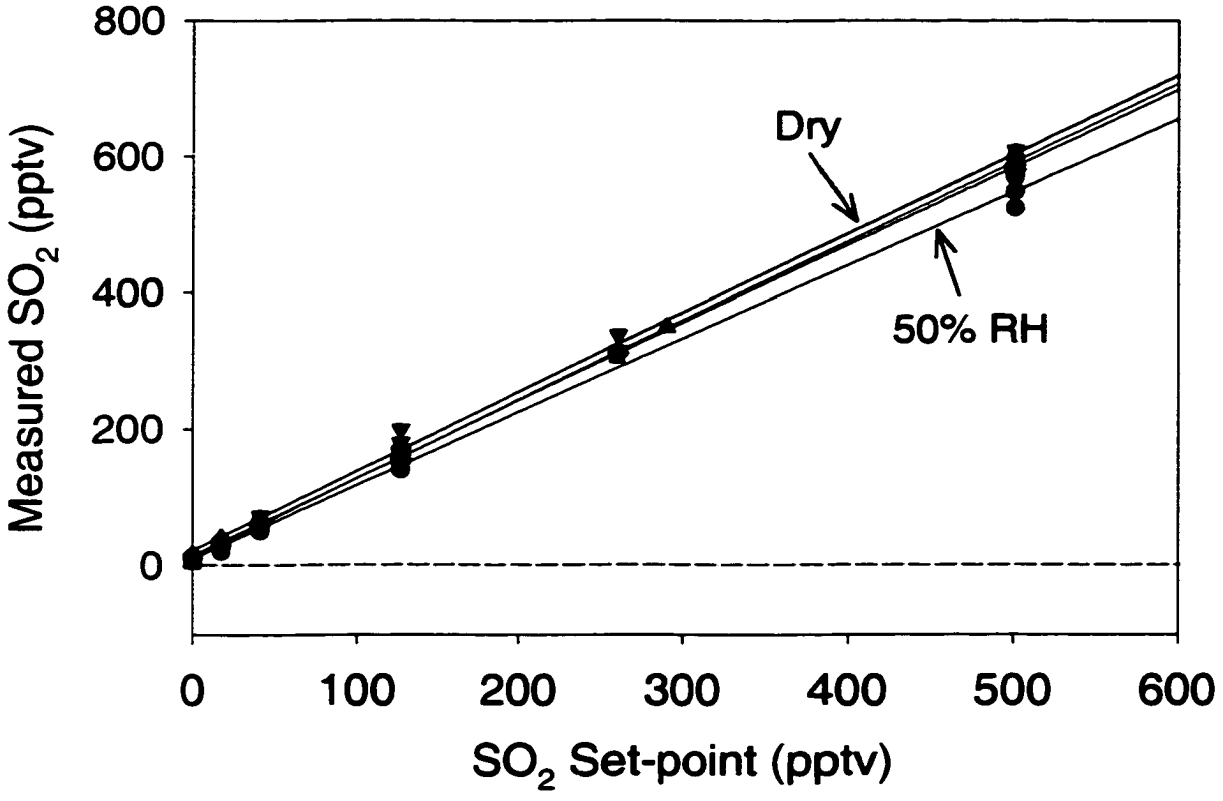

Figure 1.4 A summary of results from the Gas-Phase Sulfur Intercomparison Experiment (GASIE)
This summary of the results from GASIE is presented as an average of the measured SO_2 from each of the instruments evaluated (DD/SCD results have been omitted) compared against the SO_2 set-point. The measurements from each of these techniques correlated well. The different regression lines in the graph represent different measurements in different sample air matrices. Except for the 50% relative humidity sample air matrix, there is no significant difference between the response from each of the other sample air matrices. These results demonstrate a significant improvement since the CITE3 mission.

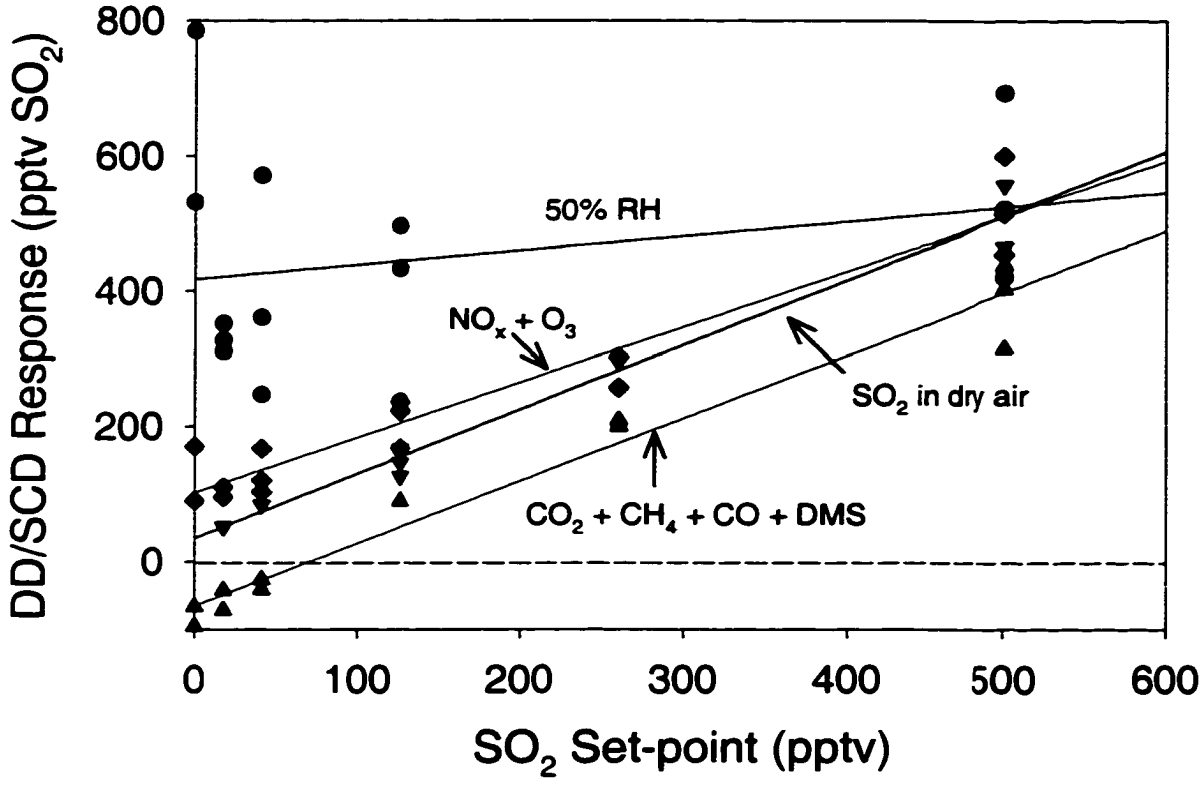

Figure 1.5 Results from the DD/SCD during GASIE
The DD/SCD results from GASIE demonstrate serious problems with water vapor and some minor problems with the sample air containing DMS and NO_x. The sample air containing no interfering gases did correlate well with the other techniques evaluated in GASIE. This demonstrated that the DD/SCD could prove to be a successful technique, if the interference problems could be resolved.

Chapter 2

Summary of GASIE-2, a rigorously blind evaluation of the Diffusion Denuder Sulfur Chemiluminescence Detector (DD/SCD) for low pptv SO_2 measurements[1]

Abstract:

The Diffusion Denuder/Sulfur Chemiluminescence Detector (DD/SCD) is a relatively new technology for making sulfur dioxide measurements in ambient air down to low part-per-trillion levels. Previously reported results with this technique revealed a large interference from water vapor and smaller interferece to other gases [Stecher et al., 1997]. The work described here is the result of a second rigorously blind evaluation of a redesigned DD/SCD. The program is known as the Gas Phase Sulfur Intercomparison Experiment Phase 2 or "GASIE-2." The protocol developed for the first phase of the intercomparison (GASIE) in 1994, when 7 different analytical systems were intercompared, was adopted for this work to ensure results would be comparable. The DD/SCD continuously measured a synthetically prepared mixture of SO_2 in air containing controlled levels of other matrix gases during a series of 90 min periods. During each 90 min sample period, the DD/SCD measured the difference in response between the sample air containing SO_2 and the same air scrubbed of SO_2 via a diffusion denduer. The differential response resulted in 6 to 7 determinations of the SO_2 mixing ratio for each

---

[1]Nicks Jr., D. K., L. Bamesberger, R. L. Benner, D. Crosley, S. O. Farwell, P. Goldan and D. MacTaggart, submitted to: *Journal of Geophysical Research*, 1999.

sample period. Sulfur dioxide mixing ratios used during the experiment ranged from 0 to 200 pptv. Other matrix gases included water vapor at 0 or 75% relative humidity, nitrogen oxides, dimethylsulfide, ozone, carbon monoxide, carbon dioxide and methane. The results reported here show that the DD/SCD performed on par with all of the techniques validated during GASIE. The serious interference from water vapor has been significantly reduced and none of the other matrix gases affected the detection of SO_2. A small but statistically significant change in the slope and intercept was seen between dry and moist air, although this could not be attributed to either the DD/SCD or the test gas delivery system. The DD/SCD could also distinguish 0 pptv from 20 pptv on any given day during the experiment.

Introduction:

Sulfur dioxide is an important trace gas in the atmosphere. It affects the environment directly through dry deposition and indirectly through its oxidation products, such as sulfuric acid (H_2SO_4). Sulfuric acid is an important contributor to acidity of precipitation. The effects of H_2SO_4 on biogeochemistry range from weathering of rock and the release of nutrients and soil minerals to formation of cloud condensation nuclei and climate change [Shaw, 1983, Charleson et al., 1987; Schlessinger, 1991, Shaw et al., 1998]. Sulfur dioxide is a major intermediate species in atmospheric oxidation of reduced biogenic sulfur gases. Anthropogenic emissions of sulfur to the atmosphere are primarily in the form of SO_2 [Cullis and Hirschler, 1980]. Estimates of the global sulfur budget

suggest that anthropogenic sources are comparable to all natural sulfur emissions combined [Andreae, 1986; Cullis and Hirschler, 1980]. Since sulfur sources are so diverse, the ability to reliably measure SO_2 in both polluted and unpolluted environments is critical to understanding the cycling of this gas through the atmosphere and its effect on Earth's complex and dynamic climate and biogeochemical systems.

Sulfur dioxide mixing ratios in polluted environments are frequently upwards of 50 parts per billion by volume (ppbv) [Brimblecombe, 1996] and have been reported to be as high as hundreds of ppbv near industrial centers [Sram et al., 1996]. In the unpolluted environment, ambient SO_2 mixing ratios are frequently 10-100 parts per trillion by volume (pptv) [Seinfeld and Pandis, 1997]. Obtaining meaningful and reproducible measurements of mixing ratios that range over five orders of magnitude has been a challenge to the atmospheric chemistry community especially when mixing ratios are less than 500 pptv. Over the past 10 years, several techniques with analytical capabilities within this range have been developed. These techniques include a pulsed fluorescence technique [Luke, 1997], high-performance liquid chromatography (HPLC)/fluorescence [Gallagher et al., 1997], mist chamber/ion chromatography (IC) [Talbot et al., 1997], diffusion scrubber/IC [Kok, et al., 1990], aqueous chemiluminescence [Jaeschke et al., 1997], isotope dilution-gas chromatograph (GC)/mass spectrometer (MS) [Bandy et al., 1993], a carbonate filter/IC [Ferek et al., 1993] and the diffusion denuder/sulfur chemiluminescence detector (DD/SCD) [Benner et al., 1997]. Each technique has certain advantages and disadvantages and thus can be used in an application depending on costs, sampling

platform, desired temporal resolution and other factors. In 1989, NASA sponsored the Chemical Instrumentation and Testing Experiment 3 (CITE3) to compare airborne measurements of SO_2 mixing ratios from several different techniques. The program included a series of flights to submit these techniques to both clean and polluted air. The results from this experiment demonstrated a lack of agreement between these state-of-the-art techniques, especially in ambient air where SO_2 mixing ratios were < 250 pptv SO_2 [Gregory et al., 1993].

In Fall of 1994, the National Science Foundation (NSF) sponsored the Gas-Phase Sulfur Intercomparison Experiment (GASIE)[Stecher et al.,1997] which incorporated seven instrumental techniques including some of the instruments tested during CITE3. In GASIE, the analytical techniques were submitted to various mixing ratios of SO_2 spanning 0-501 pptv along with several potential interfering gases added in known amounts to the sample matrices. The experiment demonstrated good correlation between the different techniques with few exceptions [Stecher et al., 1997]. One of the major findings in the GASIE study was that after one sample period in which water vapor condensed in the sample manifold, the DD/SCD response showed a dramatic effect from water vapor. The GASIE results demonstrated that in the presence of water vapor, some of the sample lines and fittings within the DD/SCD sample train appeared to be re-emitting previously adsorbed sulfur dioxide. This resulted in inaccurate response to SO_2 when the sample air matrix contained humidity. Further problems with the DD/SCD were discovered in GASIE during the tests containing potential interfering gases [Benner et al., 1997]. The

interference caused by the humid-air and NO_x/O_3 test gas matrices was explored in detail in the University of Alaska Fairbanks (UAF) laboratory after GASIE and was thought to be caused from permanent damage to the DD/SCD tubing after liquid water formed in the sample train [Benner et al., 1997]. Despite the problems encountered, the DD/SCD demonstrated good correlation with the other PI results in dry air samples [Stecher et al., 1997]. This correlation demonstrated the viability of the DD/SCD technique if the interference problems could be solved, and allowed the UAF group to identify and solve several problems with their new technique. Changes were made to the sample train set-up and materials, reducing surface effects and lowering residence time within the sample train. For details see Wu, [1995] and Benner et al., [1997].

The Gas-Phase Sulfur Intercomparison Experiment Phase 2 (GASIE-2) was conducted as a reevaluation of the DD/SCD in a rigorously blind experiment similar to the original GASIE. The Automated Sulfur Gas Dilution System (which for simplicity will be referred to in this paper as the delivery system) developed and maintained by S.O. Farwell's group at the South Dakota School of Mines and Technology (SDSM&T) was used during the retest of the DD/SCD. David Crosley of SRI International (SRI) and Paul Goldan of the NOAA Aeronomy Laboratory conducted independent oversight and analysis of the results of this experiment.

Experimental Setup:

Test Gas Delivery System:

The test gas delivery system was developed to deliver pptv-level SO_2 test gas mixtures within several synthetic gas matrices. The system successfully delivered SO_2 mixing ratios ranging from 0-501 pptv during GASIE [Stecher et al., 1997; MacTaggart et al., 1997] and was selected to deliver the test gas mixtures for the reevaluation of the DD/SCD in GASIE-2. The delivery system operated in the same manor as in GASIE, with the exception of the test gas flow rate, which was decreased from 100 slpm to 25 slpm [MacTaggart et al., 1997]. In GASIE, the higher flow rate was required to supply sample air for the seven analytical techniques. The SDSM&T group also measured the test gases to ensure the accuracy and precision of the test gas mixture during each sample period. The QA measurement scheme for the delivery system in GASIE-2 was identical to that described in GASIE [MacTaggart et al, 1997]. The test gas delivery manifold was nearly identical to that described by MacTaggart, et al., [1997] and Stecher et al., [1997]. The design ensured complete mixing and a uniform mixing ratio of the test gas sample. Residence time of the test gas within the sample manifold was less than 1 s to minimize surface interactions.

GASIE-2 Design and Procedure:

The design of this experiment was modeled after GASIE, so that the conclusions from each experiment could be compared. Some changes in the experimental set-up were made based on the results of GASIE. A summary of experimental differences between GASIE and GASIE-2 are listed in Table 1. In particular, the range of SO_2 mixing ratios in

this experiment was reduced from 0-501 pptv to 0-200 pptv because none of the instruments evaluated had problems with mixing ratios greater than 500 pptv. The potential interfering gas species and their mixing ratios were kept the same with the exception of water vapor which was increased from 50% relative humidity (RH) to 75-80% RH. The higher relative humidity in the sample matrix used in this work made for a more rigorous evaluation, which was appropriate given the problems caused by humidity with the DD/SCD during GASIE.

The number and make-up of the test gas mixtures were chosen to efficiently evaluate the DD/SCD. Four SO_2 mixing ratios and SO_2-free air were delivered for analysis several times during each sample matrix. This provided a statistically meaningful number of replicates and allowed an evaluation of precision between sampling periods. The sampling schedule consisted of 4-5 90-min long sample periods per day with 30 min between each. Preliminary results from each day were submitted to the oversight committee the following day by both UAF and SDSM&T and neither group was aware of the other's results. The final results of the experiment were sent to the advisory within two months of the end of the experiment.

Analytical System:

The DD/SCD technique is conceptually straight forward; a schematic diagram of the technique is shown in Figure 1. Solenoid valve "A" controls the source of the sample air to the DD/SCD sample train. Air from the dilution system was set as the default

sample source, with air sampled from the test gas manifold only during sample periods. When sample air is drawn into the DD/SCD sample train, it immediately passes through a 1 m long counter-flow shell-and-tube Nafion® (Permapure, Toms River, NJ) drier. The first 25cm of the Nafion® drier was heated to 40° C to prevent condensation and the last 25cm was cooled to 0° C to improve the efficiency of the drier [Leckrone and Hayes, 1997]. The sample air is then continuously analyzed by the SCD. Solenoid valve "B" alternatively allows the gas to go directly to the SCD or diverts it through a carbonate coated denuder, where SO_2 is quantitatively removed from the sample [Ferm and Sjodin, 1985; Lindgren and Dasgupta, 1989]. Because the SCD is a linear detector, the magnitude of the resulting signal modulation is proportional to the SO_2 mixing ratio in air [Schorran et al., 1994; Wu, 1995; Benner et al., 1997]. The SCD draws a sample air flow of about 180 $cm^3 \cdot min^{-1}$. An auxiliary pump downstream from the SCD sample inlet increases the total flow through the manifold to about 800 $cm^3 \cdot min^{-1}$. The higher flow rate ensures the sample air residence in the sample train is less than 1 s. The entire DD/SCD sample train is constructed of PFA (perfluoroalkoxy) Teflon® (DuPont, Willmington, DE), excluding the Nafion® membrane in the drier and carbonate coated quartz denuder. PFA Teflon® is preferred for SO_2 measurement techniques because it minimizes surface interaction in the manifold. A more detailed account of the DD/SCD has been previously described [Benner et al, 1997].

During the intercomparison, the DD/SCD was calibrated with a custom built dynamic dilution system. This dilution system is capable of dilution factors up to 10^6 with

a relative error of < 1%. It was used to perform single point calibrations during the 30 min period between sampling periods to check the instrument response throughout a test day. Automated multi-point calibrations of the DD/SCD were also conducted overnight, between testing days using the computer controlled dilution system. The calibration gas standard used in the dynamic dilution system was 0.98 ppmv SO_2 in air (Scott Marrin, Riverside, CA) certified NIST traceable by the manufacturer to have an accuracy of ± 5%. The standard gas flow rate was regulated by a crimped stainless steel capillary tube pressurized to 20 psig. The calibration gas flow into the dynamic dilution system was measured in triplicate 5-6 times a day with both a manual bubble meter (Hewlet Packard (HP), Palo Alto CA) and Gilibrator (Sensidyne-Gillian, Clearwater, FL) automated bubble meter. Room temperature and pressure were recorded with a Climatronics weather sensor package, model 102254 (Climatronics Corporation, Bohemia, NY) to convert the bubble meter flow data to standard conditions. The Gilibrator was calibrated volumetrically and the HP bubble meter was calibrated both volumetrically and gravimetrically with water. Analysis of the measured flows from both the HP bubble meter and Gilibrator show a nearly Gaussian distribution about a mean of 10.35 sccm with a 99% confidence limit of ± 0.4% throughout the duration of the 5-week experiment.

The source of SO_2-free air used in the dilution system was compressed breathing quality (BQ) air (Air Products, Allentown, PA) which underwent a 2-stage chemical scrubbing optimized to remove sulfur gases. The first stage of the scrubber was a packed bed of Purifil (Purifil Inc., Doraville, GA), followed by a packed bed of Puricarb (Purifil

Inc.). The zero air was then filtered with a 47 mm Teflon® filter to remove particles.

Data acquisition and instrument control for the DD/SCD consisted of a 16 bit A/D board (MIO16x, National Instruments, Dallas, TX) in a desktop PC. The dynamic dilution system used a 12 bit A/D board (DAQ-Pad 12, National Instruments, Dallas, TX) via a parallel port to a laptop PC. Custom software was developed for both data acquisition systems using Labview development software (National Instruments, Dallas, TX).

Results and Discussion:

At the conclusion of the first week of the experiment, it was determined that there were some problems with the stability of the delivery system sample gas concentration during sample periods 1-20. During this time, the delivery system was operated using a compressed gas calibration source containing 1000 ppmv SO_2. The high mixing ratio of the standard gas source required the delivery system to operate close to its maximum dilution factor in order to supply test gases below 200 pptv SO_2 resulting in poor reproducibility of the test gas mixtures. The standard was changed to a 100 ppmv standard that provided a considerable improvement in the reproducibility of the set-point throughout sample periods 21-66. As a result of the reproducibility problem with sample periods 1-20, only sample periods 21-66 were used in the analysis of the GASIE-2 results. The results from sample periods 21-66 are listed in Table 2.

Due to sensitivity problems with the QA measurements for the delivery system, the

DD/SCD measured mixing ratios for each sample period were compared to the delivery system set-point. This differs from the original GASIE intercomparison, where the delivery system QA measurement data were used as the independent variable during analysis. Figure 2 shows the delivery system set-point and the corresponding DD/SCD measurement of SO_2 for each sample period and demonstrates that the set-point is included within one standard deviation of the measurement for 64% of the measurement periods. Figure 3 shows regressions of DD/SCD vs: set-point for each sample matrix delivered during the experiment. Again, these data show good correlation between the delivered and measured mixing ratios over the entire range of set-points and for all sample gas matrices.

The original delivery system set-points for GASIE-2 were corrected because of inaccuracies in the dilution factors provided by the proportioning valve dilution apparatus (PVDA, MacTaggart et al., 1997) within the test gas delivery system. These inaccuracies could not be tracked during the course of GASIE-2 because the SDSM&T quality assurance analytical systems were experiencing temporary sensitivity problems. After the end of GASIE-2, these sensitivity problems were fixed. While SDSM&T was still blind to the DD/SCD results from GASIE-2, the SDSM&T quality assurance system was used to re-measure all the original GASIE-2 delivery system set-points. These re-measurements were reported to the Advisory Committee as the corrected delivery system set-points. These corrected set-points then became the basis for statistical comparison with the DD/SCD results.

In the test gas delivery system, the zero SO_2 test gas mixtures were made by shutting off any calibration gas flow to the dilution system. The result was a 0 pptv SO_2 set-point with a significantly better precision than that of the lower (<50 pptv SO_2) set-points, which biased the slope of the regressions. For this reason, the sample periods with a 0 pptv SO_2 set-point were removed from the data set. The resulting slopes and intercepts of combined sample periods from each of the matrix categories with and without the 0 pptv set-points are summarized in Table 3.

The regression lines in Figure 3 and results listed in Table 3 show excellent agreement between the delivery system set-point and DD/SCD during GASIE-2. During dry air sample periods, the regression line shows a slope of 0.99 and high correlation (r^2 = 0.99). The small, negative y-intercept from the regression (-8 pptv SO_2) may be the result of differences in the ability of each group to prepare SO_2-free air in their calibration systems. In the humid air test segments, the regression again shows excellent correlation ($r^2 = 0.99$). The slope of the regression line was 0.89 with y-intercept of 4 pptv SO_2. There was a small but significant difference between the slopes and intercepts of the wet and dry sample runs. Unfortunately, the delivery system QA data did not have the sensitivity to discern whether the change in slope was due to the test gas delivery system, the manifold, or an interference within the DD/SCD. The test segments with a sample air matrix containing 100 ppbv O_3 and 10 ppbv NO_x, showed a high correlation with the delivery system set-point ($r^2 = 0.99$) with a slope of 1.07 and an intercept of negative 10 pptv SO_2. DD/SCD measurements with the matrix containing CO_2, CH_4, CO and DMS

also showed high correlation with the delivery system set-point ($r^2 = 0.99$) with a slope of 1.01 and a small negative intercept (- 6 pptv SO_2). The slope and intercept for these two sample matrix compositions were not statistically different from those observed with dry zero air and therefore show no discernable effects from these matrix gases.

Precision and Accuracy:

In assessing the precision and accuracy of the DD/SCD, it is important to note that the variability within the reported DD/SCD measurements is a combination of the variability of the mixing ratio of the synthetically produced sample gas and the variability of the DD/SCD measurement. Since the variability of the delivery system set-point mixing ratios between-sample periods and within a single 90 min sample period could not be determined directly, the precision figures reported from GASIE-2 reflect the pooled variability of both the delivery system and DD/SCD detection systems.

The reproducibility of the set-point mixing ratios was investigated by looking at the precision of the DD/SCD measurements. Since this estimate of reproducibility includes variability from both the DD/SCD instrumental technique as well as the variability in the mixing ratio of the sample gas, this estimate represents the maximum variability in reproducing set-point mixing ratios. A graph of the standard deviations of measured values with respect to the set-point mixing ratio is shown in Figure 4 and show a general increase with increasing SO_2 mixing ratio. The absolute error in the set-point mixing ratios increases with higher SO_2 mixing ratios. However, the relative error improves to

about ± 6% at 182 pptv SO_2, for the combined delivery system and DD/SCD detection system.

The variability of the SO_2 mixing ratio produced by the delivery system within the 90 min sample period was investigated by using the standard deviation of the DD/SCD measurement. During each sample period, the DD/SCD completed between 5 and 7 complete measurement cycles. The standard deviation of these measurements would include variability from both the measurement and the delivery system, and represents a maximum variability for the delivered SO_2 mixing ratio. The graph in Figure 5 shows the standard deviations with respect to delivery system set-point. The graph demonstrates that the mixing ratio of SO_2 is fairly constant within each 90 minute sample period. The two points with the highest variability were for the 182 pptv set-point. It is important to note that although the absolute variability for these two points may be high, the relative variability is still better than ±10% of the set-point. A linear least squares fit of all the standard deviations shows a average variability of about ± 8 pptv over the entire range of set-points. A constant absolute variability results in higher relative variability for low mixing ratio set-points. This is consistent with the decision to omit the 0 pptv SO_2 set-point due to the high precision of that point which biased the slope of the regressions.

The within-sample period precision and set-point reproducibility as determined by the pooled or combined variability from the delivery system and DD/SCD are summarized in Table 4. The precision and reproducibility of the delivery system set-point was previously determined in GASIE to be at least ± (1.5 pptv + 1.5% of the set-point) and ±

(7 pptv + 2% of the set-point), respectively [Stecher et. al., 1997]. These precision estimates were based on the instrumental techniques evaluated in GASIE that demonstrated the least amount of variability. The logic being that the precision of the delivery system would be represented in the results from all of the instrumental techniques. The instrument with the best precision would define a maximum variability for the dilution system. Using this same logic, the within-sample period precision of the delivery system in GASIE-2 was ± (7.5 pptv + 0.3% of the set-point) and the reproducibility of the set-point was ± (5 pptv + 4% of the set-point).

Although the regression lines between delivery system set-point and DD/SCD measured SO_2 mixing ratio were close to unity, no conclusions regarding accuracy could be made. There is no broadly recognized standard technique for measuring or creating known mixing ratios of SO_2 at these low levels.

Detection Limit:

A single factor analysis of variance (ANOVA) was performed on the daily and day-to-day results. The results show that on any day the delivery system and DD/SCD detection systems can distinguish 0 pptv from 20 pptv and 20 pptv from 40 pptv. The day-to-day variability is larger, but the delivery and detection systems can distinguish 0 pptv from 30pptv and 30pptv from 60 pptv on different days. The detection limits from the analysis were as good as the best analytical techniques evaluated in GASIE. It is important to note that this evaluation of detection limit contains a combined variability

from both the DD/SCD measurement technique and the delivery system, and therefore is a worst case scenario for either. Presumably, each of these techniques has a detection limit better than the combined estimate stated here, based on these results.

Choice of independent variable:

A significant difference between the analysis performed on the data from GASIE and GASIE-2 was the choice of the independent variable used to evaluate the instrumental techniques. In GASIE, the delivery system QA measurements were used as the independent variable for a comparison against the mixing ratios reported by the various instrumental techniques. In this experiment the delivery system QA measurements did not have the sensitivity needed for a good comparison so the delivery system set-point was used instead. Had the delivery system QA information been available for use as the independent variable, any artifact in sample preparation or delivery resulting in loss of SO_2 within the delivery system apparatus and/or manifold would be reflected in both the QA and DD/SCD results. Likewise, any residual SO_2 in the zero air used to dilute the sample gas would also be accounted for. Since the delivery system set-point was used as the independent variable, residual SO_2 in the dilution air or changes in the sample gas mixing ratio within the sample manifold could not be determined. Any deviation from the ideal values of slope or y-intercept of 1.0 and 0 pptv respectively, would be interpreted as an interference in the DD/SCD when in fact, the sample manifold might be the cause of the non-ideal behavior.

Small but significant non-zero intercepts in both the dry and humid air samples and a small effect on the slope of the humid air samples are indicated in the data. As stated previously, these effects could not be directly attributed to either system because sample gas QA measurements were not available. Since the DD/SCD has shown no interference in either slope or intercept with these matrices as previously tested [Benner et al., 1997; Wu, 1995], the small but significant effects may have been a result of problems with the test gas delivery manifold that were not accounted for in using the delivery system set-point as independent variable.

Since the manifold design was based on the design used in GASIE, an evaluation of GASIE data using delivery system set-point instead of QA measurement may offer evidence of sample gas degradation within the delivery system. To ease the analysis of this large data set and normalize spurious results from any one instrumental technique, the principal investigator (PI) instrument responses were pooled as an average response to each of the delivery system test gas sample periods during GASIE. Instruments that demonstrated problems with the sample matrices used in GASIE were not used in this PI average. The instrumental techniques omitted from the average were the filter/IC during any sample periods containing humid air and the DD/SCD for all of the sample periods in GASIE. First, the PI averaged data was compared against the delivery system QA measurements. The group of measurements from each of the potentially interfering gas matrices was compared to dry air (control) measurements. A divergence in the slope or intercept for the sample periods containing potential interfering gases would indicate an

effect of the gas matrix within the manifold or a common measurement problem. Since the comparison involves five different analytical techniques, the probability of all five detectors demonstrating a similar interference problem is low. Thus a manifold effect would be more likely. In comparing the PI averaged measurements with the delivery system QA measurements, the regressions of each of the sample air matrices had similar slopes and intercepts when compared to the control sample periods (ie interference-free dry air). This supports the conclusions of GASIE that these instruments showed no significant interference from these matrix gases and demonstrates the viability of the PI average as a robust statistic for comparison.

The same analysis was conducted using delivery system set-point as the independent variable. The analysis shows no significant effect from all potentially interfering gas matrices, except for the periods with humidity. The plots in Figures 6 and 7 demonstrate the effect that choice of the independent variable has on the slope and intercept. A comparison of PI average verses delivery system QA measurement (the independent variable used in GASIE) in Figure 6 shows no difference in slope between the response during dry air control and humid sample periods. The comparison of PI average verses delivery system set-point (the independent variable used in GASIE-2) in Figure 7 shows a decrease of 6% in the slope for sample periods containing 50% relative humidity when compared to the dry air periods. This small but significant change in slope is consistent with the effects of surface losses of SO_2 within the delivery system manifold when humidity is part of the sample matrix.

The change in slope from the use of the delivery system set-point instead of the QA measurements should be considered in the interpretation of data from the DD/SCD during this experiment. This consideration does not change the general conclusions, which demonstrate that the DD/SCD is a successful and robust SO_2 detection system and that the delivery system has the ability to generate low pptv sample gases with a high degree of precision. However, the results do suggest that actual measurement of the analyte after passing through the sample manifold is necessary to ensure that potential wall effects are properly accounted for. For this reason, we must qualify the conclusion that a small but significant effect in response was observed from the samples containing humidity.

During GASIE-2, the PVDA within the test gas delivery system demonstrated inaccuracies similar to those experienced during GASIE. Between these two experiments, newly designed Teflon mixing chambers were machined and installed within the PVDA. This change solved the gas leakage problems experienced during GASIE [MacTaggart et al., 1997]. However, the dilution inaccuracy problems remained. In fact, they became worse when the total delivery system flow was decreased from 100 to 25 slpm. This observation, along with the observation that PVDA dilution error increased with decreased total delivery system flow, prompted the change of the delivery system source cylinder from nominally 1000 ppmv SO_2 to nominally 100 ppmv.

The behavior or the PVDA has been more thoroughly investigated since the analysis of the GASIE-2 data set. This work has pinpointed four primary factors as

responsible for the observed inaccuracies: (1) back-diffusion of vent lines into output lines, (2) zero point drifts of the output and vent pressure gauges, (3) uncontrolled pressure differentials at the first two stages of the three-stage PVDA, and (4) nonequivalent and/or nonideal valve switching behaviors. These problems have been recently ameliorated through changes in plumbing configuration, replacement of the output and vent pressure gauges with a high-precision differential pressure gauge, and installation of calibrated pressure restrictors at each of the first two stages of the PVDA. Subsequent experiments with this modified PVDA at SDSM&T have demonstrated that accuracies of 2-3% for the PVDA dilution factors utilized during GASIE and GASIE-2 are now achievable. Details on this work will be published in a separate paper.

Conclusions:

This experiment was specifically designed to re-evaluate the DD/SCD for interferences found in the previous intercomparison. This re-evaluation was more rigorous in that the range of SO_2 mixing ratios was considerably lower and the relative humidity used was considerable higher than that used in the previous experiment. The results of this work demonstrate that the previous problems with the DD/SCD technique have been solved. The effects from water vapor were minimal if not eliminated altogether, and no interferences from NO_x, O_3 and DMS, CO_2, CO, CH_4 in the sample matrix were detected. The modifications and improvements to the DD/SCD sample train and analytical technique have greatly improved the instrument's precision and limit of

detection. The precision and limit of detection reported in this work is comparable to the best techniques evaluated in the GASIE.

Table 2.1 Summary of experimental conditions for both GASIE and GASIE-2.

	GASIE	GASIE-2
SO_2 Mixing Ratios (pptv)	0, 18, 41, 127, 260, 501 pptv*	0, 27, 37, 66 and 182 pptv*
Relative Humidity (RH)	50% RH	75% RH
CO_2 CH_4 CO DMS	350 ppmv CO_2 2 ppmv CH_4 120 ppbv CO 100 pptv DMS	No Change
NO_x O_3	10 ppbv NO_x 100 ppbv O_3	No Change

* Set-points used for the delivery system, other mixing ratios were also delivered to test the calibration set-up of the delivery system throughout the experiement.

Table 2.2 Tabulated results for the DD/SCD during GASIE-2

GASIE-2 mean SO_2 mixing ratios, within-sample standard deviation and replicates for sample periods 21-66.

Date	Run	Set-point	Matrix	DD/SCD	STD	Reps	Comment:
25-May	21	37	Z	31	7.6	7	
25-May	22	182	Z	180	6.4	7	
25-May	23	137	Z*	135	12	6	
25-May	24	48	Z*	47	10	7	
26-May	25	0	Z	0	9.4	7	
26-May	26	19	Z	15	5.7	7	
26-May	27	29	Z	27	11.7	7	
26-May	28	182	Z	179	7.4	7	
28-May	29	37	W	55	11	6	DD/SCD manifold flushing SO_2.
28-May	30	27	W	25	4.5	7	
28-May	31	182	W	158	11.4	7	
28-May	32	66	Z	61	6	7	
29-May	33	66	W	67	5.8	7	
29-May	34	0	W	5	5.7	6	
29-May	35	37	Z	21	11.4	7	
29-May	36	27	W	19	4.4	7	
30-May	37	27	Z	25	9.1	7	
30-May	38	182	W	169	4.3	7	
30-May	39	66	W	71	6.2	7	
30-May	40	37	W	39	8.9	7	
1-June	41	182	N	184	15.4	7	
1-June	42	27	N	18	8.5	7	
1-June	43	37	Z	21	8.7	7	
1-June	44	0	N	-2	8	7	
2-June	45	37	N	32	4.8	7	
2-June	46	182	Z	160	6.7	8	
2-June	47	27	N	16	5.7	6	
2-June	48	66	N	54	1	1	Power outage, acquired one measurement.
3-June	49	0	Z	-4	5	4	Zero-air compressor failure.
3-June	50	66	N	70	7	6	
5-June	51	27	C	15	10.7	8	
5-June	52	182	C	162	6.8	7	
5-June	53	66	Z	56	6.1	7	
5-June	54	37	C	24	8	7	
6-June	55	66	C	74	9.9	7	
6-June	56	37	Z	26	8.5	7	
6-June	57	182	C	190	4.9	8	
6-June	58	0	C	-1	6.5	7	
8-June	59	37	C	N/M	0	0	Power failure, no data.
8-June	60	0	C	-1	10.1	7	
8-June	61	66	C	63	6.5	5	
8-June	62	27	Z	12	2.9	6	
9-June	63	182	Z	179	4	6	
9-June	64	0	Z	0	7.7	7	
9-June	65	27	C	19	8.1	7	
9-June	66	37	C	34	3.5	6	

Matrix codes: Z = SO_2 in air; Z* = sample air supplied from SDSM&T calibration system; W = 75% RH; N = 10 ppbv NO_x + 100 ppbv O_3; C = 350 ppmv CO_2 + 2 ppmv CH_4 + 100 ppbv CO + 100 pptv DMS.

Table 2.3 Summary of regression results from sample periods with different sample gas matrices

	Including periods of SO_2-free air			Without SO_2-free air periods		
Matrix	slope	y-intercept (pptv)	r^2	slope	y-intercept (pptv)	r^2
Dry air	0.99	-5.9	0.99	1.01	-8.1	0.99
Wet air	0.95	-1.8	0.98	0.89	4.0	0.99
DMS,CO, CO_2, CH_4	1.0	-4.2	0.98	1.01	-6.3	0.98
NO_x, O_3	1.0	-7.5	0.99	1.07	-9.9	0.99

Table 2.4 Comparison of within-sample period precision and set-point reproducibility from GASIE and GASIE-2.

	GASIE		GASIE-2	
	Within Sample Period	Set-point reproducibility	Within Sample Period	Set-point reproducibility
Best Average:	1.5 pptv + 1.5%	7 pptv + 2%	N/A	N/A
DD/SCD	15pptv + 1.5%	-5.2pptv + 14%	7.5 pptv + 0.3%	5.0 pptv + 4%

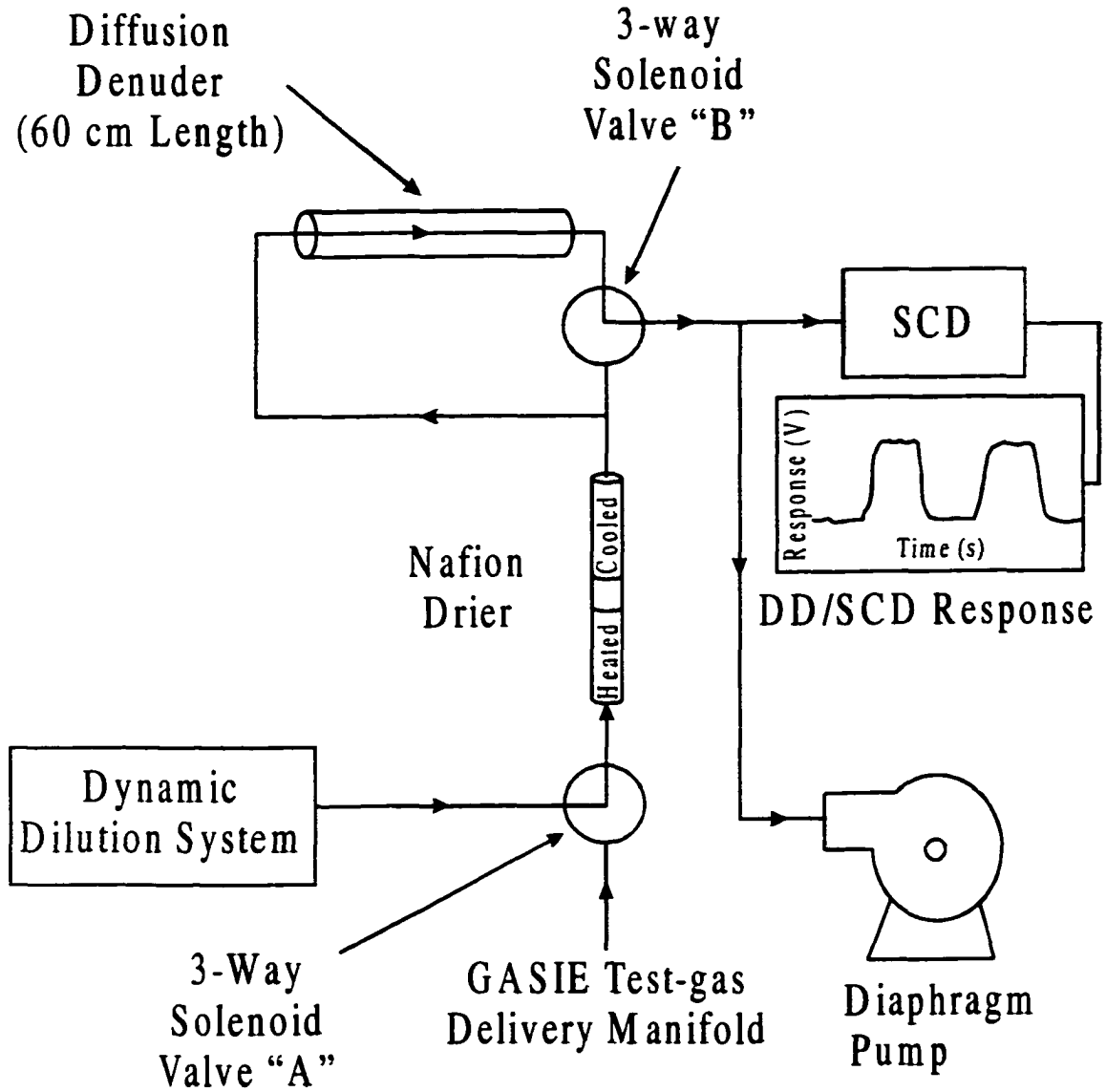

Figure 2.1 Schematic of the DD/SCD sampling system as used in GASIE
Air is sampled from either the GASIE test gas delivery manifold or the dynamic dilution calibration system via solenoid valve A. The sample gas is dried and directed to the SCD via solenoid valve B. The position of valve B selects a sample flow path either directly to the SCD or first through a denuder (for removal of SO_2). The switching of valve B results in a modulation of the SCD response, which is proportional to the SO_2 mixing ratio of the sample air.

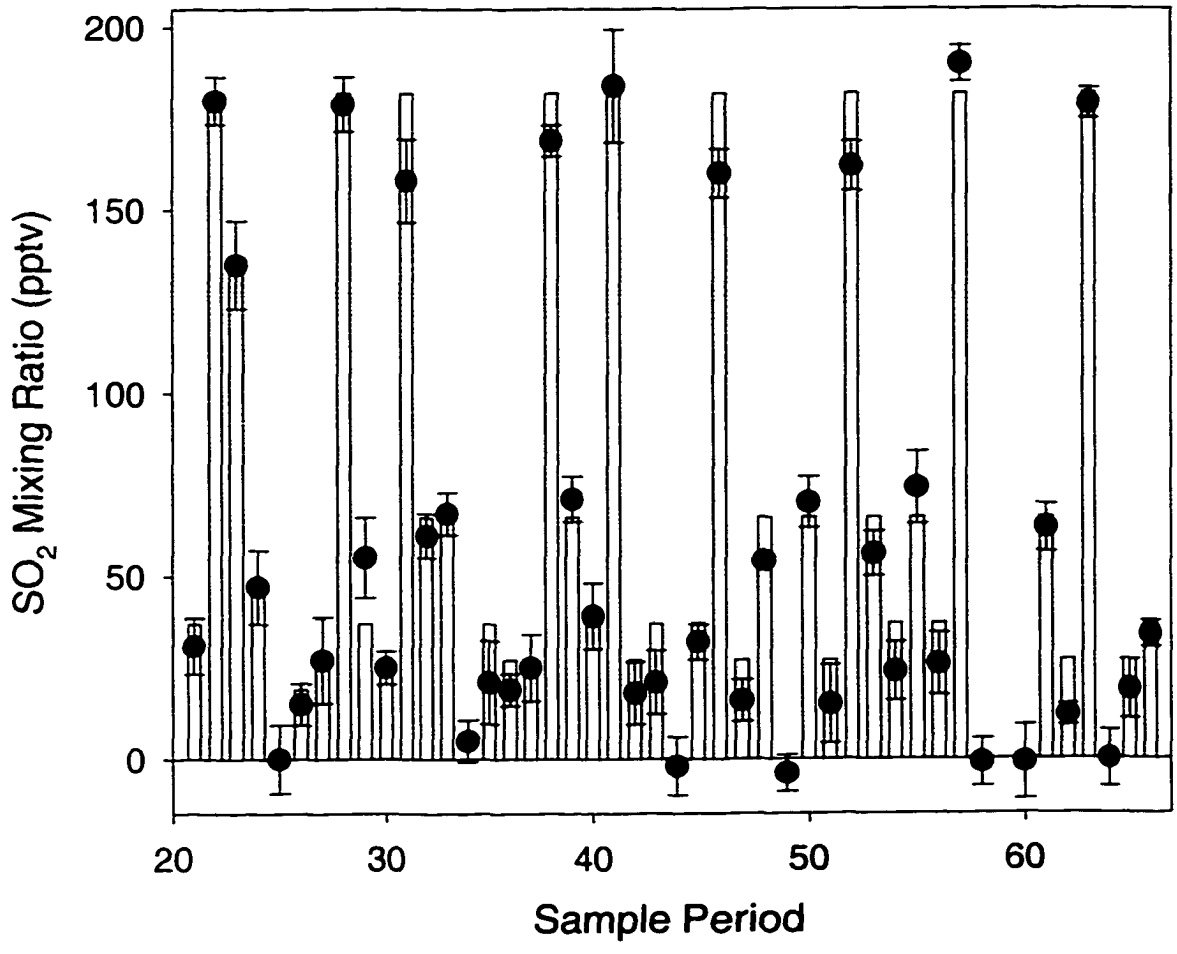

Figure 2.2 Comparison of the DD/SCD reported mixing ratio vs: delivery system set-point.
The dots represent the DD/SCD measurement with error bars representing ± one standard deviation. The bars represent the set-point mixing ratio as determined from the delivery system settings. The DD/SCD and delivery system demonstrate good agreement, with a majority of the DD/SCD measurements within one standard deviation of the set-point.

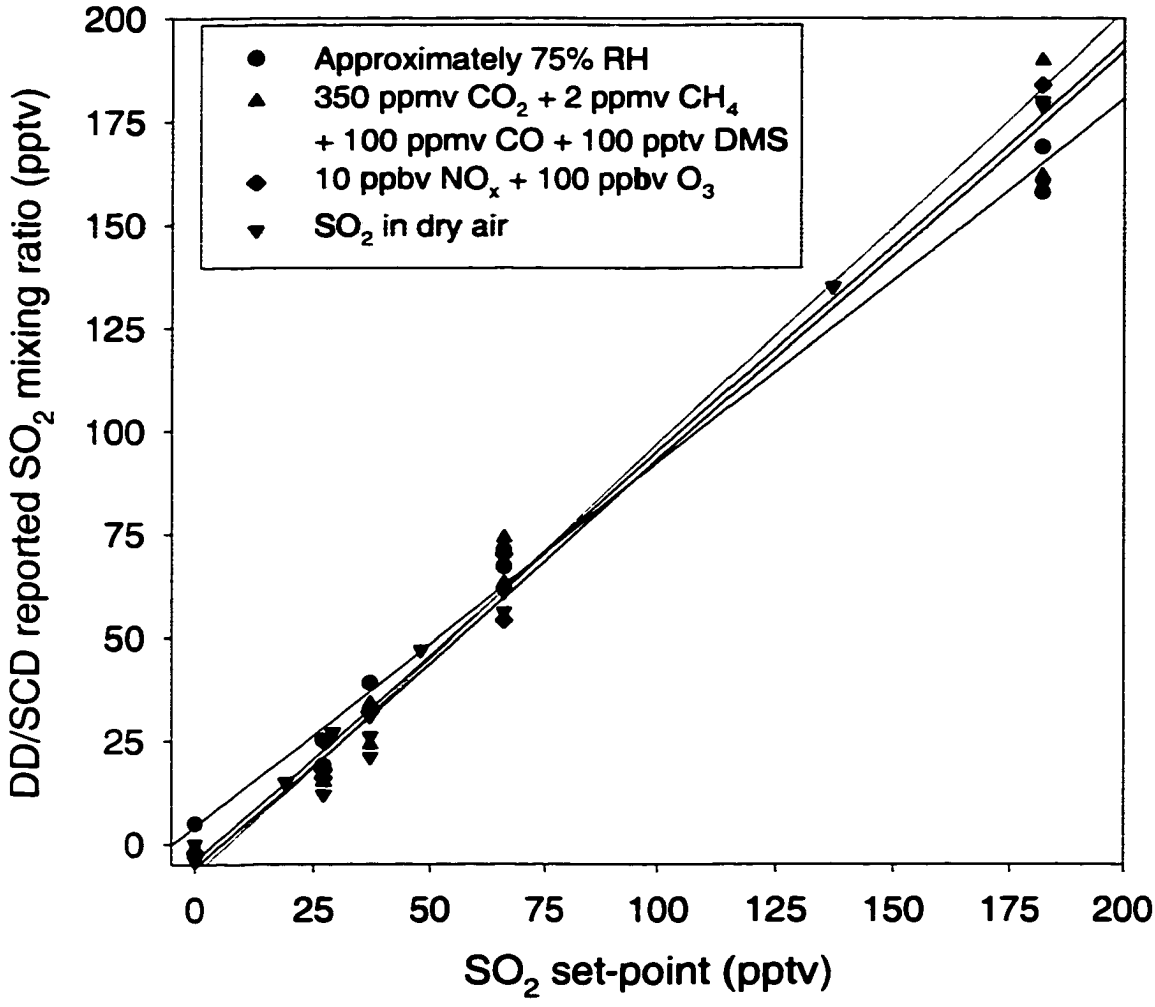

Figure 2.3 Graph of the DD/SCD reported mixing ratio and delivery system set-point separated by sample gas matrix.
The graph of the DD/SCD reported mixing ratio vs: the delivery system set-point demonstrates good correlation of the measurements from all sample gas matrices included in the experiment.

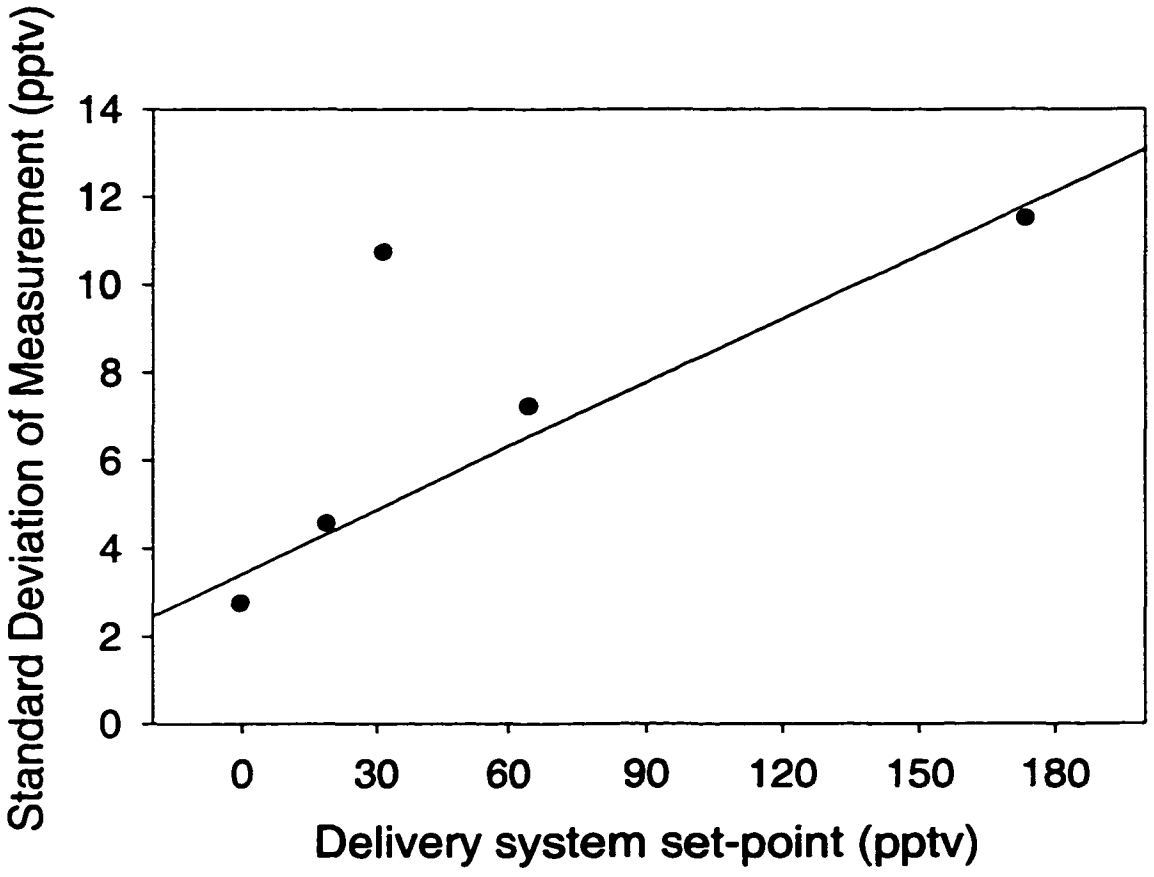

Figure 2.4 Reproducibility of the delivery system set-point during GASIE-2
The reproducibility of the set-point was determined by analyzing the standard deviation of the measurements for each of the set-points over the course of the experiment. The graph shows reproducibility is excellent, with absolute variability increasing with an increasing SO_2 mixing ratio.

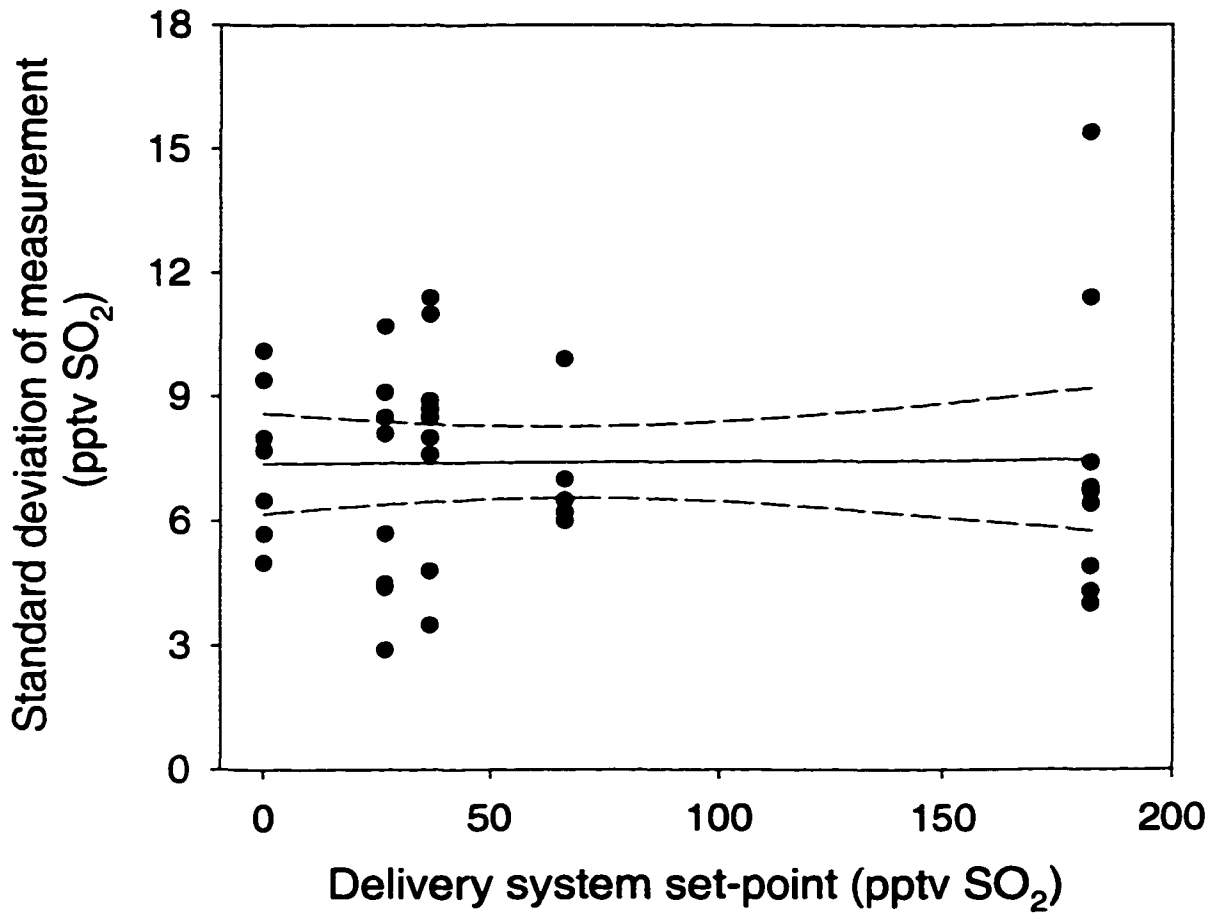

Figure 2.5 Variability of the delivery system SO_2 mixing ratio
A graph of the standard deviation of the measurement with regards to delivery system set-point demonstrates that SO_2 mixing ratio is fairly constant during the 90 minute sample period. The solid line is a linear least squares fit of the data and the dashed line represents the 95% confidence interval. The standard deviations include variability from both the DD/SCD measurement as well as the delivery system and represent a maximum variability for the test gas SO_2 mixing ratio for each set-point.

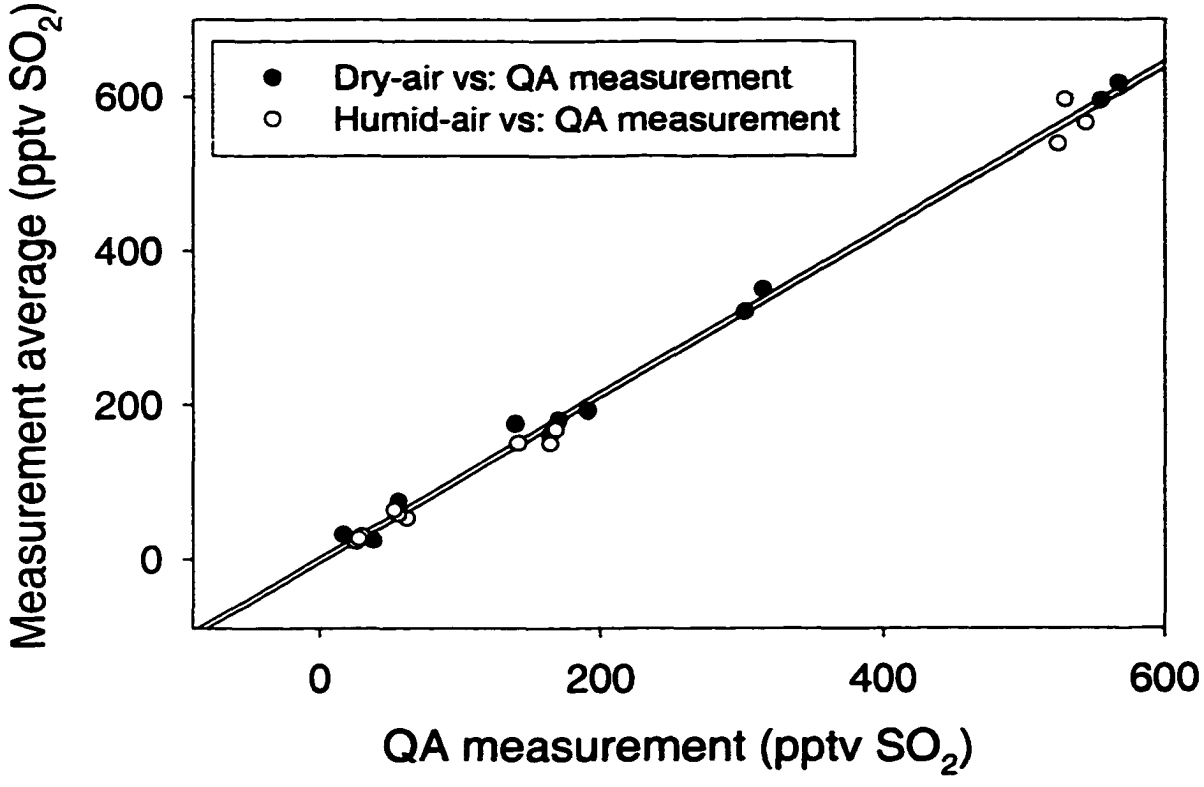

Figure 2.6 Comparison of dry control and humid air regressions vs: delivery system QA measurement during GASIE

A comparison of dry control and humid air regressions from the GASIE demonstrates negligible difference in slope due to water vapor, when the QA measurement is used as independent variable.

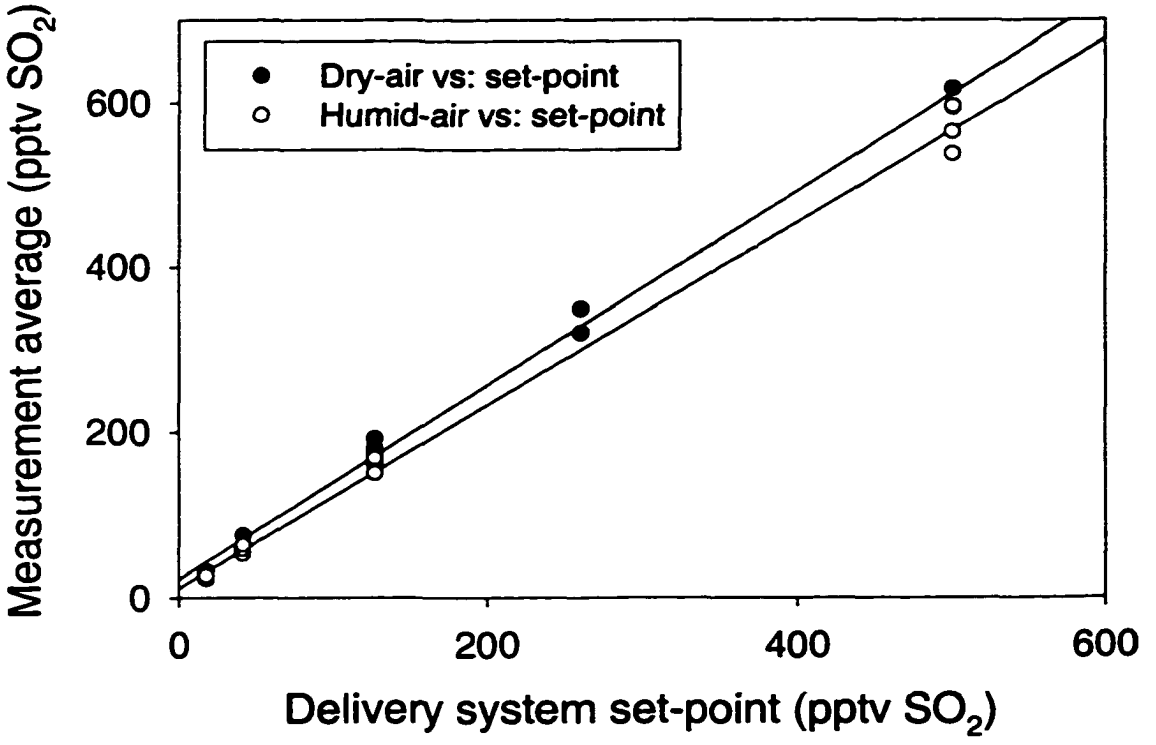

Figure 2.7 Comparison of dry control and humid air regressions vs: delivery system set-point during GASIE

A comparison of dry control and humid air regressions from the GASIE demonstrates a 6% decrease in slope from the addition of 50% relative humidity.

Chapter 3

A multi-stage dynamic dilution system for use with reactive gases

Introduction:

The desire for better sensitivity in the measurement of sulfur dioxide and other reactive trace gases in the atmosphere faces a number of challenges in analytical chemistry and instrument development. Measurement techniques aside, the challenge also involves the calibration of these new highly sensitive instruments. Results from the Gas-phase Sulfur Intercomparison Experiment (GASIE), a study that compared state-of-the-art SO_2 instrumentation demonstrate that although the measurement techniques compared well, there were major discrepancies among the different calibration methods used [Stecher et al., 1997]. These discrepancies suggest that either the commercially available standards are not meeting specifications stated by the manufacturer or the individual methods used to dilute the standards are flawed. These results warrant more detailed investigation into the standard calibration materials used as well as the methods of diluting these standards to desired mixing ratios.

The typical source for calibration materials is a National Institute for Science and Technology (NIST) Standard Reference Material (SRM) or a standard fabricated by a third party that has been calibrated and certified using a NIST standard (hereafter, both NIST and third party standards are referred to as "standard gas"). The most diluted SO_2

standard gas currently available at NIST exist in two forms, a compressed gas cylinder nominally containing 50 parts per million by volume (ppmv) SO_2 in nitrogen (SRM 1693a) and a permeation device that emits a constant 1.4 μg SO_2 min^{-1} in a temperature controlled environment (SRM 1626). The permeation rate stated above would be equivalent to 5 ppmv with a 100 cm^3 min^{-1} flow rate of dilution air. There is a ready supply of standard gas sources at these mixing ratios for SO_2. The problem is that the mixing ratios of SO_2 in the atmosphere are commonly 10^5-10^6 times less than even the lowest available mixing ratio standard gas. Because SO_2 is reactive, it cannot be stored in any known container at mixing ratios below about 1 ppmv. Using stable, higher mixing ratio standards to calibrate an instrument in the pptv range involves dilution of the standard gas. In the case of the available 50 ppmv NIST standard gas mentioned above, a dilution factor of 10^6 is needed to fabricate a calibration standard of 50 pptv SO_2, a level commonly found in the unpolluted atmosphere [Seinfeld and Pandis, 1997]. A dilution factor is the ratio of dilution air volume to standard gas volume required to obtain the desired calibration gas mixing ratio in a one-stage dilution. For instance, to obtain a dilution factor of 10^6, the volume of SO_2-free dilution air needed is 10^6 cm^3, for a standard gas volume of 1 cm^3. Because of the large quantity of dilution air needed for a modest volume of standard gas, static dilution chambers (large containers of dilution air to which a small volume of standard gas would be injected) become cumbersome due to the size of the chamber and difficulties with equilibration of such a large volume. It is more common to calibrate instruments measuring atmospheric mixing ratios of SO_2, using a dynamic dilution process.

This is where a small continuous flow of an SO_2 standard gas is mixed with a larger continuous dilution flow of SO_2-free air. In this arrangement, the two flows can be adjusted to deliver a range of mixing ratios needed to calibrate an instrument. Dynamic dilution is advantageous over static dilution chambers because of the ease in changing the mixing ratio of the calibration air. However, there is still the difficulty of high dilution factors. With a 1 cm^3 min^{-1} flow rate from a 50 ppmv NIST standard cylinder, 1,000 L min^{-1} of dilution air is needed to achieve 50 pptv SO_2 in a single stage dynamic dilution system. Fabricating and controlling this large volumetric flow of SO_2-free air in a laboratory setting is difficult and it is practically impossible to do so in a field sampling scenario. A multiple-stage dynamic dilution system can be fabricated by arranging a number of single-stage dynamic dilutions in series. This approach has an advantage in that it can achieve the needed dilution factors with a modest dilution air consumption of about 1.2 L min^{-1} compared with the 1,000 L min^{-1} for the single stage dilution. Commercial single and multiple-stage dynamic dilution systems are readily available and can achieve the dilution factors discussed here. The problem with these dilution systems is that they use materials that are incompatible with reactive gases such as SO_2. This results in systematic errors in the dilution of calibration gases from the loss of standard gas within the dilution system.

Source of standard gas:

Depending on the application as well as the availability of calibration gas

standards, it may be advantageous to use either compressed gas cylinders or permeation devices, or even a combination of the two. There are advantages and disadvantages for using either type of calibration gas source. Permeation devices are compact and light weight. They are calibrated by monitoring mass loss over long periods of time. However, for low mixing ratio applications, low loss permeation devices are preferred. With a low permeation rate, it is more difficult to determine the change in mass with time and can result in a permeation rate with a high relative error. Permeation devices with high precision often have higher permeation rates and need larger dilution factors to obtain calibration air mixing ratios of less than 100 pptv. Compressed gas cylinders do not need to be temperature controlled or equilibrated over long periods of time. Unlike permeation devices, they do not require routine analysis for mass loss. However, compressed gas cylinders are heavy, bulky and are limited in the choice of materials that can be used for both the container and regulator. Depending on the analyte, application and field site, either a permeation device or compressed gas cylinder may be the ideal calibration gas source. Thus, it is important that a dilution system be versatile enough to use both sources.

Source of Dilution Air:

The source of dilution air is also an important factor in designing a calibration system. Any residual analyte in the air used to dilute the standard gas will result in higher delivered mixing ratios than calculated based solely on dilution. Ideally, the dilution air

should have undetectable amounts of the analyte gas, although in some cases, residual analyte in the dilution air can be corrected for as long as the mixing ratio of the analyte is constant throughout the calibration. It is also important that the dilution air be similar in composition to that of the sample air. Using a dilution air that is similar in composition to that of the sample air will result in fewer systematic errors from interferences or interactions caused by other trace constituents in the sample air.

Dilution air can be fabricated using commercial "zero air generators." Zero air generators have been used to create continuous flows of dilution air containing SO_2 mixing ratios of less than a few pptv [MacTaggart et al., 1997]. Zero air generators are ideal for remote operation, since they can be operated by using a standard air compressor and do not require compressed gases cylinders. Another dependable source of dilution air can be compressed sample air treated with chemical scrubbers. Chemical scrubbers are used to remove unwanted gases from any dilution air source. The chemical composition of the scrubber is chosen to be selective for removing a certain compound or class of compounds and can be selected depending on the application. For removal of sulfur gases, a 2-stage scrubber can be used. The first stage consists of Purafil (Purafil Inc., Doraville, GA) which is a $KMnO_4$-based media and the second stage of Puricarb (Purafil Inc.) which is an activated carbon-based material which is impregnated with Cu metal. The scrubbed dilution air is then passed through a Teflon filter to remove particulate matter. The source of the air for the chemical scrubber technique can be either ambient air, which is pumped through the scrubbers or supplied from a compressed gas cylinder.

This chemical scrubber method was used successfully for the fabrication of SO_2-free dilution air for the calibration of the diffusion denuder/sulfur chemiluminescence (DD/SCD) technique during the Gas-phase Sulfur Intercomparison Experiment phase-2 (GASIE-2). Although the scrubbed dilution air has not been analyzed for residual SO_2 at the time of this writing, it contained no detectable SO_2 by the DD/SCD technique. The comparison of the DD/SCD measurements of both chemically scrubbed dilution air and dilution air from a zero air generator used in GASIE-2 indicate that the residual SO_2 mixing ratio is similar for both dilution air fabrication techniques.

The particular dilution air generation systems described above are typically designed to deliver a maximum of 100 L min^{-1} of dilution air. A dilution air flow of this magnitude is not sufficient for obtaining required dilution factors for SO_2 from commercially available standard gas sources using a single-stage dynamic dilution system. Although these dilution air generation systems could be scaled up to produce sufficient dilution air for single stage systems, it is much easier to fabricate smaller volumes of dilution air. Thus, a dilution system that utilizes smaller volumes of dilution air is preferred over one that requires thousands of L min^{-1}.

An Ideal Dilution System:

Aside from the source of standard gas and dilution air, the actual design of the dilution system is also critical. An ideal dilution system for creating low level mixing ratios of reactive gases such as SO_2 would achieve the following objectives: (1) be able to

achieve dilution factors of up to 10^6 with a minimal use of dilution air, (2) minimize surface area that the calibration gas is exposed to and use materials that are compatible with the standard gas, (3) have the capability to use either a permeation-based and/or compressed cylinder containing standard gas, (4) provide calibration air with precision and accuracy of better than ±5%, and (5) be light weight, portable, automated, and easy to implement for the calibration of both laboratory and field instrumentation.

A dilution system described by Goldan et al. [1986] accomplishes many of these criteria, including a design where the only material the resulting calibration air comes in contact with is Teflon® (Dupont, Willmington, DE). Although the system uses mass flow controllers (MFCs) which contain wetted surfaces that are incompatible with SO_2 at low levels, the design is such that the resulting calibration air never flows through a MFC. The dilution system described in this Chapter is similar to this design. Improvements to the Golden et al. design include updated MFCs with built in temperature compensation, a modern data acquisition system and computer interface and the capability for remote control via the Internet. The new system uses MFCs where the flow can be driven by a pressure difference created by high pressure at the inlet (pushing) or low pressure at the outlet (pulling). By using a combination of push and pull type flow meters, the dilution can be performed at atmospheric pressure. This is different from Golden et al., where the MFCs were only of the push-type. To drive the flow through some of the MFCs, a throttle valve at the dilution system outlet was needed to pressurize the dilution system. A throttle valve is not needed if the dilutions are at atmospheric pressure. The new dilution

system is capable of using both permeation devices and standard gas cylinders as a source for calibration gases. The final improvement was an internal calibration routine that utilizes a network of solenoids to re-direct the flows through the MFC network.

The dilution system described here was used during GASIE-2. It accomplishes the five criteria stated above and provided high quality calibration gases for the DD/SCD for the entire field mission. The mixing ratios delivered by the system ranged from 0 pptv to about 300 pptv SO_2, or dilution factors close to 10^6.

Multi-stage Dynamic Dilution System:

Operation of Dilution System

A dynamic dilution system was designed and custom-built in our laboratory. A schematic diagram of this system is contained in Figure 3.1. The standard gas, denoted "CAL", contained 0.98 ppmv SO_2 in air [Scott-Marrin, Riverside, CA] and was certified as NIST traceable by the manufacturer to have an accuracy of ± 5%. To assure the stability of this standard gas, it was re-analyzed two years after it was purchased. The re-analysis indicated that the mixing ratio was still within the original specifications. The standard gas flow rate was regulated by a crimped stainless steel capillary tube pressurized to 20 psig. The dilution air source denoted "AIR" was compressed breathing quality air (BQ air) with a 2-stage chemical scrubbing optimized to remove sulfur gases. The first stage of the scrubber was a packed bed of Purifil (Purifil Inc., Doraville, GA), followed by a packed bed of Puricarb (Purifil, Inc.). The SO_2-free air was then filtered with a 47 mm

Teflon® filter to remove particles.

The MFCs are labeled F1 through F5 (Unit Instruments Ltd., Model 1100A, Orange, CA). Flow controllers 1-4 have a range of 0 to 100 cm^3 min^{-1} and flow controller 5 has a range of 0 to 1000 cm^3 min^{-1}. Flow controllers 1, 3 and 5 are "push" type flow controllers. This means that the flow through the controller is facilitated by a pressure drop, which is caused by head pressure of SO_2-free air at the inlet. Flow controllers 2 and 4 are "pull" type flow controllers. The pressure drop across these flow controllers is maintained by a carbon vane pump (GAST Model 1031-117-G373X, Benton, MI) which applies a vacuum at the flow controller outlet.

The dilution stages are labeled C1 through C3. Each of these dilution stages has a mixing volume which consists of a 20 cm length of 1/4" Perfluoroalkoxy (PFA) Teflon® (Dupont, Willmington, DE). The flow rates in the proceeding discussion are in cm^3 min^{-1} at standard temperature and pressure, unless otherwise specified. Primary dilution is achieved in C1 by addition of the standard gas flow (F_{cal}) and the dilution air flow through F1 (F_1). The resulting mixing ratio in pptv SO_2 from the first dilution step at C1 is defined as:

$$C1 = MR * \frac{F_{cal}}{F_{cal} + F_1} \tag{3.1}$$

Where MR is the mixing ratio of the standard gas in pptv SO_2 , F_{cal} is the flow rate of standard gas and F_1 is the dilution air flow rate through flow controller 1. The total flow

at $C1$ is given in the denominator (the sum of F_{cal} and F_1). The calibration gas flow into the secondary dilution chamber C2 is controlled by flow controller 2. By adjusting the flow through F2 to be less than the total flow at C1, the calibration gas flow to the next dilution stage C2 can be controlled. The calibration air that is not removed by flow controller 2 is then diluted in the second stage by dilution air from flow controller 3. The resulting mixing ratio in pptv SO_2 at $C2$ from the first and second dilution stages combined is defined as:

$$C2 = C1 * \frac{(F_{cal} + F_1 - F_2)}{(F_{cal} + F_1 - F_2 + F_3)} \tag{3.2}$$

Where $C1$ is the final mixing ratio from the primary dilution stage in pptv, F_2 is the flow through flow controller 2 and F_3 is the flow from flow controller 3. The total flow at $C2$ is given in the denominator. Similar to the previous dilution step, a portion of the calibration gas is removed, this time by flow controller 4. The calibration air that is not removed by flow controller 4 is then diluted by the flow through F5. The mixing ratio in pptv at the final dilution step $C3$ is defined as:

$$C3 = C2 * \frac{(F_1 + F_{cal} - F_2 + F_3 - F_4)}{(F_1 + F_{cal} - F_2 + F_3 - F_4 + F_5)} \tag{3.3}$$

Where $C2$ is the mixing ratio in pptv from the previous dilution step, F_4 is the flow through flow controller 4 and F_5 is the flow from flow controller 5.

The available data acquisition and control system (DAQPad-1200, National Instrument, Dallas, TX) contains only 2 analog output signals so some of the flow controllers were controlled in tandem. Flow controllers 1 and 3 are controlled by one analog output and 2 and 4 on the second analog output. Flow controller 5 was set at 987 $cm^3\ min^{-1}$, or close to 100% full scale. With flow controller 5 set at close to full scale, the dilution system is optimized for maximum dilution factors and maximum volumetric output of calibration gas.

Operation with a permeation device:

Permeation devices can be used in the dilution system by adding them to a temperature controlled chamber between F1 and C1. The flow from F1 is then directed through the temperature controlled chamber, where the permeated standard gas is introduced to the system. Incorporating permeation devices into this multi-stage dynamic dilution system is easy, as the dilution system is plumbed for this application. When using a permeation device, the formula for the final mixing ratio of the calibration gas is:

$$C3 = \left(\frac{m(t)RT}{F_1 P M_w}\right) * \left[\frac{F_1 - F_2}{F_1 - F_2 + F_3}\right] * \left[\frac{F_1 - F_2 + F_3 - F_4}{F_1 - F_2 + F_3 - F_4 + F_5}\right] \quad (3.4)$$

Where *m(t)* is the permeation rate in mass per unit time (g/min), M_w is the molecular weight of the permeating species (g/mol), *R* is the gas constant (83145 $cm^3 \cdot mb \cdot mol^{-1} \cdot K^{-1}$), *T* is the temperature of the dilution air (K) and *P* is atmospheric pressure (mb). All other flow rates are the same as described earlier. Since pressure and temperature are needed to convert the permeation rate to a mass flow, the dilution system is configured with both a pressure and temperature sensor. The SO_2 gas flow from the permeation device can be left out of the denominator without a significant loss in accuracy because it is 10^{-6} times that of any of the other flow rates.

By using a permeation device, there is an advantage that may lead to improved accuracy of the resulting calibration gas. The permeation device's contribution to the error in the calibration gas is only from the determination of the permeation rate, whereas the error from the calibration gas cylinder contains error in both the measured flow from the cylinder and the accuracy of the mixing ratio of the calibration gas. A more accurate and precise calibration standard may be achieved by using a permeation device, if the precision and accuracy of the permeation rate is better than that of the combined precision and accuracy of both the calibration gas flow and the standard gas mixing ratio.

Dilution air requirements:

One of the primary advantages of multi-stage dynamic dilution is that high dilution factors can be achieved with relatively low volumes of dilution air. In the system described here, dilution factors of close to 10^6 are achieved with a maximum of 1.2 L min^{-1}

of the SO_2-free dilution air. Mass flow meters 1 and 3 each delivering 100 cm^3 min^{-1} and flow meter 5 delivers close to 1000 cm^3 min^{-1}. The equivalent single stage dynamic dilution would require roughly 1000 times as much dilution air to achieve the same dilution factor. Multi-stage dynamic dilution alleviates the problem of synthesizing large volumes of SO_2-free dilution air in the field.

Data Acquisition and Instrument Control:

The multi-stage dynamic dilution system is interfaced to a laptop computer by a DAQPad-1200 (National Instruments, Dallas, TX) data acquisition system. Ambient temperature and pressure were obtained by a meteorological instrument package (Climatronics Corp, Model 102254, Bohemia, NY). MFC readings, temperature and pressure were acquired at 1s intervals. Custom software written in Labview (National Instruments) saved 10s averages of these data to disk. The dynamic dilution system software also controlled the mass flow controller settings.

An automated routine for delivering gases for multi-point calibrations was also embedded within the dilution system software. In this routine, the operator enters the desired number of calibration points, the mixing ratio of each of the points and the length of time each point will be delivered. Since multi-point calibrations can take many hours to complete depending on the analytical system being calibrated, this feature saves the operator from being present during the calibration. During GASIE-2, the operators could setup the dilution system for a 6 hour calibration of the DD/SCD at the end of the day, to

be run overnight. The automated calibration routine was used over 25 times during the course of a 5 week GASIE-2 intercomparison. The automated calibration feature literally saved hundreds of hours of operator time in this study alone.

Another advantage of having an automated, computer controlled dilution system is that it can be configured for remote control. This would be advantageous in remote field sampling campaigns. Using Internet technology and modern client/server architecture, it would not be difficult to collect information on the range of mixing ratios being sampled at the remote site. Calibration points could then be selected so that the range covered in the calibration was similar to the range of the observed mixing ratios. Some progress has been made in modifying the existing dilution system software for Internet remote control. Due to time and budgetary constraints, these modification have not yet been completed at the time of this writing.

Calibration and estimates of accuracy:

Calibration of standard gas flow:

The calibration source used in this study was a compressed gas cylinder of 0.98 ppmv SO_2 in air, as mentioned previously. The flow rate of the standard gas was controlled by a crimped piece of stainless steel capillary tubing which was pressurized to 20 psig. Stainless steel and even the wetted surfaces of mass flow controllers are suitable for handling SO_2 in the ppmv levels [MacTaggart et al., 1997]. The flow rate through this crimped capillary was calibrated over the period of one month with approximately 130

triplicate measurements of flow with two separate flow meters. The flow was measured with both a Gilibrator (Sensidyne-Gillian, Clearwater, FL) automated bubble meter and a standard bubble-type flow meter (Hewlett-Packard, CA). The Gilibrator flow cell is a bubble-type flow cell that has optical sensors that trigger a timing circuit that replaces the stopwatch used in a standard bubble-type flow meter. The particular Gilibrator flow cell that was used is rated for flows ranging from 0.1 to 250 cm^3 min^{-1}. The Gilibrator is calibrated by the manufacturer under laboratory conditions of approximately 70° F, with a pre-humidified air source and corrected to standard pressure. For mass flow measurements, the Gilibrator flow must be corrected from operating to standard temperature, pressure and the difference in the vapor pressure of water from 70° F to the operating temperature. In this experiment, the laboratory temperature was close to 70° F, and the difference in the vapor pressure over water was found to be negligible. The Gilibrator flow was only corrected for standard temperature and pressure for use in this evaluation. The Gilibrator factory calibration was confirmed by using a mass flow controller which had been calibrated to a NIST traceable standard. To best simulate the SO_2 standard gas from the cylinder the air used for the calibration was from a cylinder of breathing quality air which was not humidified. The graph in Figure 3.2 shows the calibration of the small Gilibrator cell, which showed excellent precision and linearity over the range of 0 to 100 cm^3 min^{-1}.

The HP manual bubble meter was calibrated gravimetrically. The calibrated volume of the glass bubble meter was filled with deionized water. The mass of the water

was then determined to the nearest 0.1 mg by using a Mettler electronic balance (Mettler Toledo International, Model AJ100, Greifensee, Switzerland). The mass of the water was then converted to volume using the density of water at the ambient temperature. This gravimetric determination of the volume was repeated 5 times. The 10 cm^3 marked volume on the flow meter was calibrated to be 10.09 cm^3 with a relative standard deviation of 0.2%. This volume was used to correct the calibration gas flows as measured by the HP bubble meter.

After the HP bubble meter and the Gilibrator were calibrated for mass flow. The standard gas flow rates measured over a one-month period were combined to obtain an average flow for that period of time. The graph in Figure 3.3 contain over 130 triplicate measurements of the standard gas flow which was controlled by the crimped stainless steel capillary tube. The measured mean flow over the course of a month was 10.35 $cm^3\ min^{-1}$ and a 95% confidence interval of better than ±1%. This demonstrates that the crimped stainless steel tube is an excellent and inexpensive method of controlling mass flow from a compressed gas cylinder. It is conceivable that with higher pressures and a smaller oriface on the stainless steel capillary, the flow rate may be controlled with even better precision. Further improvements in the precision of the mass flow may be realized with the addition of a sensor to monitor the delivery pressure to the capillary tube. By detecting small changes in the delivery pressure, the mass flow through the oriface may be predicted with better accuracy.

Calibration of the Mass Flow Controllers:

Calibration of each of the mass flow controllers in the dynamic dilution system was conducted using a Califlow (MKS Instruments Inc., Andover, MA) at the South Dakota School of Mines and Technology. The Califlow has a NIST traceable accuracy of ± 0.2% of the measured flow rate. Each of the flow controllers was isolated and calibrated independently. The 0-100 cm^3 min^{-1} flow controllers where calibrated over the range of 10 to 100 cm^3 min^{-1} and the 1000 cm^3 min^{-1} flow controller was calibrated only near full scale (1000 cm^3 min^{-1}). The 1000 cm^3 min^{-1} (flow controller 5) was operated and calibrated near full scale because this setting results in the maximum dilution and delivers the maximum volume of calibration gas. All of the flows were measured in triplicate, so that a standard deviation could be calculated for each of the flow rates. Calibration curves for each of the mass flow controllers show excellent accuracy, precision and linearity over the 100 cm^3 min^{-1} range. The calibration curves for flow controllers 1 and 3 are shown in Figure 3.4. Calibration curves for flow controllers 2 and 4 are shown in Figure 3.5. The flow controllers demonstrate a linear response in the 0 to 100 cm^3 min^{-1} range. The excellent precision of these MFCs is also demonstrated, as each set-point on the calibration curve is actually a group of at least 3 separate points, although they can hardly be distinguished from one another. It is important to note that although the absolute error in the MFCs is small throughout the entire calibration range, the relative error increases as the mass flow set-point decreases. This effect is demonstrated in Figure 3.6. This is not a problem, since in normal operation MFCs 1 and 3 are set at or near 90 cm^3 min^{-1} and

MFCs 2 and 4 are set in the range of 60 to 99 cm^3 min^{-1}.

The information from the calibrations was incorporated into a model to estimate the accuracy of the dilution system over a range flows encountered. In the model, the error from each flow controller was assumed to be random and independent of the other flow controllers. The independent errors are then combined in the mixing ratio calculation so that error propagation is included in the result. The results of the model, as shown in Figure 3.7, are presented as the estimated error versus the dilution factor. The maximum error is the standard deviation relative to the resulting mixing ratio. The two data sets on the graph represent the error in the dilution system including the error in the calibration gas flow and without the calibration gas flow error. The data set representing a smaller amount of error is based on the errors resulting from only the mass flow controllers within the dilution system and is independent of the calibration gas flow or permeation rate. The added error from including the error in standard gas flow is significant. Presenting the error estimation in this way demonstrates that the small error in calibration gas flow results in significantly higher error in the delivered mixing ratio. This accentuates the importance of controlling the flow or permeation rate of the calibration gas standard to a high degree of accuracy.

Mass flow controllers zero:

Mass flow controllers typically have trouble with changes in ambient temperatures. The primary problem caused by temperature fluctuations is a shift in zero reading. A zero

reading is the voltage output from a mass flow controller when no gas is flowing through it. Zero reading changes of approximately 0.1% of full scale per °C have been observed [Goldan, et al., 1986]. The mass flow controllers used in the dynamic dilution system described here have built-in electronic temperature compensation. To evaluate the effectiveness of the temperature compensation feature, the zero readings of the mass flow controllers were monitored over the course of a month. During this time, the room temperature fluctuated between 20-30 °C. In Figure 3.8, a graph of the zero readings over time suggests that the temperature compensation routine works well over this range of operating temperatures. Even though the change over time was small, the mass flow data was corrected for the recorded zeros.

Internal Calibration routine:

One of the subtle features of this dilution system is the capability for internal calibrations of the mass flow controllers. A schematic diagram of the dilution system as operated in internal calibration mode is shown in Figure 3.9. The series of solenoid valves shown are switched on so that the flow can be routed through the mass flow controllers sequentially. With the solenoids in calibration position, the flow begins through MFC 1 and is routed directly to MFC 2, the flow is then routed through MFC 3 and finally to MFC 4 and MFC 5. The Teflon® mixing chambers, pressurized SO_2-free air supply and vacuum lines are by-passed so that the MFCs can be isolated from the rest of the system. In this calibration mode, a known mass flow of air (or any other dilution gas) is passed

through each of the mass flow controllers. This is advantageous in that the flow controllers do not need to be removed from the instrument and can be calibrated concurrently. If the operator wants to isolate one mass flow controller, the other flow controllers can be shut off using manual switches that are accessible from the front panel of the instrument.

Since the internal calibration routine is electronic, the data acquisition and control instrumentation can be modified to allow remote control via the Internet. In this mode, the MFCs could be cross calibrated to MFC 1, which would be controlling the flow through the other MFCs. This option would be especially useful in a field situation where the dilution system is deployed in a remote location.

Conclusions:

The dynamic dilution system described here is a robust instrument capable of delivering sub-ppbv calibration gases from higher mixing ratio standard gas sources. Dilution factors of 3×10^5 have been achieved with a relative standard deviation of less than ±5%. The dilution system is capable of using both permeation devices or compressed gas cylinders as the source of calibration gas. The system is designed for handling reactive gases such as SO_2. Even though the system uses mass flow controllers which have wetted surfaces not compatible with SO_2, the design is such that the resulting calibration gas comes in contact with only PFA Teflon® surfaces. If necessary, the system can be modified to use other materials that may be better suited for the chosen analyte. The

dilution system is fully automated and computer controlled. The custom software includes an automated calibration routine, so that multi-point calibrations can be conducted without the operator being present. Further software enhancements can create a client/server architecture that takes advantage of Internet technology. This would allow the dilution system to be controlled remotely, which would be especially useful in the field. For quality assurance purposes, an internal calibration for the MFCs is also incorporated into the system. This feature makes it easier to conduct quality assurance on the dilution system and MFCs within. The multi-stage dynamic dilution system was operated for a month during the GASIE campaign as a source of calibration gases for the DD/SCD. The dilution system proved to be crucial to the intercomparison effort and performed flawlessly over the one month experiment.

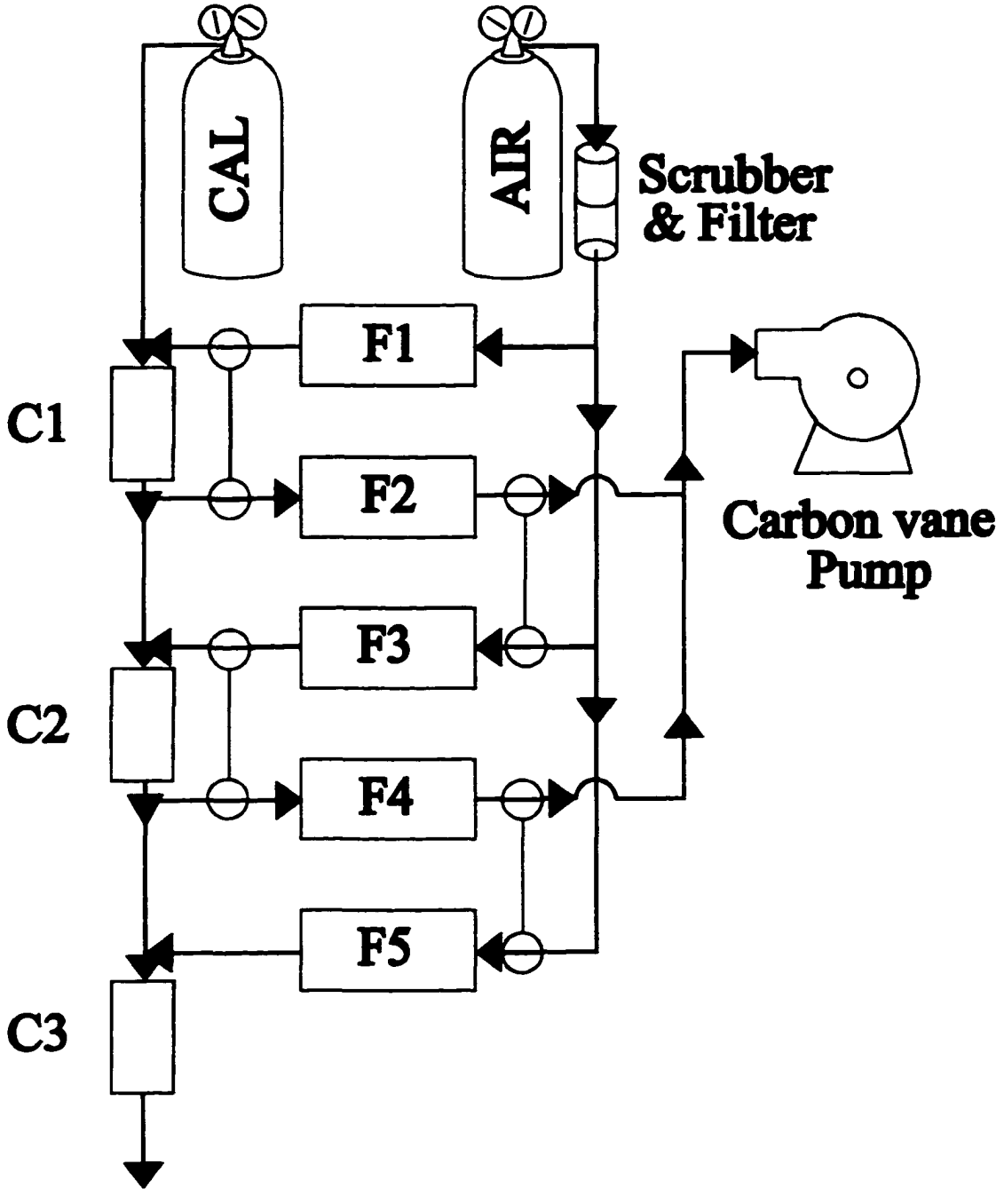

Figure 3.1 A schematic diagram of the multi-stage dynamic dilution system. Mass flow controllers 1-5 are denoted F1-F5 and C1, C2 and C3 represent dilution stages 1-3. The arrows in the diagram demonstrate the flow through the dilution system. The system shown is configured for use with a compressed gas cylinder standard gas source. The system can be used with permeation devices by adding an optional temperature controlled chamber between F1 and C1.

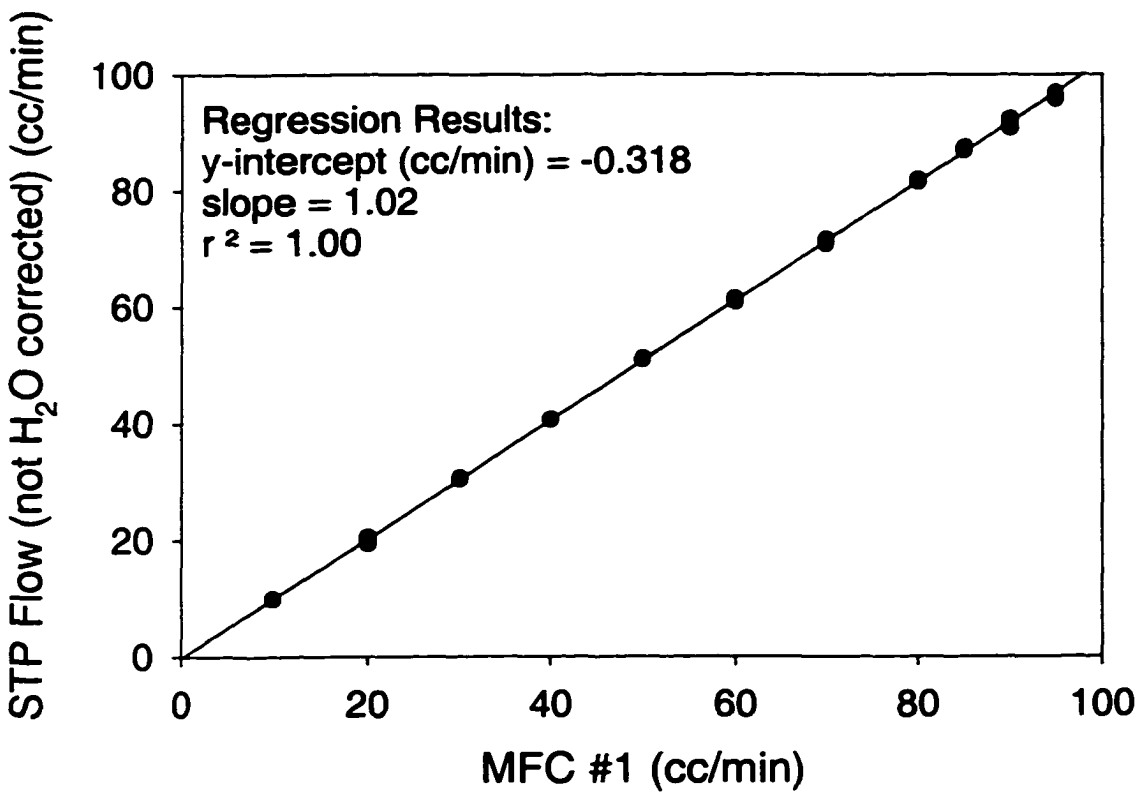

Figure 3.2 Calibration curve of the Gilian Gilibrator®.
The calibration of the Gilibrator small flow cell demonstrates an excellent linear range. The Gilibrator flow was corrected for both temperature and pressure. The flow was not corrected for water vapor because it is already accounted for in the calibration method used by the manufacturer.

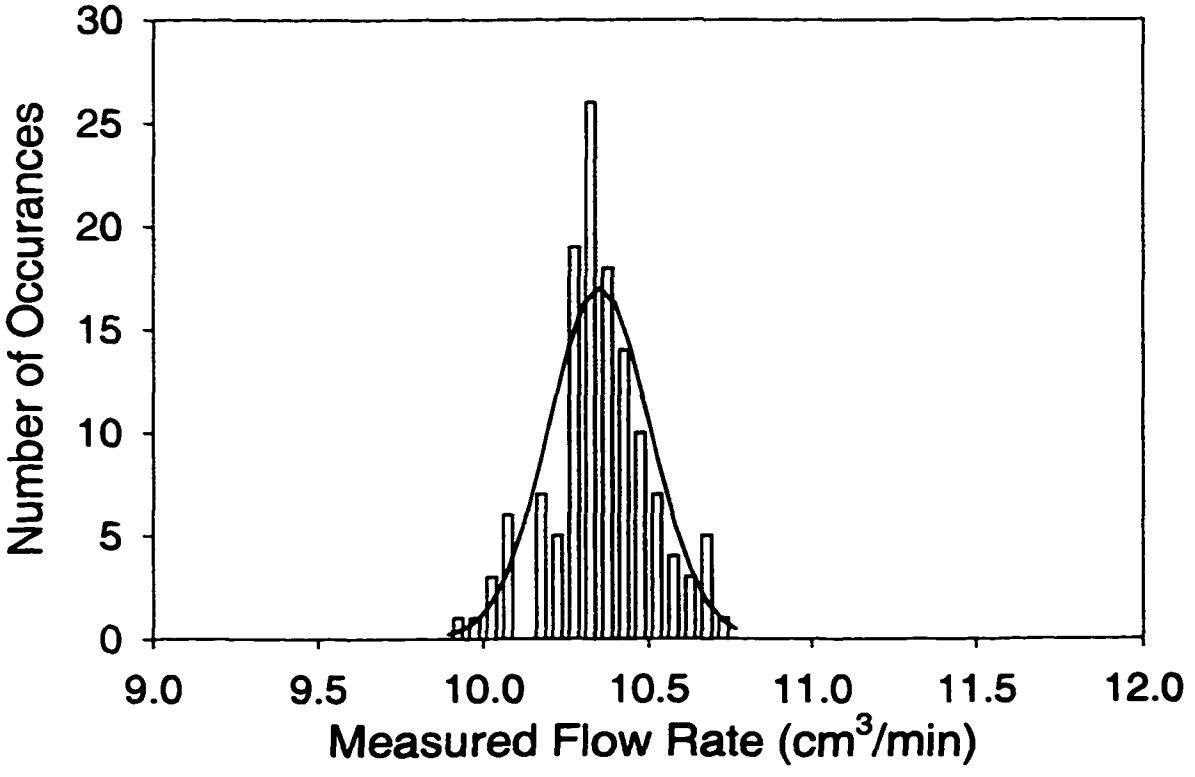

Figure 3.3 Frequency distribution of the SO_2 standard gas flow measurements. Frequency distribution of SO_2 calibration gas flow measurements from both the Gilibrator and HP bubble meter. The two flow meters were corrected for standard conditions as described in the text. The measurements and Gaussian fit are the results of over 130 flow measurements, each done in triplicate, over the course of one month. The average flow was determined to be 10.35 cm^3 min^{-1} with a standard deviation of 1.4%.

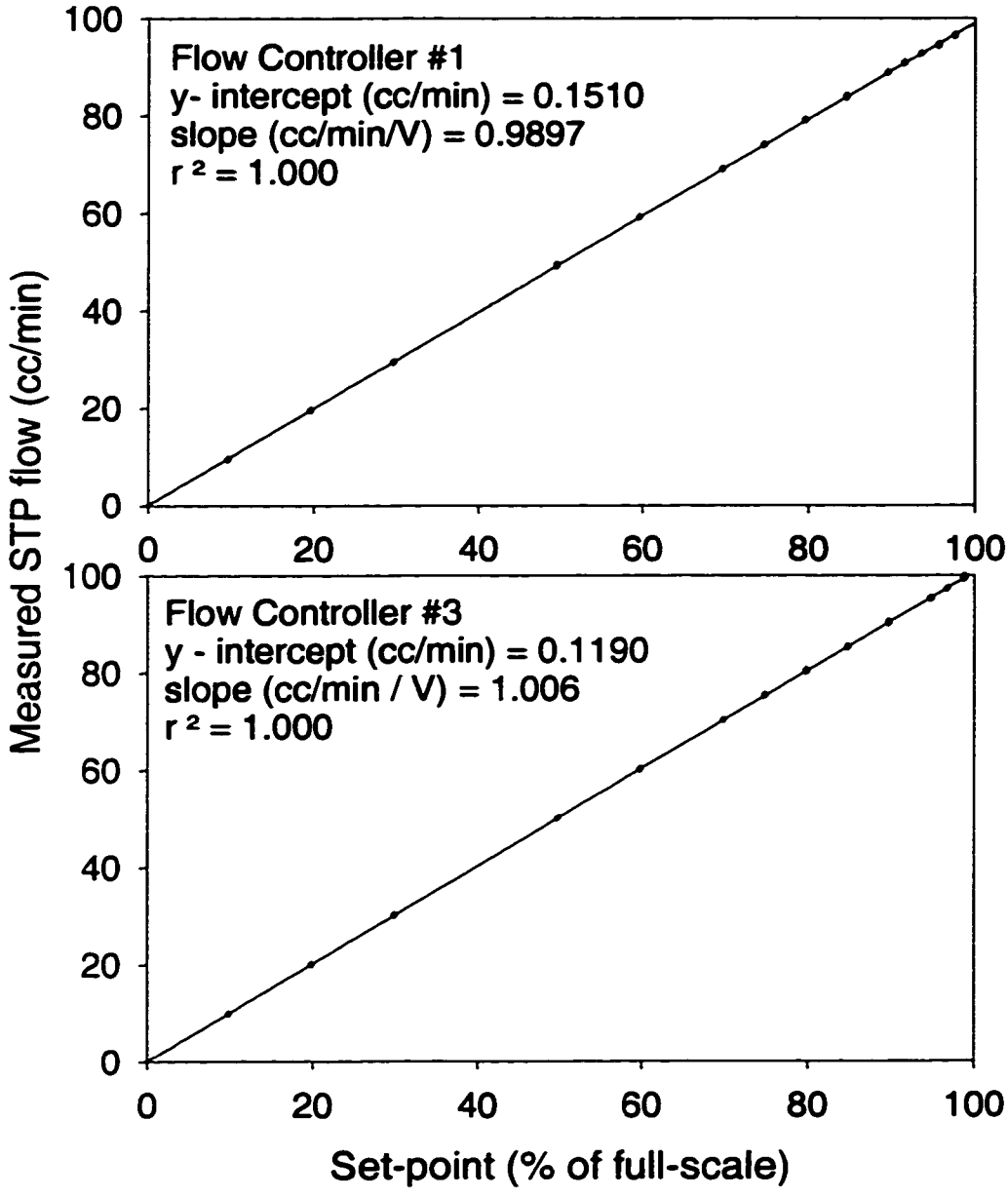

Figure 3.4 Calibration curve of mass flow controllers 1 and 3.
The calibration curve of mass flow controllers 1 and 3 show excellent linearity and precision over the 100 cm^3 min^{-1} range. The flow was measured in triplicate at each response level. The flow rate is precise enough that there is no noticeable scatter at any of the MFC set-points.

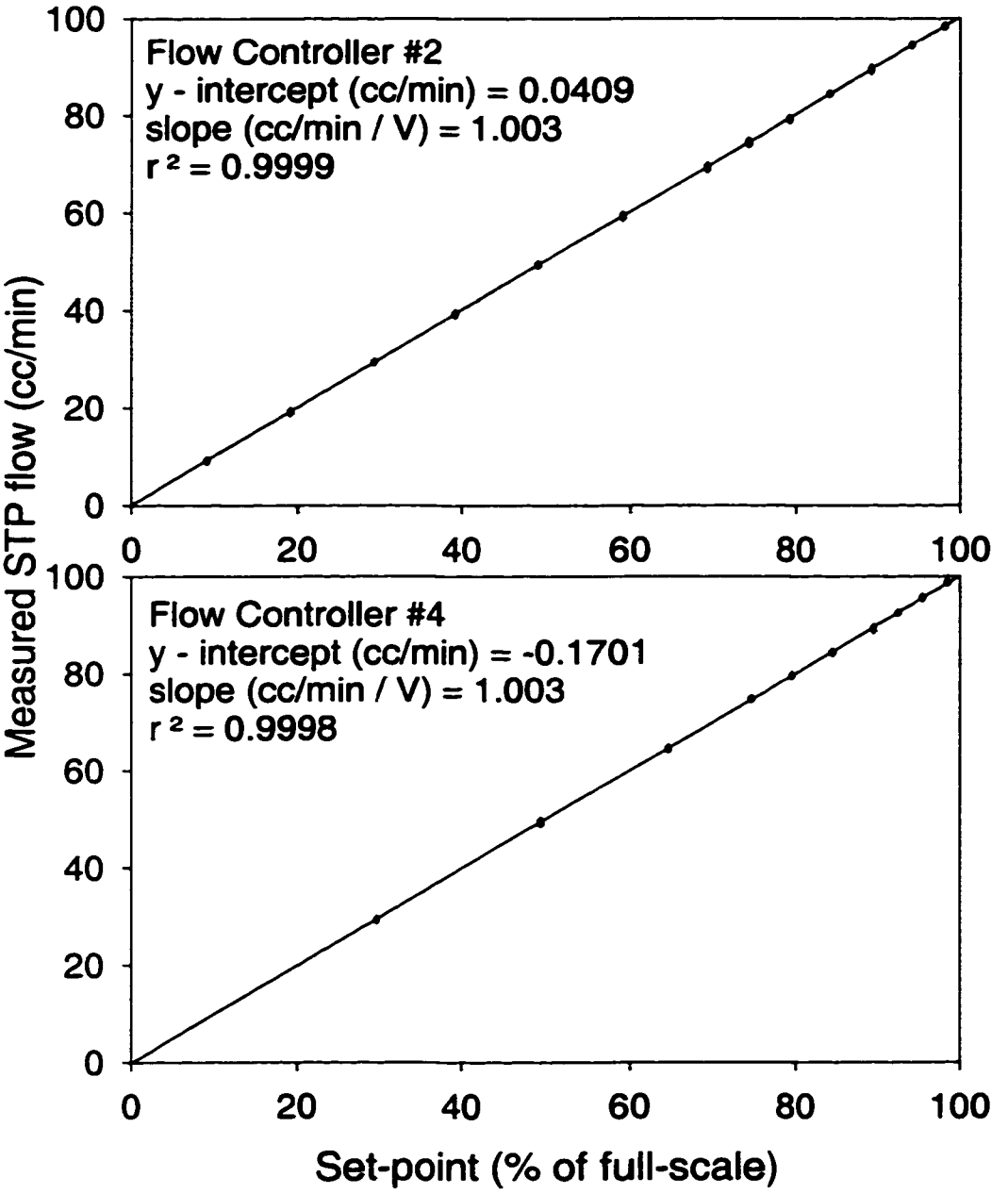

Figure 3.5 Calibration curve of mass flow controllers 2 and 4.
The calibration curve for mass flow controllers 2 and 4 show excellent precision, accuracy and linearity over the 100 cm^3 min^{-1} range. The flow was measured in triplicate at each response level. The flow rate is precise enough that there is no noticeable scatter for any of the MFC set-points.

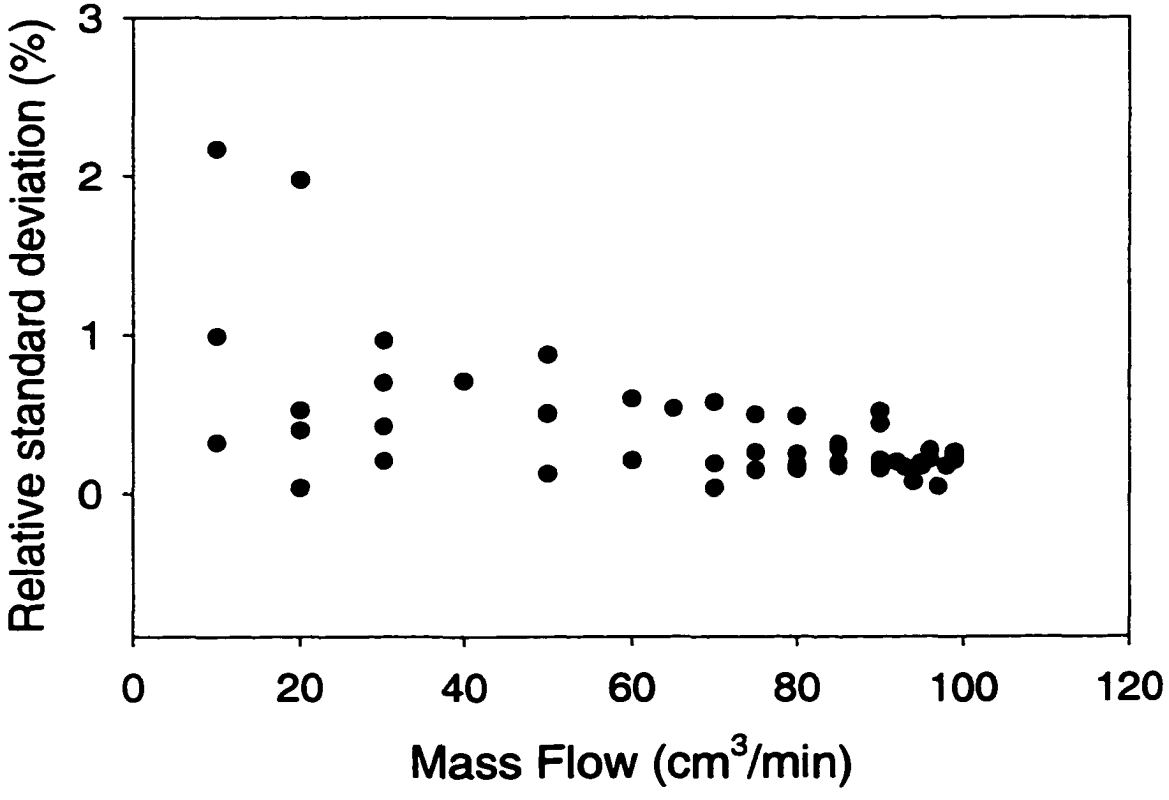

Figure 3.6 Relative standard deviation of mass flow controllers 1-4 as a function of the mass flow.
The mass flow controllers demonstrate excellent precision over the entire range, with higher relative standard deviations as the flow decreases. During the GASIE-2 experiment, the flow controllers were operated between 60 and 100 cm^3 min^{-1}.

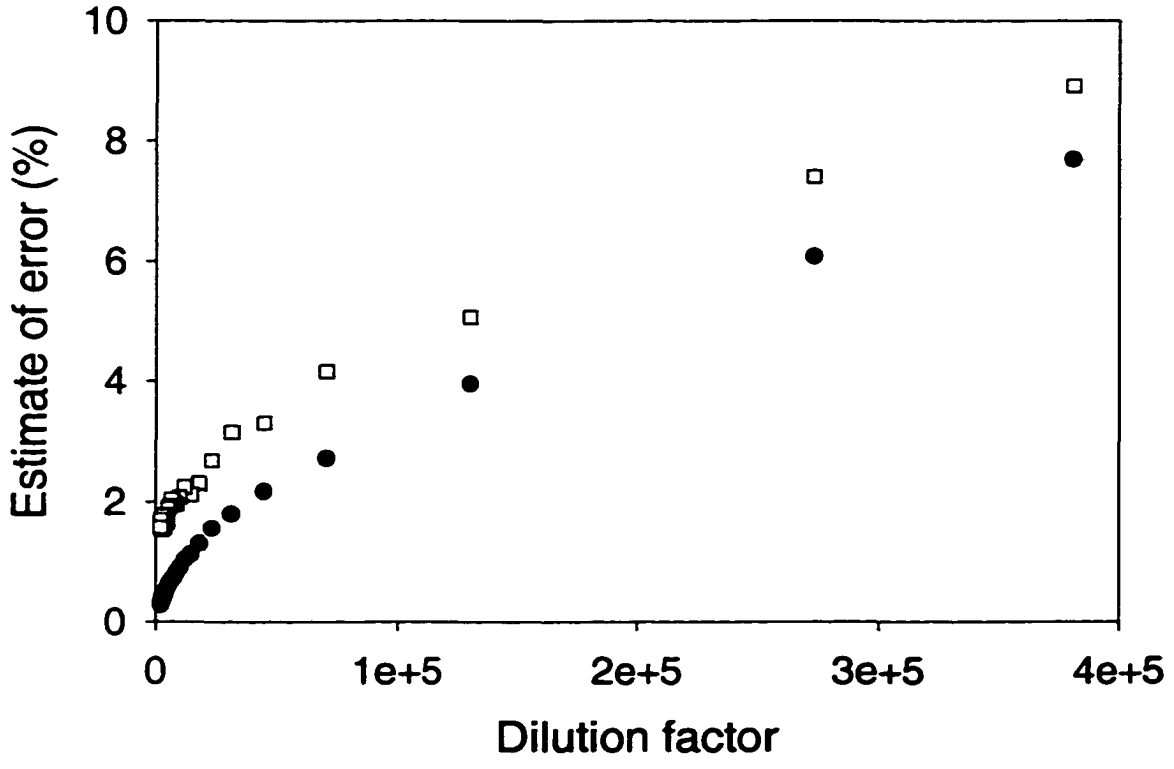

Figure 3.7 Estimate of relative error in calibration gas mixing ratio for a large range of dilution factors.
The error estimate is one standard deviation and is given as a percent of the resulting mixing ratio. The data set represented by open squares is the estimated error when the error of the calibration gas standard flow is included. The data set represented by the dark circles includes the error from the mass flow controllers only. Using the estimated error of only the mass flow controllers better evaluates the dilution system's capabilities for use with a permeation device. In both cases, dilutions of larger than 10^5 can be achieved with errors of less than ± 5%.

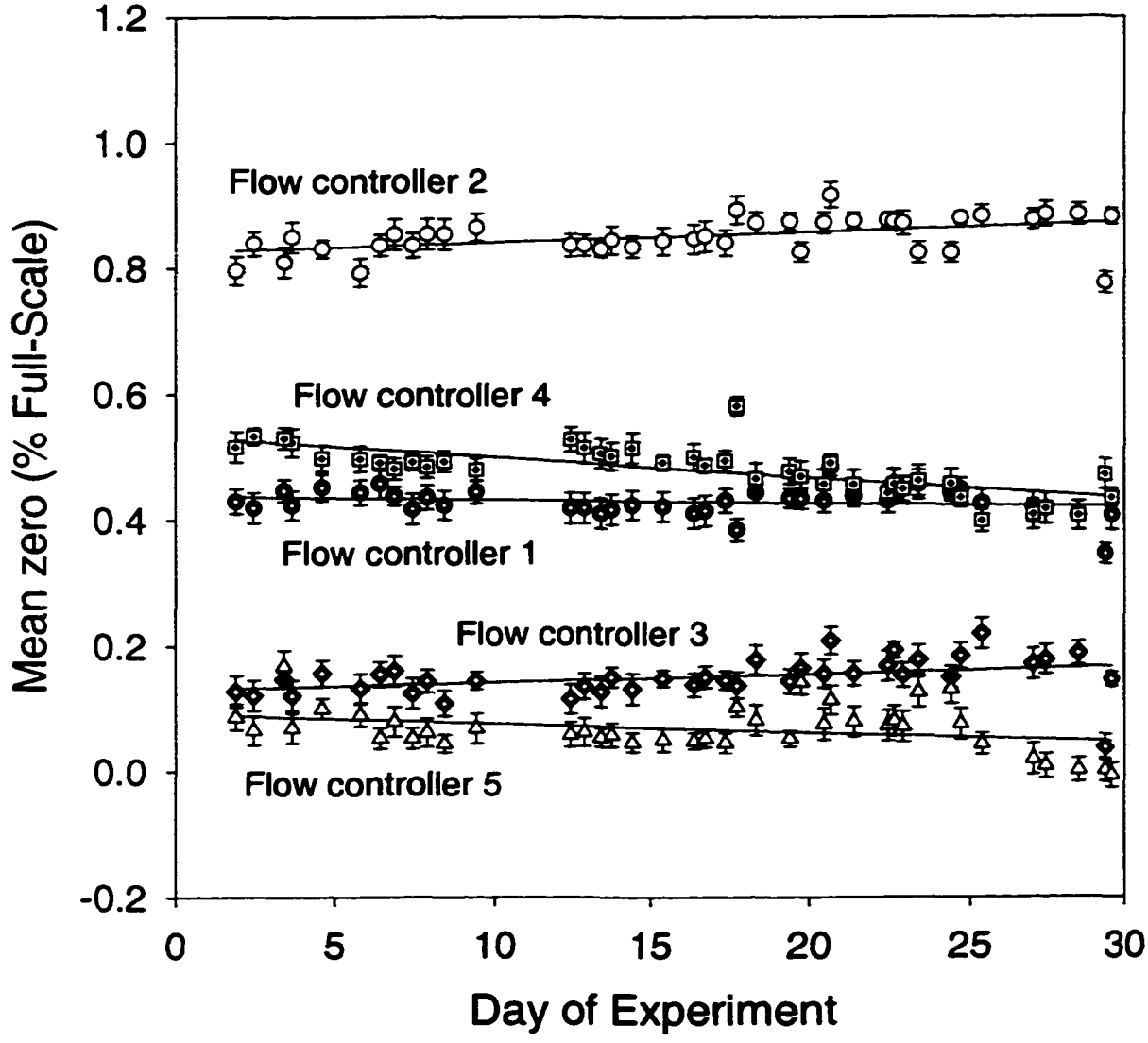

Figure 3.8 Control chart for the mass flow controller zeros over the course of a month.

The mean zero is in % full-scale, the scale of the mass flow controllers is 0-100 cc/min for MFC 1-4 and 0-1000 for MFC 5. This chart demonstrates that the flow controllers have a very consistent zero reading over the period of a month.

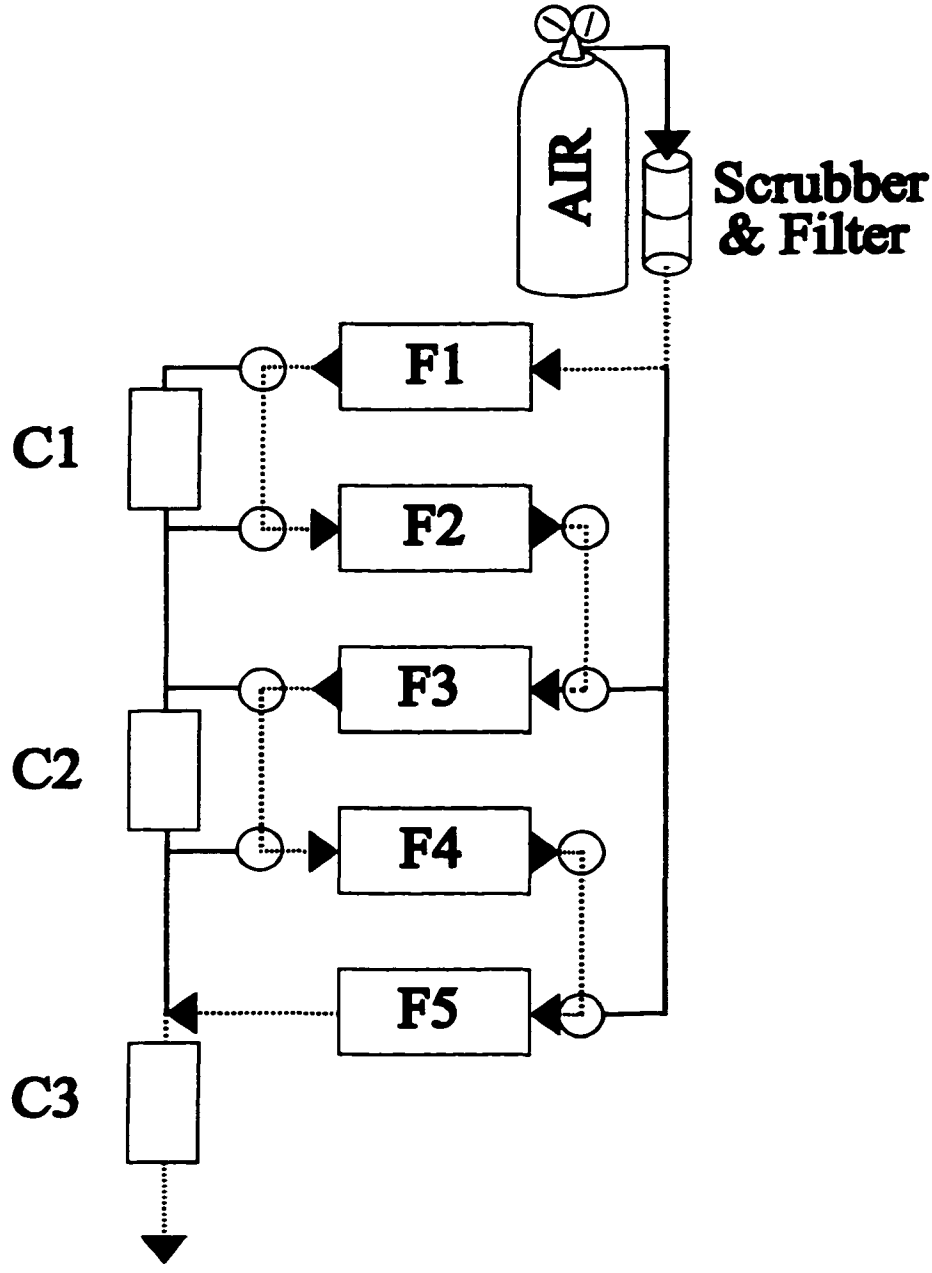

Figure 3.9 Schematic diagram of the multi-stage dynamic dilution system in internal calibration mode.
Internal calibration mode is different from dynamic dilution mode. In dynamic dilution mode, the solenoid valves are not engaged. With the solenoid valves engaged, the flow is directed sequentially into each of the 5 mass flow controllers. The dotted lines with arrows demonstrate the flow pattern when the system is in internal calibration mode. In this configuration, the flow controllers can be calibrated at the same time without being removed from the instrument.

Chapter 4

The Continuous SO_2 Detector (CSD)

Introduction:

In comparison to the conclusions from the CITE3 mission, results of the GASIE campaigns are quite impressive. The instrumental techniques that had showed no correlation at mixing ratios less than 200 pptv SO_2 in CITE3, had excellent correlation in this range in GASIE and GASIE-2. An overview of the instruments evaluated in the GASIE campaigns is shown in Table 4.1 [Benner et al, 1997; Stecher et al, 1997; Nicks et al, 1999]. In these experiments, the instruments fared well in the controlled laboratory environment. The instruments showed little to no interference from potentially interfering gases such as CO, NO_x, CO_2, DMS, O_3, CH_4 and water vapor. In comparing limits of detection as determined in the GASIE campaigns, the evaluated instruments are similar in that they can differentiate between at least zero and 40 pptv SO_2. The significant difference between the instruments was in the sample time required to obtain the sensitivity required for effective measurements of SO_2 in the unpolluted environment. The instruments evaluated in GASIE and GASIE-2 required sampling and measurement time of between 4 and 90 minutes. These instruments require time intensive procedures such as preconcentration and chromatographic separation, or significant signal averaging times of 20 or more minutes [Stecher et al. 1997; Luke, 1997]. The DD/SCD was the only

instrument evaluated in the GASIE campaigns where the sampling and measurement time was not inherently limited by a preconcentration, separation or significant signal averaging time. The diffusion denuder technique was originally developed because of this feature and its simplicity in separating SO_2 from other sulfur gases. By excluding the time intensive steps of preconcentration and chromatography, the technique can take advantage of the fast response of the SCD.

A 4 to 30 minute measurement for SO_2 is quite useful when observing events such as diurnal cycles or longer-term events from a stationary point. They are also effective in determining average mixing ratios for a given location, which can be used to infer background levels of SO_2 over a more general region. Stations such as this have helped to define background levels for generic locations such as "continental" or "clean marine." Any of the techniques evaluated in GASIE would be suitable for such a task. However, there are many compelling reasons for developing a real-time SO_2 detector. Ground-based stationary sampling cites do not allow one to conduct transects of a given air mass or vertical profiles of SO_2 mixing ratios in the atmosphere. Thus, the information collected at the site may not necessarily be representative of a larger region, and is limited to the conditions at the site. A sensitive, real-time instrument installed on a moving platform, such as an airplane, would be better suited for studying regional atmospheric chemistry, and would also be capable of determining vertical profiles. Experimenters would have the option to follow interesting atmospheric phenomena, and if necessary, make another pass through a particular air mass. At typical speeds of 200 ms^{-1}, a 4-min sampling time

represents an average mixing ratio over a distance of 48 km. Without sensitive SO_2 measurements on the order of seconds, the interpretation of atmospheric chemistry is often limited to steady-state assumptions. The availability of an SO_2 detection scheme which is capable of these types of measurements would open up new applications in atmospheric chemistry.

As far as real-time measurements of SO_2 in the atmosphere are concerned, the research has been limited to applications where the ambient mixing ratios are greater than 1 part-per-billion by volume (ppbv). This research includes urban pollution studies and the fate and transport of emissions from smoke stacks . Currently, the pulsed fluorescence technique is being used for real-time SO_2 measurements in these polluted areas. The technique has been used successfully in both stationary and moving platforms and has a detection limit of 0.3 to 2.0 ppbv with signal averaging times ranging from 30 seconds to a few seconds [Hübler et al., 1998; Ryerson et al., 1998; Ferek et al., 1997]. The longer the signal averaging time for the pulsed fluorescence detector, the better the detection limit. During GASIE, a signal averaging time of 30 min was needed to obtain detection limits of 20-40 pptv and an equal amount of time was used to establish the instrument baseline before and after the measurement [Stecher et al, 1997, Luke, 1997]. The pulsed fluorescence technique is adequate for real-time measurements in polluted areas where the mixing ratio of SO_2 can easily reach 10's of ppbv. However, the technique does not have the sensitivity for real-time measurements in unpolluted or even moderately polluted areas. The research conducted with the pulsed fluorescence technique has aided in the

understanding of localized and semi-regional pollution effects such as acid rain and degradation of visibility. While this research is important for understanding the atmospheric chemistry of urban centers and the affected localized areas, it does not address atmospheric chemistry on a global or large-scale, regional level.

Biogenic sources of reduced sulfur gases, that are oxidized to SO_2 in the atmosphere are ubiquitous. The magnitude of these emissions are not well known, but are estimated to be equal to that of the total anthropogenic loading of sulfur gases, which is primarily SO_2 [Cullis and Hirschler, 1980; Andreae et al., 1986]. While the study of roughly half of the atmospheric sulfur emissions can be completed in and around urban centers, the geographic area represented is a tiny fraction. The ambient SO_2 mixing ratios present in a vast majority of Earth's atmosphere are controlled by biogenic emissions of gases such as hydrogen sulfide (H_2S) and dimethylsulfide (DMS). During oxidation in the atmosphere these biogenic sulfur gases are converted to SO_2 then further oxidized to sulfate (SO_4^{2-}). The mixing ratios of SO_2 in the natural environment are often less than 100 pptv [Seinfeld and Pandis, 1998; Andreae et. al, 1986; Möller, 1984]. In order to understand the atmospheric chemistry in the remote atmosphere, an instrument must be sensitive enough to measure these low mixing ratios and be mobile in order to obtain measurements over large geographical regions. An instrument with these capabilities is crucial to the study of the global biogeochemistry of sulfur and primarily the effects of aerosol sulfur chemistry on the radiative balance of Earth's climate system [Shaw, 1983; Charlson et al., 1987; Charlson et al., 1991; Charlson et al., 1992; Andreae and Crutzen,

1997].

The goal of the work presented in this chapter is to further develop and refine the successful technology of the DD/SCD, to achieve near real-time SO_2 measurements in the low pptv range. This new research demonstrates a relatively inexpensive, and robust system that accomplishes this goal. The Continuous SO_2 Detector (CSD) is based on the same analytical principles of the DD/SCD, but has been optimized for sensitive, high-time resolved measurements of SO_2 in air. This optimization has resulted in a new instrument that has similar sensitivity as the instruments evaluated in GASIE, but accomplishes it with a sampling time of less than 1 min.

Experimental Section:

A diagram of the CSD is shown in Figure 4.1. Sample air is drawn through a custom built counter-flow shell and tube type Nafion Drier (Permapure, Toms River, NJ) to remove water vapor. The sample stream is then split, half of which flows through a CO_3^{2-} coated diffusion denuder, that selectively and quantitatively removes SO_2 from the sample [Ferm and Sjodin, 1985; Lindgren and Dasgupta, 1989]. The other half of the sample stream flows through 1/8" Perfluoroalkoxy (PFA) Teflon tubing (DuPont, Willmington, DE). Splitting the sample air flow between the Teflon tube and denuder pathways creates a continuous sample flow through these two channels in the CSD sample train. This is different than the DD/SCD, where the sample gas flow was alternately switched with a solenoid valve either through the denuder or Teflon tube. Therefore, in

the original DD/SCD technique, sample air was only flowing through one channel at a time. When the sample flow was switched, the equilibration of the sample air to the surface of the tubing caused the SCD response to be unstable for a few minutes. The new continuous flow configuration significantly reduces the equilibration time as the sample air and denuded air are alternately sampled, resulting in a faster SO_2 measurement.

In the new configuration, the SCD alternately samples the continuous gas stream flowing through each of the two pathways of the sample train. A PTFE Teflon 3-way solenoid valve (Parker-Hannafin Corp. Fairfield, NJ) directs the flow from the sample train to the SCD through PFA Teflon tubing who's length has been minimized. The length of tubing required to equilibrate after a valve switch has been reduced from 30 cm in the DD/SCD to 5 cm in the CSD for the undenuded channel and from 130 cm in the DD/SCD to 5 cm in the CSD for the denuded channel. The SCD measures the total sulfur content of the sample air containing SO_2 and then measures the same sample air that has SO_2 removed. Similar to the DD/SCD, the resulting periodic signal has an amplitude that is proportional to the SO_2 mixing ratio of the sample air. The period of the signal is controlled by the switching or modulation frequency of the solenoid valve driven with a BK Precision model 3022 function generator (Chicago, IL) and CRYDOM (San Diego, CA) model D2W203F solid state relay.

The SCD response and solenoid valve position were recorded on a National Instruments MIO16x, 16 bit A/D board (Dallas, TX) in a desktop PC. A low-pass RC filter with a 20 Hz cutoff frequency (-3 decibels (dB)) was used to avoid aliasing effects.

The -3dB cutoff frequency is where a periodic signal is attenuated by about 29%. A dB is defined in the following formula:

$$dB = 20 \log_{10} \frac{A_2}{A_1} \tag{4.1}$$

Where A_1 and A_2 are the unattenuated and attenuated signals, respectively. Custom software for the data acquisition and instrument control was developed using National Instruments Labview development software (Dallas, TX). Signals were sampled at a rate of 10 Hz and saved to disk.

Calibration gases for the instrument were delivered by a custom built dynamic dilution system. This dilution system, described in detail in Chapter 3, is capable of dilution factors of up to 10^6 with high precision and reproducibility. The calibration gas standard used in the dynamic dilution system was 0.98 ppmv SO_2 in air (Scott Marrin, Riverside, CA) certified NIST traceable by the manufacturer to have an accuracy of ± 5%. The standard gas flow rate was regulated by a crimped stainless steel capillary tube, pressurized to 20 psig. The crimped capillary tube delivered a constant standard gas flow rate of 11.4 sccm, as measured by a Gilibrator (Sensidyne-Gillian, Clearwater, FL) automated bubble meter. The source of the SO_2-free air used in the dilution system was compressed breathing quality air which underwent a 2-stage chemical scrubbing optimized to remove sulfur gases. The first stage of the scrubber was a packed bed of Purifil (Purifil Inc., Doraville, GA), followed by a packed bed of Puricarb (Purifil, Inc.). The SO_2-free

air was then filtered with a 47 mm Teflon filter to remove particulate matter.

The performance of the CSD was evaluated using modulation frequencies ranging from 2 to 60 cycles per minute (0.03 - 1.0 Hz). A series of 6 different sample gas compositions ranging from 0 to 900 pptv SO_2 was delivered over a period of 30 minutes. This series of experiments were designed to evaluate the ability of the CSD to make sensitive, high time resolved measurements. Signal-to-noise ratios for the CSD were also determined using a series of SO_2-free air and 500 pptv SO_2 in air measurements with different modulation frequencies. By evaluating the instrument using a broad range of modulation frequencies, the instrument's frequency dependent noise characteristics were studied and the instrument's response time determined.

Results and Discussion:

Response Characteristics:

The resulting time series from the experiments using 6 different SO_2 mixing ratios were plotted and compared. Figure 4.2 shows the resulting time series of raw detector signals read and recorded at 10 Hz, with 3 different solenoid modulation frequencies. The 2-cycle per minute (0.03 Hz) time series shows a distinct square wave pattern and the 4-cycle per minute (0.067 Hz) time series begins to resemble more of a sawtooth pattern. In both cases, it is easy to differentiate the frequency of the solenoid modulation from the time series and the changing levels of SO_2 in the sampled air. When the sampling rate is increased to 15-cycles per minute (0.25 Hz) and more solenoid valve modulations are

applied per unit time, the data resembles more a pattern of noise with changing amplitudes, but there is still a pronounced difference between the amplitudes observed with low mixing ratios compared to high mixing ratios.

In the 0.25 Hz data, the baseline of the measurement seems to increase with increasing SO_2 in the sample air. It is important to note that since this technique is a differential measurement, where the SO_2 mixing ratio is proportional to the difference between the signal from air with SO_2 and air without SO_2. As long as the instrument response to SO_2 is linear and does not change over time, baseline drift of the detector is unimportant at frequencies other than the modulation frequency. Although the shift in the data was not critical to the data collected with the technique, understanding it can offer insights to allow for full optimization of the technique. What appears to be a baseline shift associated with increasing SO_2 mixing ratios at 0.25 Hz modulation frequency has been determined to be caused by attenuation of the signal modulation. This effect is caused by the modulation frequency being faster than the total response frequency of the instrument. When the instrument is sampling the air containing SO_2, the solenoid valve switches to the air without SO_2. At faster modulation frequencies (0.25 Hz and faster) the valve switches from one channel to the other before the sampling train materials equilibrate allowing the detector to fully respond. The attenuation effect is illustrated Figure 4.3. The figure contains a 1Hz sine wave that simulates the signal of the CSD. The sine wave is then attenuated by either a 1 Hz or 0.5 Hz lowpass filter. When the sine wave is attenuated by a 0.5 Hz lowpass filter, there is a noticeable change in minimum signal seen in the times

series. The time constant of the filter (2 s) is too slow for the SCD to react fully to the change in the faster signal (1 Hz).

The attenuation is dependent on the modulation frequency of the solenoid that selectively samples between air containing SO_2 and air scrubbed of SO_2. The faster the modulation frequency, the more the attenuation. As shown in 0.25 Hz data in Figure 4.2, the period of the signal is noticeably faster than the equilibration time of the new air sample in the affected manifold tubing. The graph in Figure 4.4 shows the fraction of the total response that is detected in the CSD as a function of the solenoid modulation frequency and the response of the detector alone to pulses of SO_2 delivered at different frequencies. The response of the CSD falls off very quickly with increased modulation frequency, whereas the SCD response begins to fall off at a pulse frequency of about 2 Hz. What this means is that the CSD is not limited by the response time of the detector but rather the sample train of the CDS. If the equilibration time within the affected, or critical section of the denuder manifold can be reduced, the response time of the CSD will be improved. A faster equilibration time would allow a faster solenoid modulation frequency and faster SO_2 measurement time, without the loss of response due to attenuation.

The critical section of the manifold is shown in Figure 4.5. This section of the manifold is where air is sampled via a solenoid valve from the two gas streams. This critical area was identified early in the development of the CSD. The cause of this equilibration time-lag is the physical process of adsorption. Adsorption is caused by van der Waals forces or intermolecular electrostatic attraction between SO_2 and the molecules

at the inner surface of the manifold tubing. The amount of SO_2 adsorbed to the surface depends on the surface material and the mixing ratio of SO_2 in the sample stream. It is important to differentiate between physical *adsorption* and chemical *absorption*. Chemical absorption causes a chemical change, where the absorbed molecule forms a chemical bond with the surface. Physical adsorption is governed by electrostatic attraction and is a much weaker attraction than that of the chemical bond formed in absorption. A portion of the SO_2 adsorbs to the inner surfaces of the Teflon tubing in the critical section of the manifold. This adsorption process causes a "memory effect" or delay in the response of the detector to the SO_2 in the sample air, which contributes to the equilibration time. When the SO_2-free air is sampled, the adsorbed SO_2 is released from the tubing into the SO_2-free sample air. This desorption also causes a delay in the detector response to the SO_2-free air, contributing to the equilibration time. This adsorption/desorption process can be minimized by reducing the interaction between the sample air and the manifold tubing. This can be accomplished by minimizing the "surface effects" of the critical section of the manifold. The surface effects can be reduced by minimizing surface area of the tubing, decreasing the residence time of the sample air within the tubing, or making the tubing surface less hospitable to the physical adsorption of SO_2.

In numerous revisions of the critical section of the manifold, the response time of the CSD was improved. The equilibration time was reduced by minimizing the surface area of the tubing and minimizing interactions between sample air and the inner surfaces of

the sampling train. In an attempt to further reduce the residence time of the sample in the manifold, a PFA Teflon solenoid valve was replaced with a PTFE Teflon valve because of the smaller internal surface area and volume of the PTFE valve. The smaller volume solenoid valve also improved the equilibration time. Since PTFE Teflon is quite porous, it is not the ideal material to use with SO_2 at low levels, as it does not equilibrate as quickly as a material such as PFA Teflon [Kuster and Goldan, 1987]. Further improvements in equilibration time could be realized by using a low-volume PFA Teflon valve, which we were unable to find from any manufacturer. The equilibration time may also be improved further by heating the tubing to decreases the adsorption of SO_2 on the Teflon surface. Reductions in the equilibration time may also be realized by increasing the sample flow rate through the critical section by adding an auxiliary pump between the solenoid and detector. This would decrease the residence time of the sample within the tubing, minimizing surface effects. Lastly, consideration of new materials for the wetted surface of the critical section may also decrease surface effects. A decrease in surface effects may be realized if a replacement for PFA Teflon is more compatible for use with low levels of SO_2. The -3dB response frequency of 0.4 Hz for the CSD as shown in Figure 4.4 is a noted improvement over earlier prototypes. Further improvements in the response time of the CSD will be realized if the proposed future modifications lead to reduced equilibration time.

Data Analysis and Deconvolution

Given the increased signal modulation frequency of the CSD, the simple averaging analysis technique employed with the DD/SCD was no longer efficient. To better deconvolute this information, a digital filtering routine based on a Fourier transform to create a power spectrum was developed.

In this algorithm, the time series was separated into sequential sub-sets. Each sub-set contained data from the same number of measurement cycles. The minimum size of the sub-set was limited to one full measurement cycle. Each sub-set was transformed into a power spectra via Fast Fourier Transform (FFT) algorithm. The signal power at the solenoid modulation frequency is obtained from the power spectra and used to quantify the instrumental response to SO_2. An example of the resulting power spectra from a time series obtained with this routine is shown in Figure 4.6. In this figure, 30 s of data from the CSD while sampling 500 pptv SO_2 in air is shown along with the resulting power spectra. This 30 s time series contains data acquired at 10 Hz, using a 0.25 Hz modulation frequency. Visual inspection of the time series reveals a low frequency modulation with higher frequency noise. Two power spectra are also shown in Figure 4.6. One in which 4 s of contiguous data were analyzed for power at the modulation frequency and the other with 20 s long subsets contiguous of data. the length of the data subsets is equivalent to integration time of the signal. The bin resolution of the 4 s integration time is less than that of the 20 s integration time. The resolution of a power spectrum is dependent on the sampling frequency and the number of data points in the data used to

compare the power spectra. The 4 s and 20 s power spectra contained 40 and 200 data points respectively. This results in a bin width of 0.125 Hz for the 4s and 0.025 Hz for the 20s integration times. The smaller sized bins are preferred because they exclude noise from frequencies close to, but not resulting from solenoid modulation. The noise exclusion leads to an enhanced signal to noise ratio. This advantage is more important as the signal-to-noise ratio of the measurement decreases. For instance, consider the power spectra in Figure 4.6. The response to 500 pptv SO_2 in the modulation frequency bin (0.25 Hz) is much larger than the response from noise at any other frequency. The noise component from the near-by frequencies are small compared to the response at 0.25Hz. Thus with high signal-to-noise ratios, a high resolution power spectrum has no significant advantage over that of a low resolution power spectrum because the signal dominates the noise. This changes dramatically when considering a time series with low signal to noise ratios. Figure 4.7 contains a 30 second sample of 0 pptv SO_2 obtained with a modulation frequency of 0.25 Hz and a data acquisition rate of 10 Hz. There is no discernable pattern in the time series. In the power spectra of the data with 4 s and 20 s integration times, noise from near-by frequencies becomes more important. By using a longer integration time and obtaining higher bin resolution in the power spectrum, the noise component of the power at the modulation frequency (0.25 Hz) is reduced. By using a low resolution power spectra with low signal-to-noise ratios, the added noise from near-by frequencies will result in a noticeable positive offset, or positive y-intercept in calibration curves.

Considerations in using a Power Spectrum

A potential problem with using a FFT-based power spectrum for this type of application is the assumption that the data consists of sine waves of different frequency and amplitude. Square wave and sawtooth patterns that have been transformed with a power spectrum routine tend to have shoulder peaks at harmonics of the modulation frequency. This effect would certainly be more noticeable in the data with a lower modulation frequency such as 2 min^{-1}, where the data resembles more of a square wave than a sinusoidal pattern. Since we are interested in obtaining near real-time measurements of SO_2, the primary interest is in faster modulation frequencies. In the extensive analysis of data acquired with modulation frequencies 0.25 Hz and higher, there has been no significant artifact due to the lack of an ideal sine wave in the data. The graph in Figure 4.8 demonstrates what the resulting power spectrum of a 0.25 Hz sine wave, square wave and sawtooth pattern looks like. Each of these patterns had the same amplitude and the resulting powers have been normalized to unity with the power of the sine wave. The FFT of the sine wave has only one peak, which is at the modulation frequency. The FFT of the sawtooth pattern results with a power of roughly half of the power in the FFT of the sine. The square wave pattern FFT results in a power that is roughly1.6 that of the sine wave. The reason for the difference in power at the modulation frequency is due to the amplitude of the sine wave that best represents the pattern. The amplitude of a sine wave that best-fits a square wave pattern has a larger amplitude than the original square wave. The sine wave that best fits a sawtooth pattern

has an amplitude that is smaller than that of the sawtooth pattern. What this means is that a sine, square and sawtooth pattern with the same amplitude will have different power in the modulation frequency when transformed using a FFT-based power spectrum. The power in the different harmonics of the modulation frequency are also dependent on the type of waveform. The sawtooth pattern has a beat at each multiple of the modulation frequency. The power from the square pattern shows a beat at every other multiple of the modulation frequency. In evaluating the power spectra from the CSD at a 0.25 Hz modulation frequency, there appears to be a small response in the 0.75 Hz bin and nothing noticeable in the 0.50 Hz bin. This would suggest that the response from the CSD better resembles a square wave than a sawtooth. The discussion of the non-ideal nature of the response is interesting, but not critical to the technique. The response to different mixing ratios of SO_2 using this analysis technique was linear from 0 to over 2000 pptv, suggesting that the waveform shape does not change with increased SO_2 mixing ratios. In the worst case, some of the power from the CSD response pattern may be lost in some of the shoulder peaks in the power spectrum. As demonstrated in Figure 4.6, the power in the 0.75 Hz bin is small (about 10%) compared to the 0.25 Hz modulation frequency. It may be possible to enhance the sensitivity of the technique by including the power from the 0.75 Hz bin in the analysis. This idea has not been investigated, however it would only be beneficial if the added signal from the harmonic was significantly greater than the added noise. Thus, improvements in sensitivity of the technique by including harmonics of the modulation frequency would only be achieved when analyzing samples that already

contain a high signal to noise ratio.

Converting power to response

The power spectra used in our analysis algorithm is a two-sided spectra where the real and imaginary parts of the solution are "folded over." To obtain the analytical response, we must take the square-root of the power. This results in a linear response to SO_2 over mixing ratios ranging from 0 to over 1000 pptv. Once the response to SO_2 was quantified for integration time, the response from each is recombined into a time series. A graph of the deconvoluted SO_2 response for the 0.25Hz modulation frequency is shown in Figure 4.9. The deconvoluted time series also demonstrates the advantage of having the option to post-process the data. The first graph shows the results of the power spectra routine when one integration time contains only one modulation cycle. At 0.25 Hz modulation, the cycle is 4s in length. Since each integration time must include at least one full cycle, this defines the fastest response time for the instrument at that modulation frequency. With a 4s integration time containing only one measurement, the noise level is quite high. In the following two graphs with 12 and 20 second integration times, each integration time contains 3 and 5 measurement cycles respectively. The precision of the measurement increases as the number of measurement cycles per integration time increases. This improvement in the precision of the measurement is proportional to the inverse of the square-root of the number of measurements (n) per sub-set, as predicted by statistics [Davore, 1991]. The improved precision with longer integration time comes at

the expense of temporal resolution. What this means is that the data analysis can be optimized for the environmental conditions after the data has been acquired. The analysis can be optimized for fast response time by choosing an integration time containing only one measurement cycle. If sensitivity to low SO_2 mixing ratios is required, the precision can be improved by using a longer integration time, containing multiple measurement cycles.

Sensitivity and modulation frequency

As discussed previously, the response to SO_2 is dependent on the modulation frequency of the solenoid valve in the CSD. At faster modulation frequencies, the response of the CSD is attenuated due to equilibration affects in the tubing. An improvement in the precision of the measurement with increased integration time during data processing was also described. To understand the sensitivity of the instrument, it is important to separate and compare these two effects. The graph in Figure 4.10 shows the detection limit of the instrument, as defined by three times the standard deviation of the noise. The noise of the measurement was defined as the response to 0 pptv SO_2 at the modulation frequency, over a period of 8 min. The analysis was performed for each of the 6 modulation frequencies that were evaluated. The analysis was also conducted using 4 different integration times. As shown in Figure 4.10 there is an improvement in the detection limit with longer integration times. The improvement is roughly proportional to the square-root of the number of measurement cycles contained in the data set.

Interestingly, the data shows no improvement in detection limit with increasing modulation frequencies. One might expect an improvement due to the increased number of measurement cycles per unit time with faster modulation frequencies. One explanation for this is that the attenuation of the response that occurs with increasing modulation frequencies, offsets the improvement expected from having more modulation cycles in the data. If the attenuation of the signal can be reduced, it is probable that an improvement in detection limit would be achieved with faster modulation frequencies.

Another interesting effect seen in the graph is the improved signal to noise ratios with the 4s and 8s integration times at 15 cycles min^{-1} (0.25 Hz) compared to other modulation frequencies with the same integration time. It is possible that this frequency contains a smaller noise component than the others evaluated in this experiment. Understanding the frequency of the noise is important in optimizing the signal-to-noise ratio. Choosing a modulation frequency where the noise is minimal, while maintaining instrument response to SO_2 enhances the signal-to-noise ratio and therefore the detection limit of the instrument. While the data in Figure 4.10 suggests that 0.25 Hz may be an optimum modulation frequency, the data is not sufficient for any certainty in this conclusion. The noise characteristics may change due to environmental conditions such as temperature or proximity to sources of electromagnetic noise. The evaluation of the instrumental noise is a continuous process. With regard to noise, more work is needed to define an optimum modulation frequency for the operation of the CSD.

Conclusions:

The CSD is a new instrumental technique for measuring SO_2 at low pptv levels. It is based on the analytical principles of the DD/SCD, a robust and sensitive technique that has been evaluated in two rigorously blind evaluations. The new instrument represents a significant improvement over the state-of-the art techniques, in that it can measure SO_2 in the 10s of pptv in less than a minute. In comparison, the fastest technique evaluated in the GASIE campaigns required 4 minutes for the same measurement. The CSD is still in the development stage and it is possible that further improvements in sensitivity and measurement time can be realized. The novel data analysis technique employed can efficiently quantify the instrument response to SO_2, while excluding noise. The analysis routine is also very versatile and can be optimized for the atmospheric conditions that were encountered by the instrument after the data has been collected. The advantage of post-processing the data is significant since the analysis can be optimized for high sensitivity to SO_2 when the ambient mixing ratios are low. If the mixing ratio of SO_2 is high, sensitivity can be traded for measurements with better time resolution. The CSD is also an ideal technique for field measurements since it is straightforward in design and does not require cyrogenic materials, which can be difficult to handle in field deployment. Having a near real-time, versatile and field ready instrument for the measurement of SO_2 is especially important for moving vehicle or aircraft based campaigns. A fast response technique would also be beneficial for observing dynamic processes in the atmosphere such as gas-to-particle conversion, scavenging, oxidation and deposition velocities.

Measurements of this type would allow for new research in atmospheric chemistry and the study of biogeochemistry over large geographic areas.

Table 4.1 Summary of detection limits and sampling times for the instruments evaluated in the GASIE campaigns.
The two numbers for limit of detection define a range of sensitivity as determined by an impartial oversight committee. The detection limits stated are specified for the corresponding sample time.

Method	Limit of Detection (pptv)	Sample Time	Method Type
Aqueous Chemiluminescence	20 to 40	10-35 min	preconcentration
Modified (TECO) pulsed fluorescence	20 to 40	25 min	signal averaging
Isotope Dilution/GC/MS	0 to 20	3-8 min	cyrogenic preconcentration with GC
Diffusion Denuder/SCD	0 to 30	10 min	differential
Fluorescence/HPLC	0 to 20	4 min	preconcentration with HPLC
Carbonate Filter/IC	0 to 20	90 min	preconcentration with IC

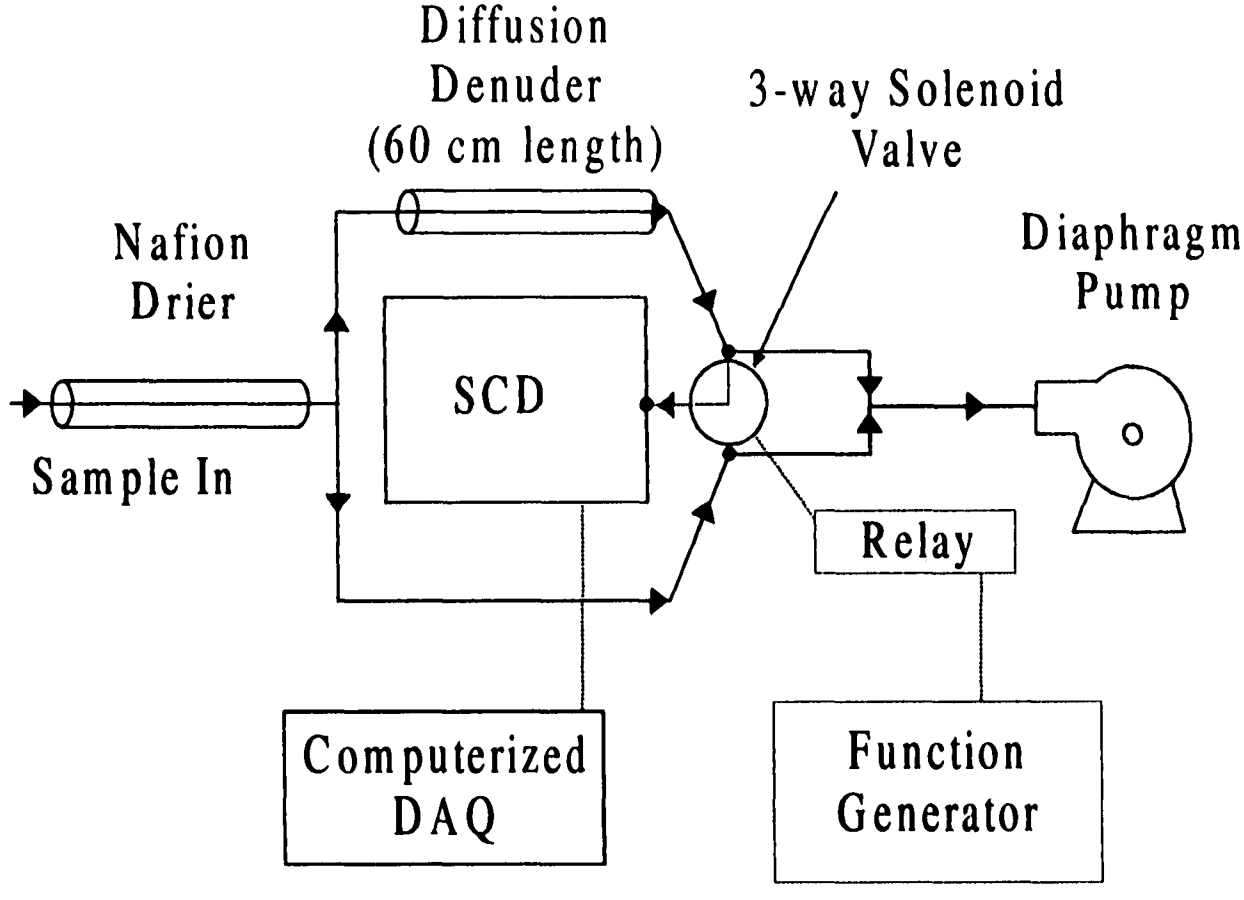

Figure 4.1 Schematic diagram of the Continuous SO_2 Detector (CSD).
The sample air is dried and split between two channels of the CSD sample train. The sample air flowing through the upper channel passes through a carbonate-coated denuder which selectively and quantitatively removes SO_2 from the sample air. The lower channel consists of a PFA Teflon tube, which does not remove SO_2. the 3-way solenoid valve alternately samples air from each of the two pathways. The sampled air is then detected by the SCD. The SO_2 mixing ratio is proportional to the difference in response between the air containing SO_2 and the air denuded of SO_2

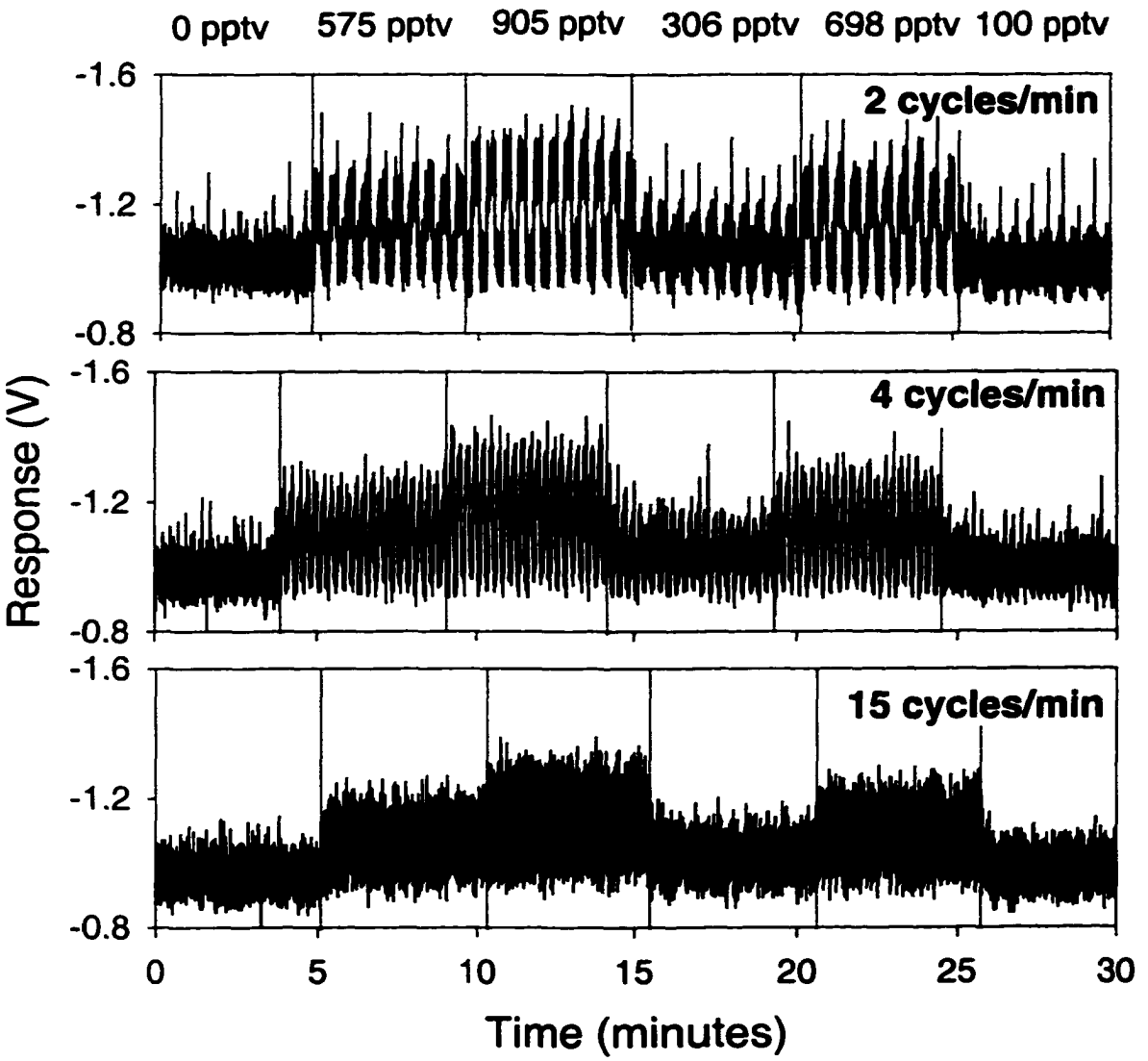

Figure 4.2 CSD response to different SO_2 mixing ratios using different modulation frequencies.

CSD response to 6 different SO_2 mixing ratios acquired at 10 Hz using different modulation frequencies is shown. A distinct pattern of high and low response is discernable in the 2 and 4 cycle per minute modulation frequency data. When the modulation frequency is increased to 15 cycles per min, the distinction between high and low is not obvious. The increase in amplitude of the response is proportional to the increase in the SO_2 mixing ratio. The response at 15 cycles per minute (0.25 Hz) is attenuated due to an equilibration effect, which results in an apparent baseline shift.

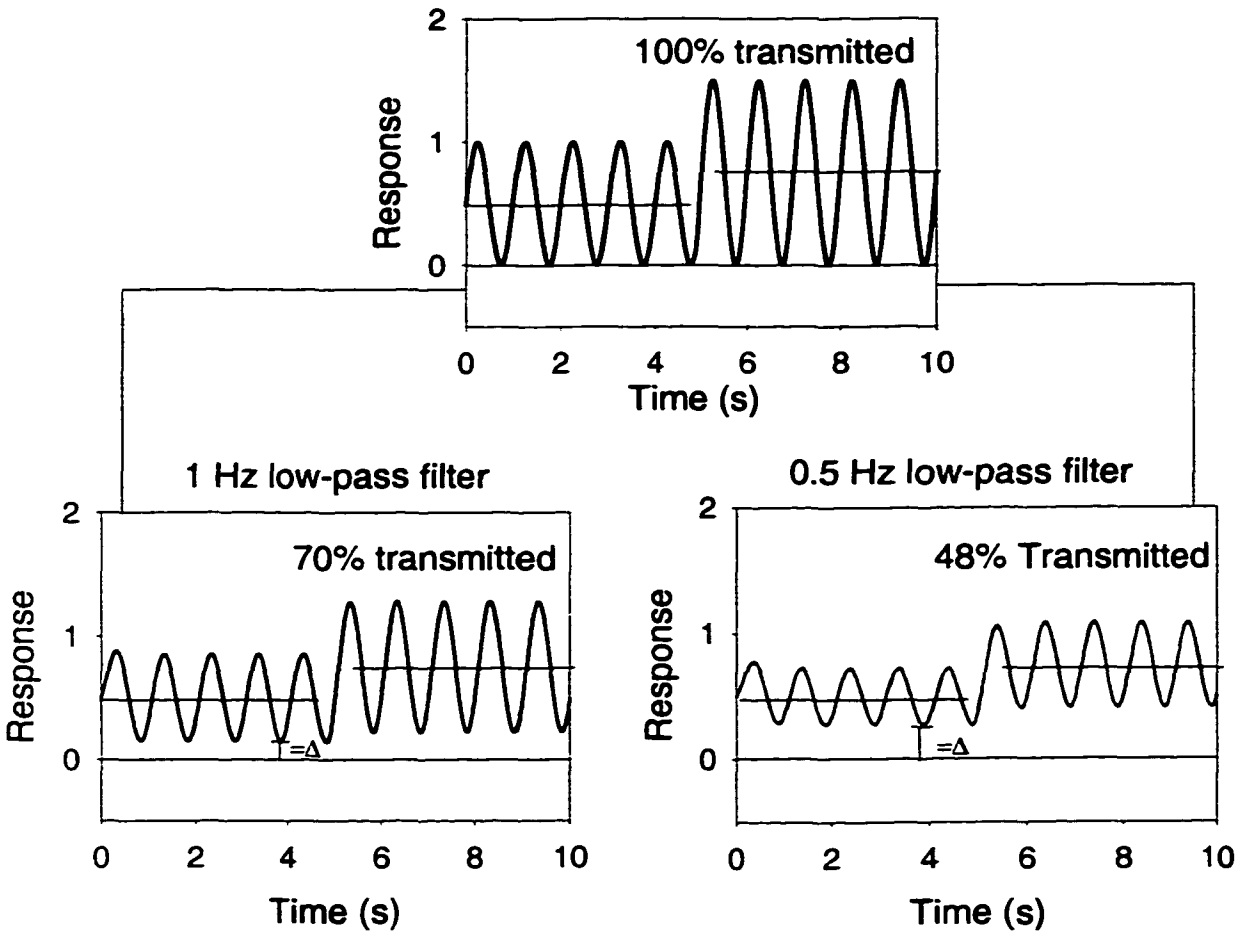

Figure 4.3 Example of an attenuation effect which creates an offset to the response of the CSD.

The 100% transmitted 1 Hz sine wave is an idealized response from the CSD. When the amplitude of this sine wave increases, as it would with increasing SO_2 mixing ratios, while the minimum value of the sine wave remains at zero. When this same sine wave is attenuated using a low-pass filter, the minimum value of the sine wave increases When the sine wave is attenuated using a low-pass filter. Δ is the offset of the minimum signal caused by attenuation of the sine wave.

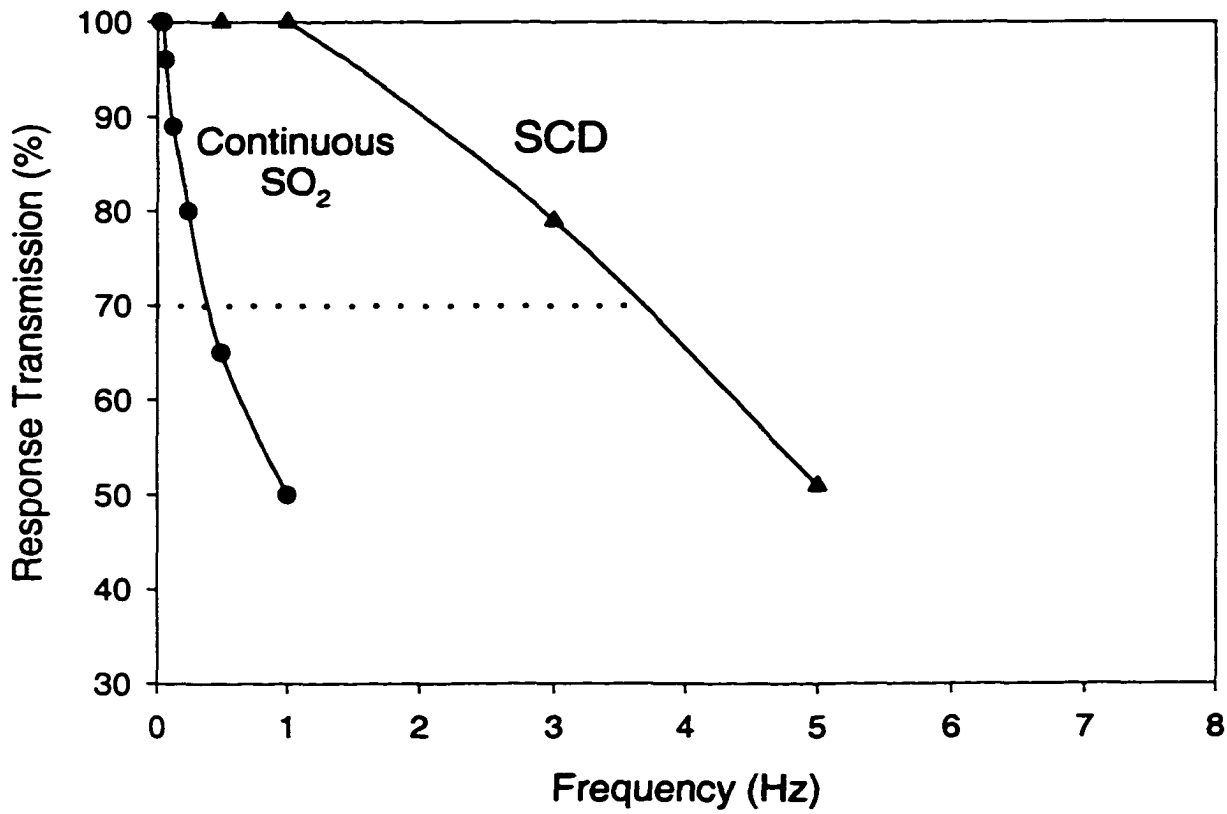

Figure 4.4 Comparison of response characteristics of the CSD and the SCD. The dotted line is where the signal has been attenuated by 30% which is also known as -3 dB . As the solenoid modulation frequency increases, the response of the CSD is significantly attenuated (-3 dB at 0.4 Hz). In comparison, the SCD has a -3 dB attenuation at about 4 Hz. This means that the CSD is not limited by the response time of the detector.

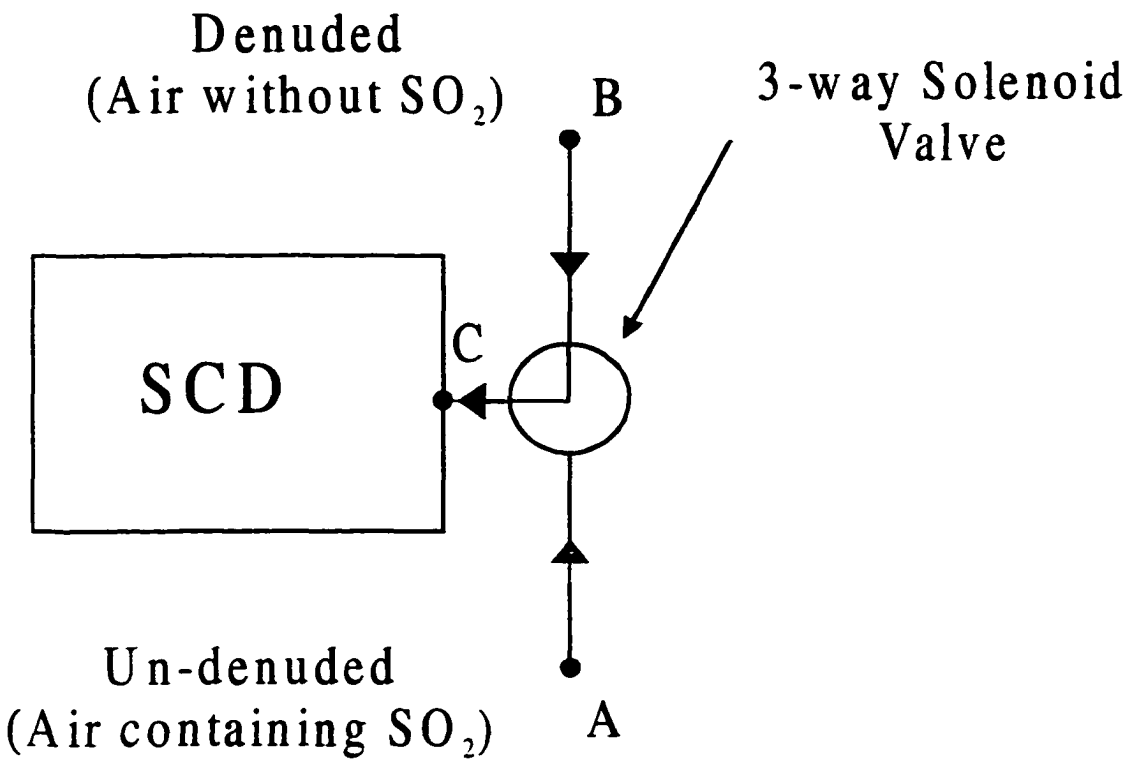

Figure 4.5 The critical section of the CSD manifold.
The equilibration effect that results in the attenuation of response at higher switching frequencies originates from this section of the CSD manifold. This is where the 3-way solenoid valve alternately samples from the two sample stream pathways in the CSD manifold. The diagram shows the solenoid valve position sampling air that has been scrubbed of SO_2 by the diffusion denuder. By minimizing the interactions between the sample air and the wetted surfaces in this section of the manifold, the equilibration time was improved, which resulted in an improvement in the response time for the CSD.

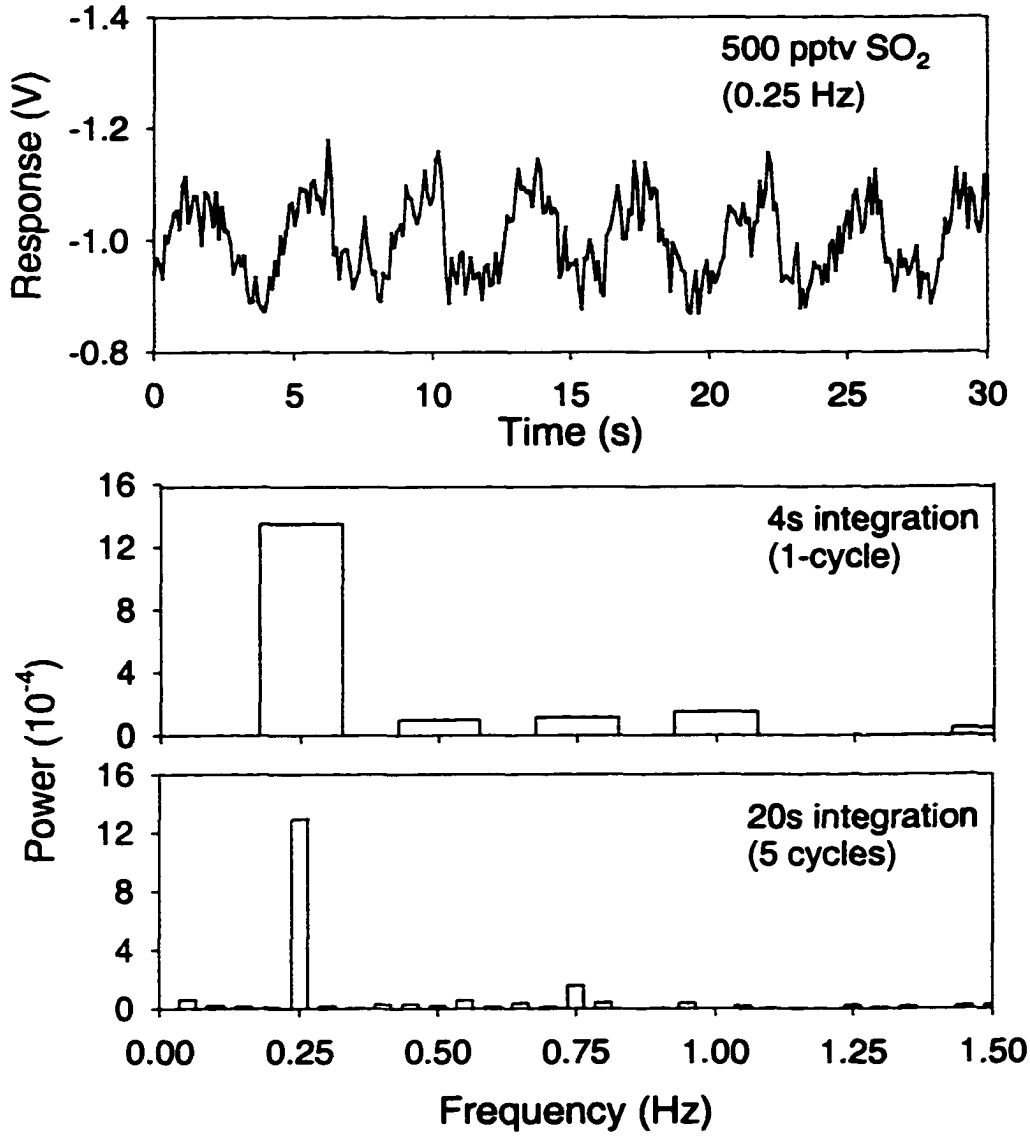

Figure 4.6 CSD response to 500 pptv SO_2 and the resulting power spectra for 4 and 20 second integration times.

A subset of a CSD time series and the results of a power spectrum transform using a 4 and 20 second integration time. There is a significant response at 0.25 Hz switching frequency from the 500 pptv SO_2 sample air. This digital filtering technique successfully excludes noise from higher frequencies. As the integration time increases, the resolution of the power spectrum obtained from an FFT improves so that noise from near-by frequencies are not included in the response.

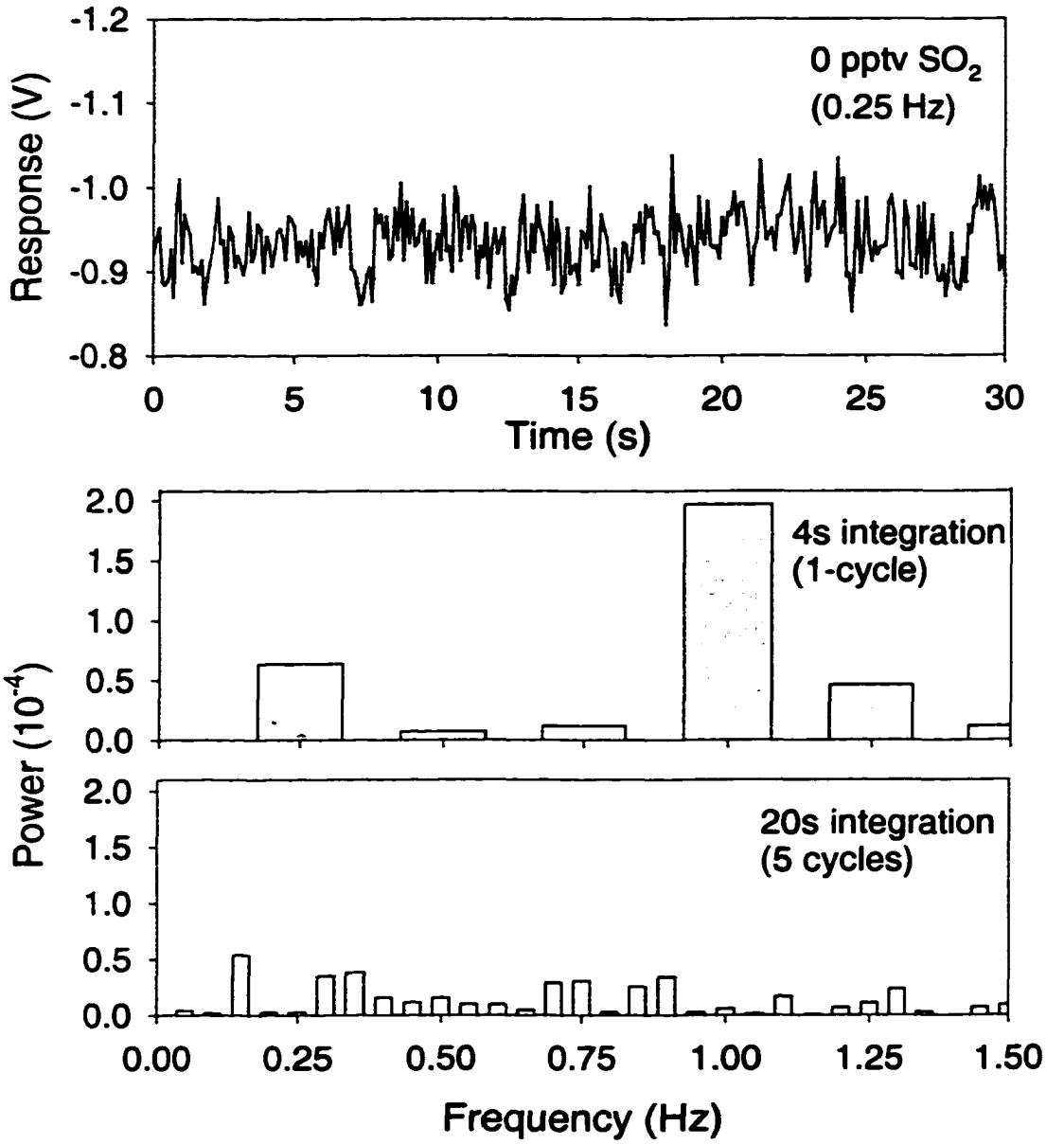

Figure 4.7 CSD response to 0 pptv SO_2 and the resulting power spectra for 4 and 20 second integration times.

Power spectrum at low signal-to-noise ratios. With sub-sets of data containing response from low mixing ratios of SO_2 the better bin resolution associated with longer integration times becomes important. The wide bandwidth associated with the 4 s integration time includes more noise from near-by frequencies than the narrow bandwidth of the 20 s integration time. The 4 s integration time will result in a zero-offset or positive y-intercept when the response is plotted against the SO_2 mixing ratio of the sample air.

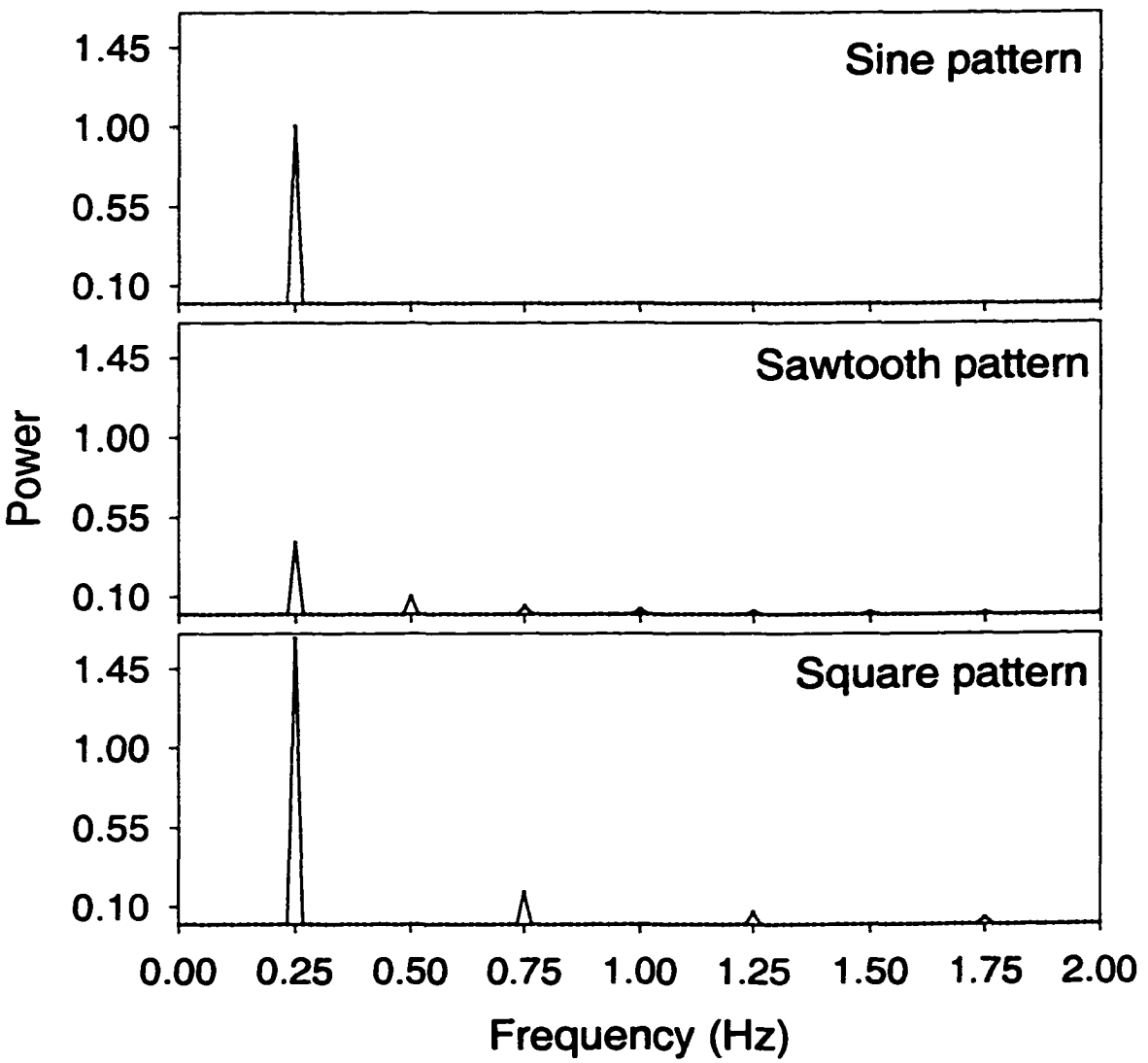

Figure 4.8 Comparison of power spectra for sine, sawtooth and square pattern waveforms.
Each of these waveforms had a modulation frequency of 0.25 Hz and an amplitude of 1. The power spectrum of a sine wave shows all of the power at the modulation frequency. The sawtooth and square patterns have most of the power at the modulation frequency, but do contain power in harmonic frequencies as well. The sawtooth pattern has harmonics at every multiple of the modulation frequency, which the square wave has harmonics at every other multiple. The magnitude of the power was normalized to the power spectra of the sine wave.

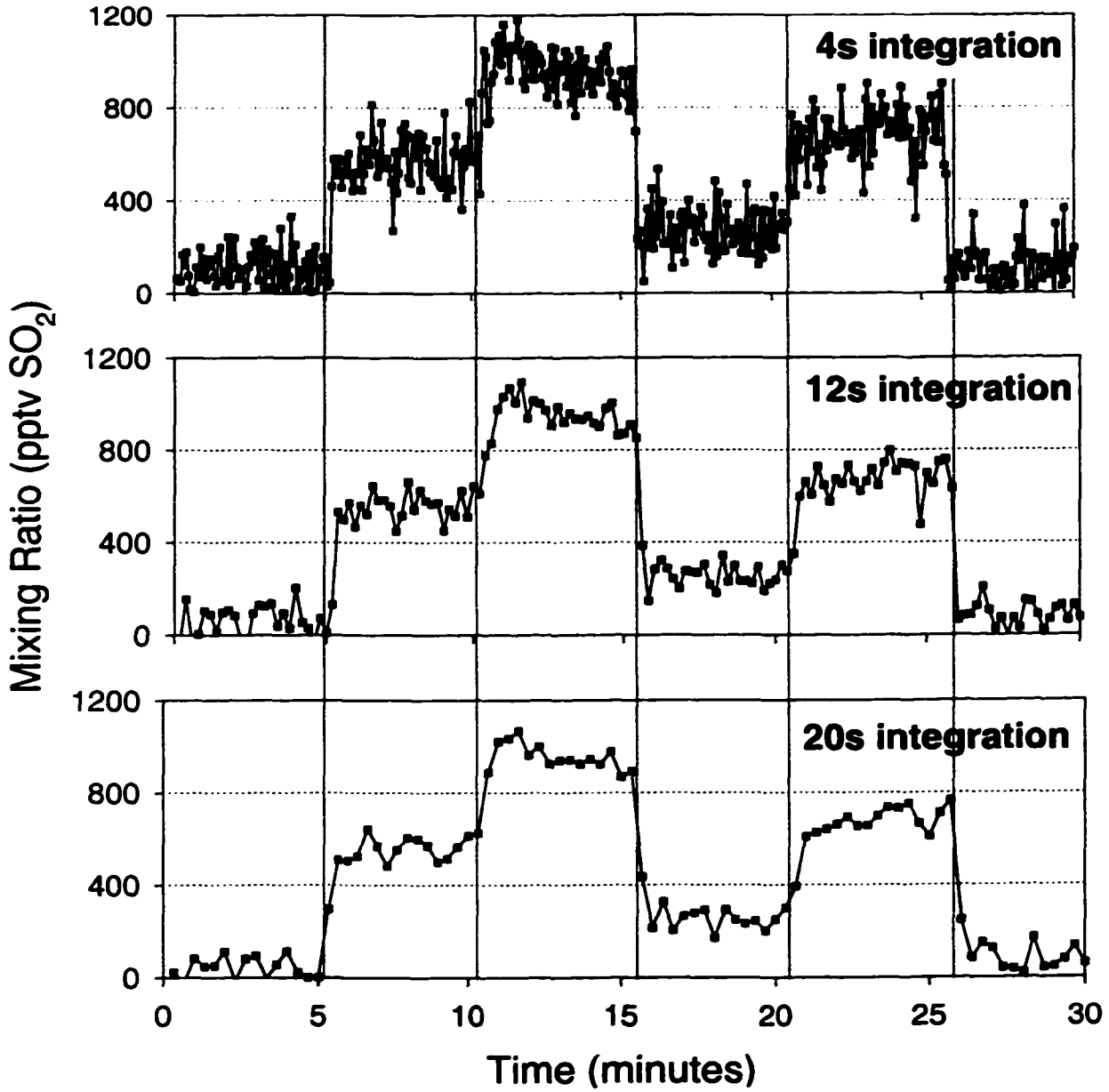

Figure 4.9 Analysis of the 0.25 Hz modulation frequency data using different integration times for the power spectra.
The graphs demonstrate both the versatility of the digital filtering technique and the ability of the CSD to measure trace-levels of SO_2 on a very short timescale. The analysis using a 4 s integration time includes a high level of noise. As the integration time is increased, the noise level is reduced. The integration time can be chosen after the data has been collected, optimizing for either sensitivity or response time. Even with the longer 20s integration time, the CSD has a sampling time that is over 10 times faster than any of the instruments evaluated in the GASIE campaigns. In the same 30 min time span, the DD/SCD would have made only 3 SO_2 measurements.

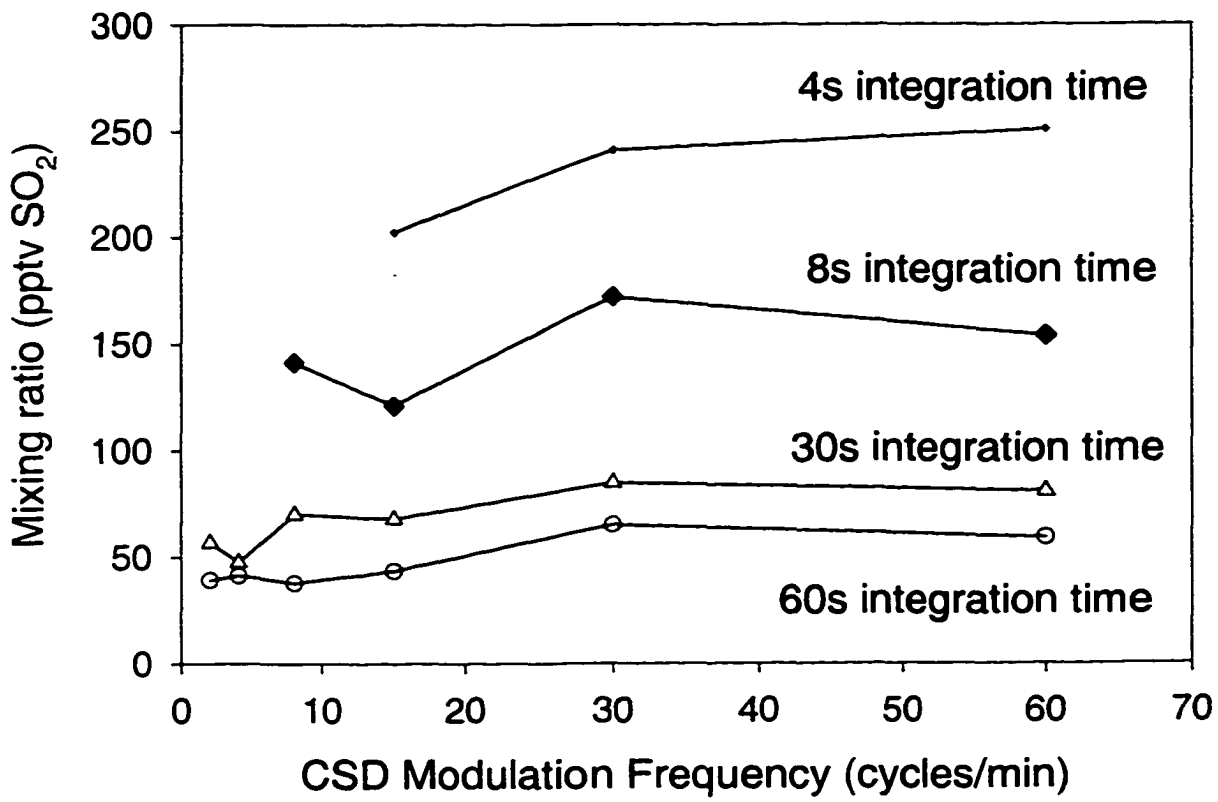

Figure 4.10 Limit of detection for the CSD for different integration times and modulation frequencies.
The limit of detection was defined as 3 times the standard deviation of the noise at 0 pptv SO_2. The graph shows that the precision of the measurement is better with longer integration times. The improvement is roughly proportional to the square-root of the number of samples (n) contained in the sub-set of data, as would be predicted by statistics. It is interesting to note that there is no significant improvement in precision with increasing modulation frequencies.

Chapter 5

Summary and recommendations for future work

The development and testing of the DD/SCD, dynamic dilution system and CSD make up a complete suite of instruments for the measurement of SO_2 in the atmosphere. The DD/SCD has been rigorously evaluated in the GASIE-2 blind comparison. The results from this comparison demonstrate that the DD/SCD is a successful technique with minimal to no interferences and sensitivity comparable to other state-of-the-art SO_2 instruments. The work from the intercomparisons represents a significant improvement in SO_2 detection technology. GASIE and GASIE-2 demonstrated that the instruments had good correlation, even in the sub-100 part per trillion by volume (pptv) range. This is a noted improvement over a previous study where the instruments had no correlation for mixing ratios less than 200 pptv.

A dynamic dilution system was developed for fabricating calibration standards of reactive gases, such as SO_2. The dilution system is versatile, portable and easy to use. It is designed so that both compressed gas and/or permeation devices can be used as the source for standard gas. The system is designed such that the only wetted surface the resulting calibration gas comes in contact with is Perfluoroalkoxy (PFA) Teflon®. The dilution system is fully automated and computer controlled. The automated multi-point calibration routine saved over 100 hours of operator time in one field campaign alone. The dilution system was used to calibrate the DD/SCD during the entire GASIE-2

campaign. During GASIE-2, the calibration system fabricated SO_2 calibration gases with mixing ratios ranging from 0 to 250 pptv. This represents dilution factors of up to 0.3 x 10^6, with a relative standard deviation of ± 5%.

The Continuous Sulfur Dioxide Detector (CSD) is a sensitive, high time resolution instrument for reliable measurements in the atmosphere. This new technology is based on the DD/SCD, a successful SO_2 measurement technique involving sulfur chemiluminescence detection (SCD) that has been validated in a rigorously blind experiment sponsored by the National Science Foundation (NSF). Due to the sensitivity of the SCD, efficient denuder separation technology and optimized pneumatic system, the CSD is capable of measuring trace levels (<100 pptv) of sulfur dioxide on the order of seconds. Novel digital signal processing with phase-locked amplification of the detector signal enhances the precision and temporal resolution of the CSD. By recording the raw detector signal at 10 Hz the data retrieval can be optimized for any particular application by modifying the parameters used in the data processing. The analysis can therefore be tailored to the environmental conditions, enhancing signal-to-noise ratio when sulfur dioxide levels are low and optimizing for temporal resolution when levels are high. The instrument has advantages over existing technologies such as chromatography in that it provides accurate and reliable measurement of low pptv sulfur dioxide in sub-minute time resolution. The high temporal resolution and sensitivity of the CSD allows for more detailed study of the atmosphere from a moving platform such as an aircraft. The CSD has applications in many fields where sulfur dioxide is found in air, including process stream

monitoring, pollution source monitoring and pollution receptor/compliance monitoring as required by the Clean Air Act.

Recommendations for future work:

Atmospheric measurements:

The development of these instruments in the laboratory is just the beginning of a work in progress. Now that a complete suite of instruments exists for the measurement of SO_2 in the atmosphere, the next step is to deploy these instruments to obtain field measurements. The integration of the DD/SCD and dynamic dilution system would be best suited for measurements from a stationary ground based sampling platform. The sensitivity of the DD/SCD is such that it can be used to measure natural background levels of SO_2, which can be as low as 10 pptv.

The CSD is capable of measuring SO_2 at levels as low as 50 pptv in less than one minute. Previously, high-time resolved measurements of SO_2 in the atmosphere were limited to polluted air masses with mixing ratios of at least a few ppbv. Averaging times of a few seconds with a modern UV-pulsed fluorescence detector yield a standard deviation of close to 1 ppbv SO_2 and a detection limit (2σ) of 300 pptv for a 30s average [Ryerson, et al., 1998; Hübler, et al., 1998]. For a 30 s average, the CSD has a detection limit (2σ) of about 50 pptv. The CSD represents a significant improvement in near real-time SO_2 measurements.

Near real time measurements of atmospheric SO_2 would benefit future studies of

the atmospheric chemistry of sulfur. The fast response of the CSD would be beneficial for observing dynamic processes in the atmosphere such as gas-to-particle conversion, scavenging, oxidation and deposition velocities. The sensitivity of both the CSD and DD/SCD would allow for new research into the natural oxidation of biogenic sulfur gases to SO_2, by determining ambient mixing ratios of SO_2 in remote, unpolluted locations. This research would add to a better understanding of the atmospheric cycling and biogeochemistry of sulfur.

The dynamic dilution system:

The automated dynamic dilution system developed as part of this Thesis work is a very useful tool. The dilution system can be improved with better control of the calibration gas flow. A more precise and accurate calibration gas flow would ultimately increase the precision and accuracy of the resulting calibration air. Since the dilution system works with SO_2, it is probable that other reactive trace gases may also be used with this dilution system. Further research into the use of this dilution system with other reactive trace gas species may be a worthwhile endeavor.

Further study of the flow rate reproducibility and stability of the mass flow controllers is important. The evaluation of this dilution system was conducted over the course of a few months. A long term study of these issues is important for understanding the characteristics of this dilution system.

Although the internal calibration routine has been used multiple times, it can be

improved with further automation. This can be achieved by better incorporating the internal calibration routine into the dynamic dilution system control software.

Since the dynamic dilution system is automated and computer controlled, the software can be improved in order for the instrument to be operated remotely. By adding TCP/IP functionality, the dilution system could be completely controlled via the Internet. With Internet capabilities, the operator could also check the measured ambient mixing ratios of SO_2 at any time. The calibrations could then be tailored so that the mixing ratios of calibration gas cover the range of observed ambient SO_2.

The results from GASIE demonstrate the there is a significant discrepancy between the calibration methods and/or supplies used by the different investigators during the experiment [Stecher et al., 1997). The discrepancy in calibration resulted in an added uncertainty of about ± 25% for mixing ratios less than 250 pptv SO_2. The precision of the individual analytical techniques used in GASIE was much better than ± 25%, suggesting that the accuracy of the techniques is limited to the uncertainty in the accuracy of the calibration gases. The accuracy of the calibration gases is a function of the dilution system, as well as the standard gas source used. By using the same standard gas source with different dynamic dilution systems, the error from the standard gas source can be isolated. It may then be possible to objectively compare and contrast different dynamic dilution schemes and identify systematic errors.

The Continuous SO_2 Detector:

There are many possible improvements for the CSD. As mentioned in this text, the response time of the instrument is not limited to the response time of the detector, but to a physical adsorption or memory effect within a critical section of the manifold tubing. If the memory effect within this critical section of the manifold can be reduced, the response time of the technique may be improved. Improving the response time of the CSD is important because it would allow for a faster SO_2 measurement. The faster measurement would also improve the detection limit, as more measurements per unit time could be averaged.

A continued study of the instrumental noise may lead to improvements in the detection limit of the instrument. If the optimum low-noise region can be defined within the 0-4 Hz operating frequency, the instrument could be operated at region, which would improve the signal to noise ratio.

Real-time measurements of SO_2 may also be achieved with the CSD technique by running two detectors in parallel. In this configuration, information from both the SO_2 containing and SO_2-free sample air channels would be recorded simultaneously. In order for the dual channel CSD to work, there are many challenges that need to be met. Changes in the instrument's baseline response would have to be accounted for on both detectors. Similarly, changes in the response to sulfur gases would also have to be accounted for. Baseline drift may be accounted for by alternating the sample flows from one SCD to the other. By periodically alternating the SCD sample flows, each detector

will measure the SO_2-free air for a specified period of time. This will establish a baseline for which to compare the air containing SO_2 and should account for any changes to the baseline in either of the two SCDs. In order to monitor the response to sulfur for the two SCDs, they would have to be routinely calibrated. Between calibrations, an internal standard may be added periodically to the sample gas stream. If a gas such as SF_6 were added to the sample gas stream, it would not be removed by the denuder. The response to a known amount of SF_6 could then be compared and changes and differences in the instrument response could be accounted for.

Another difficulty in using a dual detector CSD is the increased costs associated with such a configuration. The cost of this technique is primarily the cost of obtaining and operating a sulfur chemiluminescence detector, the cost of a dual detector system effectively doubles the cost of the instrument. The operation, maintenance and calibration time also increases with the addition of a second detector.

If the difficulties of a dual channel continuous SO_2 detector can be overcome, the benefit of real-time SO_2 measurements in the low pptv range may be well worth the additional cost. Currently, there is no analytical technique capable of these measurements with a 1Hz sampling time. If the surface effects of SO_2 on the sampling train can be minimized, the sampling time of a dual channel CSD would be limited to about 4 Hz, which is the response time of the SCD itself.

Future studies with diffusion denuders:

The source of the "unknown sulfur gas" being emitted from the CO_3^{2-} denuder with humid air is perplexing. Since this effect was noticed with a CO_3^{2-} denuder which was significantly loaded with SO_2, it is probable that the source of emission would be a SO_4^{2-} /SO_3^{2-}/HSO_3^- system which changes under humid conditions. Further studies with the CO_3^{2-} diffusion denuder under humid conditions are warranted. An extensive search of the literature revealed no previous problems with diffusion denuders, or CO_3^{2-} coatings with humidity. One study on the inhalation of aerosols which described a SO_3^{2-}/HSO_3^- aerosol generation system, observed the formation of SO_2 from a bulk solution as well as SO_3^{2-} aerosols [Dasgupta et al., 1980]. If this system can be applied to the CO_3^{2-} denuder chemistry, then it may offer new insight into the emission of this unknown sulfur gas.

If the unknown sulfur gas emission is due to chemistry involving the thermodynamically less-stable S(IV) oxidation state, than this problem may be resolved with the addition of an oxidizing agent such as H_2O_2 to the CO_3^{2-} denuder coating. The added oxidant could further oxidize the S(IV) to S(VI), which would make it more thermodynamically stable, as less apt to be re-emitted as a sulfur gas.

Understanding the chemistry of the CO_3^{2-} denuder and other CO_3^{2-}-based SO_2 collection schemes and the observed sulfur gas emission under humid conditions may alter current and historical air quality measurements. For instance, emission of an unknown sulfur gas also occurs when using a CO_3^{2-} filter technique, the loss of sulfur from a CO_3^{2-} filter would result in a measurement which was biased-low. In GASIE, the filter/IC

method did indeed show about a 20% loss in sulfur under humid conditions. The use of the CO_3^{2-} filter technique is widespread, especially for long term average measurements of atmospheric SO_2.

The collective work presented in this Thesis represents a significant contribution to the field of atmospheric chemistry. Previously, measurements of 10's of pptv SO_2 have not been achieved on time scales of less than a few minutes. This makes the sensitivity and fast response of the CSD especially exciting. This instrument in concert with the dynamic dilution system may lead to a better understanding of the sources, sinks and chemical processes of sulfur in the atmosphere.

References:

Andreae, M. O., The Ocean as a Source of Atmospheric Sulfur Compounds, In: The Role of Air-sea Exchange in Geochemical Cycling, *edited by* Buat-Menard, pp 331-362, D. Reidel, Norwell, Mass., 1986.

Andreae, M. O., and P. J. Crutzen, Atmospheric aerosols: Biogeochemical sources and role in atmospheric chemistry, *Science, 276*, 1052-1058, 1997.

Bandy, A. R., D. C. Thornton and A. R. Driedger III, Airborne measurements of sulfur dioxide, dimethyl sulfide, carbon disulfide and carbonyl sulfide by isotope dilution gas chromatography/mass spectrometry, *Journal of Geophysical Research, 98,* (D12), 23,423-23,433, 1993.

Benner, R.L., Development of the sulfur chemiluminescence detector, Ph.D. Dissertation, University of Denver, Denver, CO, 1991.

Benner, R.L. and D.H. Stedman, Universal sulfur detection by chemiluminescence detector, *Analytical Chemistry*, 61, 1268-1271, 1989.

Benner, R.L. and D.H. Stedman, A field evaluation of the sulfur chemiluminescence detector, *Environmental Science and Technology*, 24, 1592-1596, 1990.

Benner, R. L., J. Wu, and D. K. Nicks Jr., Development and evaluation of the diffusion denuder-sulfur chemiluminescence detector for atmospheric SO_2 , *Journal of Geophysical Research, 102,* (D13), 16,287-16,291, 1997.

Boatman, J. F., M. Luria, C. C. Van Valin, and D. L. Wellman, Continuous atmospheric sulfur gas measurements aboard an aircraft: A comparison between the flame photometric and fluorescence methods, *Atmospheric Environment, 22*, (9), 1949-1955, 1988.

Bunce, N., Environmental Chemistry, Wuerz Publishing Ltd, Winnipeg, Canada, 1991.

Cullis, C. F., and M. M. Hirschler, Atmospheric Sulphur: Natural and Man-made Sources, *Atmospheric Environment, 14*, 1263-1278, 1980.

Charlson, R. J., Langer, J., Rodhe, H., Leovy, C. B., and Warren, S. G., Perturbation of the norther hemisphere radiative balance by backscattering from anthropogenic sulfate aerosols. *Tellus, 43ab*, 152-163, 1991.

Charlson, R.J., J.E. Lovelock, M.O. Andreae and S.G. Warren, Oceanic phytoplankton, atmospheric sulfur, cloud albedo and climate, *Nature, 326*, 655-661, 1987.

Charlson, R. J., Schwartz, S. E., Hales, J. M., Cess, R. D., Coakley, J. A., Hansen, J. E., and Hofman, D. J., Climate Forcing by Anthropogenic Aerosols, *Science, 255*, 423-430, 1992..

Dasch, J. M., S. H. Cadle, K. G. Kennedy, and P. A. Mulawa, Comparison of annular denuders and filter packs for atmospheric sampling, *Atmospheric Environment, 23*, 2775-2782, 1989.

Dasgupta, P. K., A diffusion scrubber for the collection of atmospheric gases, *Atmospheric Environment, 18*, (8), 1593-1599, 1984.

Dasgupta, P. K. and T. R. Duvall, Study of bisulfite and metabisulfite aerosol generation systems, *American Industrial Hygiene Association, 41*, 666-671, 1980.

Davore, J. L., Probability and Statistics for Engineering and Science, 3rd ed., Duxbury Press, Belmont, CA, 1991.

Driedger III, A. R., D. C. Thornton, M. Lalevic and A. R. Bandy, Determination of part-per-trillion levels of atmospheric sulfur dioxide by isotope dilution gas chromatography/mass spectrometry, *Analytical Chemistry, 59*, 1196-1200, 1987.

Dockery, D. W., C. A. Pope III, X. Xu, J. D. Spengler, J. H. Ware, M. E. Fay, B. G. Ferris Jr, and F. E. Speizer, An association between air pollution and mortality in six U.S. cities, *The New England Journal of Medicine, 329*, (24), 1753-1759, 1993.

Eatough, D. J., L. J. Lewis, M. Eatough and E. A. Lewis, Sampling artifacts in the determination of particulate sulfate and SO_2(g) in the desert southwest using filter pack samplers, *Environmental Science and Technology, 29*, 787-791, 1995.

Farwell S. O., and C. J. Barinaga, Sulfur-selective detection with the FPD: Current enigmas, practical useage, and future directions, *Journal of Chromatographic Science, 24*, 483-494, 1986.

Febo, A, F. De Santis, C. Perrino and M. Giusto, Evaluation of laboratory and field performance of denuder tubes: A theoretical approach, *Atmospheric Environment, 23*, (7), 1517-1530, 1989.

Ferek, R. J., P. A. Covert, and W. Luke, Intercomparison of measurements of sulfur dioxide in ambient air by carbonate-impregnated filters and Teco pulsed fluorescence analyzers, *Journal of Geophysical Research, 102*, (D13), 16,267-16,272, 1997.

Ferek, R. J., D. A. Hegg, J. A. Herring and P. V. Hobbs, An improved filter pack technique for airborne measurement of low concentrations of SO_2, *Journal of Geophysical Research, 96*, (D12), 22,373-22,378, 1991.

Ferm, M, A Na_2CO_3-coated denuder and filter for determination of gaseous HNO_3 and particulate NO_3^- in the atmosphere, *Atmospheric Environment, 20*, (6), 1193-1201, 1986.

Ferm, M., and A. Sjodin, A sodium carbonate coated denuder for determination of nitrous acid in the atmosphere, *Atmospheric Environment, 19*, (6), 979-983, 1985.

Gallagher, M.S., D.B. King, P. -Y. Whung and E. S. Saltzman, Performance of the HPLC/fluorescence SO_2 detector during the GASIE instrument intercomparison experiment, *Journal of Geophysical Research, 102*, (D13), 16,247-16,254, 1997.

Gaines, K. K., W. H. Chatham, and S. O. Farwell, Comparison of the SCD and FPD for HRGC determination of atmospheric sulfur gases, *J. High Resolut. Chromatogr., 13*, 489-493, 1990.

Goldan, P. D., W. C. Kuster and D.L. Albritton, A dynamic dilution system for the production of sub-ppb concentrations of reactive and labile species, *Atmospheric Environment, 20*, (6), 1203-1209, 1986.

Gormley, P. G. and M. Kennedy, Diffusion from a stream flowing through a cylindrical tube, *Proc. R. Ir. Acad.* **52A**, 163-169, 1949.

Gregory, G. L., D. D. Davis, N. Beltz, A. R. Bandy, R. J. Ferek, and D. C. Thornton, An intercomparison of aircraft instrumentation for tropospheric measurements of sulfur dioxide, *Journal of Geophysical Research, 98*, (D12), 23,325-23,352, 1993.

Hoell Jr, J. M., D. D. Davis, G. L, Gregory, R. J. McNeal, R. J. Bendura, J. W. Drewry, J. D. Barrick, B. W. J. H. Kirchhoff, A. G. Motta, R. L. Navarro, W. D. Dorko and D. W. Owen, Operational overview of the NASA GTE/CITE 3 airborne instrument intercomparisons for sulfur dioxide, hydrogen sulfide, carbonyl sulfide, dimethyl sulfide, and carbon disulfide, *Journal of Geophysical Research, 98*, (D12), 23,291-23,304, 1993.

Hübler, G., R. Alvarez, P, Daum, R. Dennis, N. Gillani, L. Kleinman, W. Luke, J. Meagher, D. Rider, M. Trainer, and R. Valente, An overview of the airborne activities during the Southern Oxidants Study (SOS) 1995 Nashville/Middle Tennessee Ozone Study, *Journal of Geophysical Research, 103*, (D17), 22,245-22,259, 1998.

Intergovernmental Panel on Climate Change (IPCC), *Climate Change 1995: The Science of Climate Change*, J. T. Houghton et al., Eds., Cambridge Univ. Press, Cambridge, 1996.

Ito, K., G. D. Thurston, C. Hayes and M. Lippmann, Associations of London, England, daily mortality with particulate matter, sulfur dioxide, and acidic aerosol pollution, *Archives of Environmental Health, 48*, (4), 213-220, 1993.

Jaeschke, W., N. Beltz, W. Haunold and U. Krischke, Improvement of the tetrachloromercurate absorption technique for measuring low atmospheric SO_2 mixing ratios, *Journal of Geophysical Research, 102*, (D13), 16,279-16,286, 1997.

Jodwalis, C. M., Oceanic emissions of Sulfur: Application of new techniques, Ph.D. Thesis, University of Alaska Fairbanks, 1998.

Jodwalis, C. M. and R. L. Benner, Sulfur gas fluxes and horizontal inhomogeneities in the marine boundary layer, *J. Geophys. Res.*, 101, 4393-4401, 1996.

Kelly, D.P. and N.A. Smith, Organic Sulfur Compounds in the Environment, *Advances in Microbial Ecology II*, 345-385, 1990.

Kok, G. L., A. J. Schanot, P. F. Lindgren, P. K. Dasgupta, D. A. Hegg, P. V. Hobbs, and J. F. Boatman, An airborne test of three sulfur dioxide measurement techniques, *Atmospheric Environment, 24*, (7), 1903-1908, 1990.

Koutrakis, P., J. M. Wilson, J. L. Slater, M. Brauer, J. D. Spengler, R. K. Stevens and C. L. Stone, Evaluation of an annular denuder/filter pack system to collect acidic aerosols and gases, *Environmental Science and Technology, 22,* (12), 1988.

Kuster, W. C. and Goldan, P. D., Quantitation of the losses of gaseous sulfur compounds to enclosure walls, *Environmental Science and Technology, 22*, (8), 810-815, 1987.

Lee H. S., R. A. Wadden and P. A. Scheff, Measurement and evaluation of acid air pollutants in Chicago using an annular denuder system, *Atmospheric Environment, 27A*, (4), 543-553, 1993.

Leckrone, K. J., and J. M. Hayes, Efficiency and temperature dependence of water removal by membrane dryers, *Anal. Chem., 69,* 911-918, 1997.

Lindgren, P. F., and P. K. Dasgupta, Measurement of atmospheric sulfur dioxide by diffusion scrubber coupled ion chromatography, *Anal. Chem., 61,* (1), 19-24, 1989.

Luke, W. T., Evaluation of a commercial pulsed fluorescence detector for the measurement of low-lovel SO_2 concentrations during the Gas-Phase Sulfur Intercomparison Experiment, *Journal of Geophysical Research, 102*, (D13), 16,255-16,265, 1997.

Luther III, G. W. and H. A. Stecher III, Preface: Historical background, *Journal of Geophysical Research, 102*, (D13), 16215-16,217, 1997.

MacTaggart, D. L., S. O. Farwell, T. J. Haakenson, W. L. Bamesberger, and W. D. Dorko, Generation and evaluation of test gas mixtures for the Gas-Phase Sulfur Intercomparison Experiement (GASIE), *Journal of Geophysical Research, 102,* (D13), 16,237-16,245, 1997.

Möller, D., On the Global National Sulfur Emission, *Atmospheric Environment,* 18, 29, 1984b.

Muller III, C. H., K. Schofield, M. Steinberg and H. P. Broida, Sulfur chemistry in flames, *Int. Symp. Combust., 17,* 867-829, 1979.

Murphy D. M., and D. W. Fahey, Mathematical treatment of the wall loss of a trace species in denuder and catalytic converter tubes, *Analytical Chemistry, 59,* 2753-2759, 1987.

National Research Council (NRC), *Protecting visibility in National parks and wilderness areas,* National Academy Press, Washington DC, 1993.

National Research Council (NRC), Panel on Aerosol Radiative Forcing and Climate Change (J. Seinfeld, Chair), *A Plan for a Research Program on Aerosol Radiative Forcing and Climate Change,* National Academy Press, Washington DC, 1996.

Nicks Jr., D. K., R. L. Benner, S. O. Farwell, D. MacTaggart, L. Bamesberger, D. Crosley and P. Goldan, Summary of GASIE-2, a rigorously blind evaluation of the Diffusion Denuder Sulfur Chemiluminescence Detector (DD/SCD) for low pptv SO_2 measurements, *submitted to Journal of Geophysical Research,* 1999.

Okabe, H., P. L. Splitstone and J. J. Ball, Ambient and source SO_2 detector based on a fluorescence method, *Journal of Air Pollution Control Association, 23,* 514-516, 1973.

Raatz, W. E. and G. E. Shaw, Long-range tropospheric transport of pollution aerosols into the Alaskan arctic, *Jounal of Climate and Applied Meteorology, 23,* 1052-1064, 1984.

Reichhardt, T., Weighing the health risks of airborne particulates, *Environmental Science and Technology, 29,* (8), 360A-364A, 1995.

Ryerson T. B., M. P. Buhr, G. J. Frost, P. D. Goldan, J. S. Holloway, G. Hübler, B. T. Jobson, W. C. Kuster, S. A. McKeen, D. D. Parrish, J. M. Roberts, D. T. Sueper, M. Trainer, J. Williams, and F. C. Fehsenfeld, *Journal of Geophysical Research, 103*, (D17), 22,569-22,583, 1998.

Ryerson, T. B, A. J. Dunham, R. M. Barkley and R. E. Sievers, Sulfur-selective detector for liquid chromatography based on sulfur monoxide-ozone chemiluminescence, *Analytical Chemistry, 66*, 2841-2851, 1992

Saltzman, E. S., S. A. Yvon and P. A. Matrai, Low-level atmospheric sulfur dioxide measurement using HPLC/fluorescence detection, *J. Atmospheric Chemistry, 17*, 73-90, 1993.

Samet, J. M. and M. J. Utell, The environment and the lung, changing perspectives, *Jounal of the American Medical Assocition, 266*, (5), 670-674, 1991.

Schlesinger, W.H., *Biogeochemistry, An Analysis of Global Change*, Academic Press, Inc., San Diego, CA, 1991.

Schorran, D. E., C. Fought, D. F. Miller, W. G. Coulombe, R. E. Keislar, R. Benner, and D. Stedman, Semicontinuous Method for Monitoring SO_2 at Low Parts-per-Trillion Concentrations, *Environ. Sci. Technol., 28*, (7), 1307-1311, 1994.

Schwartz, S. E., and M. O. Andreae, Uncertainty in climate change caused by aerosols, *Science, 272*, 1121-1122, 1996.

Seinfeld, J. H. and S. Pandis, *Atmospheric Chemistry and Physics: From Air Pollution to Climate Change*, Wiley-Interscience, New York, 1997.

Shaw, Glenn, Bio-Controlled Thermostasis Involving the Sulfur Cycle, *Climate Change, 5*, 297-303, 1983.

Shaw, G. E., Aerosol measurements in central Alaska, 1982-1984, *Atmospheric Environment, 19*, (12), 2025-2031, 1985.

Shaw, G. E., R.L. Benner, A.D. Clarke and W. Cantrell, On the regulation of climate: A sulfate particle feedback loop involving deep convection, *Climate Change, 39*, 23-33, 1998.

Sram, R. J., I. Benes, B. Binkova, J. Dejmek, D. Horstman, F. Kotesovec, D. Otto, S. D. Perreault, J. Rubes, S. G. Selevan, I. Skalik, R. K. Stevens and J. Lewtas, Teplice Program - The impact of air pollution on human health, *Environmental Health Perspectives, 104*, (4), 699-714, 1996.

Stecher III, H. A., G. W. Luther III, D. L. MacTaggart, S. O. Farwell, D. R. Crosley, W. D. Dorko, P. D. Goldan, N. Beltz, U. Krischke, W. T. Luke, D. C. Thornton, R. W. Talbot, Barry L.L., E. M. Scheuer, R. L. Benner, J. Wu, E. S. Saltzman, M. S. Gallagher, and R. J. Ferek, Results of the Gas-Phase Sulfur Intercomparison Experiment (GASIE): Overview of experiemental setup, results and general conclusions, *Journal of Geophysical Research, 102*, (D13), 16,219-16,236, 1997.

Sugden, T. M, E. M. Bulewicz and A. Demerdache, Some observations on oxides and hydrides of nitrogen and sulfur in flame gases containing atomic hydrogen, atomic oxygen, and hydroxyl radicals, In *Chemical Reactions in the Lower and Upper Atmosphere*, Wiley, New York, pp 89-108, 1962.

Talbot, R. W., E. M. Scheuer, B. L. Lefer and W. T. Luke, Measurements of sulfur dioxide durring GASIE with the mist chamber technique, *Journal of Geophysical Research, 102*, (D13), 16,273-16,278, 1997.

Thornton, D. C., and A. R. Bandy, Sulfur dioxide and dimethyl sulfide in the Central Pacific troposphere, *J. Atmospheric Chemistry, 17*, 1-13, 1993.

Wu, J., The DD/SCD analytical method for SO2 at part-per-trillion, M.S. thesis, Univ. of Alaska Fairbanks, 1995.

Yvon S. A., and E. S. Saltzman, Atmospheric sulfur cycling in the tropical Pacific marine boundary layer (12°S, 135°W): A comparison of field data and model results 2. suflur dioxide, *Journal of Geophysical Research, 101*, (D3), 6911-6918, 1996.

Zulifiqur, A., C. L. Thomas and J. F. Alder, Denuder tubes for sampling gaseous species, A review, *Analyst, 114*, 759-769, 1989.